THE UNIVERSITY OF CHICAGO

DEFINING ASSEMBLY OF A TRANSLOCON FOR MULTIPASS MEMBRANE PROTEIN BIOGENESIS

A DISSERTATION SUBMITTED TO

THE FACULTY OF THE DIVISION OF THE BIOLOGICAL SCIENCES

AND THE PRITZKER SCHOOL OF MEDICINE

IN CANDIDACY FOR THE DEGREE OF

DOCTOR OF PHILOSOPHY

GRADUATE PROGRAM IN CELL AND MOLECULAR BIOLOGY

BY

FRANK WANG ZHONG

CHICAGO, ILLINOIS

DECEMBER 2023

TO MY MOTHER, FATHER, AND BROTHER, WHO HAVE CONSTANTLY SUPPORTED ME THROUGHOUT MY JOURNEY. THANK YOU FOR EVERYTHING. I COULD NOT HAVE DONE IT WITHOUT YOU

Table of Contents

List of Figures

Acknowledgements

As I think back on the 6 years I have spent in the Keenan Lab, I find myself thinking about the young scientist who excitedly joined thinking that he would publish a paper in 3 years and graduate. While it took 6 years, not 3, I did manage to publish a paper and am about to graduate. Nevertheless, it is my good fortune that I have been a part of a multitude of different projects and worked in an intensively collaborative effort with many brilliant scientists in which good science was discussed and many new research paths were opened. To my advisor, Robert Keenan, I cannot overstate the importance of how important to my growth, you were and are. You have never hesitated in your support of the projects of the lab (from TMCO1 to RAMP4 to FKBP11) and am ever grateful you allowed a young aspiring molecular biologist and biochemist to join a lab that was initially very structurally focused. I will remember fondly our discussions on experiments and strategies. You opened my thinking on how to think about hypotheses and to at least entertain possibilities that I thought impossible.

Throughout my Ph.D., the Keenan Lab has functioned in a collaborative effort for which I am eternally grateful. When I first started, I worked with Andrei, an excellent mentor who got me excited about the TMCO1-translocon and convinced me to join the Keenan Lab. Thanks Andrei. Throughout the bulk of my Ph.D. I worked closely with Arun on both the initial TMCO1-translocon paper as well as our paper defining multipass assembly at the Sec61 complex. Arun, you taught me so much. Thanks for shaping me into the scientist that I am and thanks for all the memories these past 6 years. I'll treasure the time we have spent together. Others in the lab have been instrumental in discussions and experiments, JoJo (honestly the backbone of the lab, how did you survive 5 years of me and Arun), Mel (my cohort buddy! We

entered the Keenan Lab at the same time and it's been a pleasure the last 6 years), Madeline, Ben, Amanda, Phil, Natasha, Szymon, thanks so much.

Thanks to all the people around me at the University of Chicago who helped me throughout my years here. From the BMB office: Bulent, Amy, Lisa, Alicia, and Shani, thank you for keeping me caffeinated, fed, and helping in any way they could. Thanks to Stephanie from CMB for checking in and keeping me on track. Also thanks to the Benzanilla Lab who welcomed me with open arms during our morning coffee sessions, thanks Carlitos, Yichen, Bernardo, Sarah.

I would be amiss if I did not thank the funding that I have received over the course of my Ph.D. My work here has been funded, in great part by the NIH, from the molecular biology training grant to the R01 and R35 awarded to the Keenan lab for this work. I would also like to thank both the CMB and BMB departments for providing funding throughout the 6 years.

Thank you to my family for supporting me throughout my life and during my Ph.D. Thanks dad for encouraging my scientific curiousity from a young age and thanks mom for always worrying and fretting about me and asking me if I need anything. Also thanks Randy, you've been here for my entire Ph.D. and I am not sure how I would have been able to finish without your support. I am also most grateful of to my girlfriend Jen Kwok. She has been supportive in all facets and encouraged me to no end. Her belief in me is what allowed me to power through the last couple months.

Lastly, I need to thank all my friends both within UChicago and outside that have supported me throughout these six years. There are too many names to name but thank you for being there for me. Thanks for tolerating my complaints and keeping my spirits up in dark times.

Abstract

The cellular proteome is comprised of both soluble proteins and membrane proteins. Membrane proteins make up 30% of the human proteome and defects in their biogenesis results in a wide range of diseases. While biogenesis of membrane proteins with a singular transmembrane domain (TMD) is relatively well understood, the biogenesis of membrane proteins with multiple TMDs ("multipass") is less clear. The TMDs of multipass membrane proteins are diverse, with varying hydrophobicities, and require folding within the lipid bilayer. To overcome this set of challenges, the Sec61 translocon has been shown to assemble various complexes during protein synthesis. Here, we show that for multipass membrane proteins, a Sec61 translocon specific for this class of membrane proteins exists and is assembled in response to defined signals. Furthermore, we show that two different novel accessory factors associate with the Sec61 translocon and are involved in protein biogenesis.

We first define the existence of a "multipass translocon." The multipass translocon is distinguished by three components that selectively bind the ribosome–Sec61 complex during multipass protein synthesis: the GET- and EMC-like (GEL), protein associated with translocon (PAT) and back of Sec61 (BOS) complexes. We show that assembly of the multipass translocon is in response to defined signals and depletion of multipass translocon components results in multipass membrane protein biogenesis and topogenesis defects both in vivo and in vitro. These results establish the mechanism by which nascent multipass proteins selectively recruit the multipass translocon to facilitate their biogenesis.

In addition to this work, we characterize the role of two translocon accessory factors, RAMP4 and FKBP11, and their role in protein biogenesis. For both proteins, we demonstrate

that they are involved in the synthesis of proteins with long lumenal loops. Specifically, for FKBP11, RNA sequencing of ribosome-translocon complexes implicates a bias for proteins that have long translocated lumenal domains. Analysis of insertion intermediates shows dynamics of FKBP11 association with the Sec61 translocon, with recruitment being concomitant with the oligosaccharyl transferase complex (OST). Depletion of FKBP11 further leads to membrane protein instability at the cellular level. In summation, this work defines the ER translocon as a dynamic assembly whose subunit composition adjusts co-translationally to accommodate the biosynthetic needs of its diverse range of substrates, from single-pass to multi-pass.

1. Introduction

1.1. A brief overview of transmembrane proteins

Living cells are defined by two key features: the cytoplasm, and the cellular membrane. Of particular importance and interest is the cellular membrane. Its presence allows the cell to clearly define an exterior and interior space as well as function as a gatekeeper for what can enter and exit the cell. Furthermore, the cellular membrane allows cells to partition intracellular compartments which in turn have specific roles and functions. These biological membranes consist of a lipid bilayer (comprised of phospholipids, sphingolipids, and sterols) and proteins (Watson, 2015). Two different classes of proteins associate with biological membranes. Extrinsic proteins are membrane proteins that are only loosely associated with the membrane. The interactions between these proteins and the membrane consist of weak molecular interactions with the polar head group of lipids or integral proteins. Intrinsic proteins, however, are embedded within the membrane itself and the interactions are direct hydrophobic interactions with the phospholipids of the bilayer. While some intrinsic proteins do not completely span the bilayer, a class of intrinsic proteins in fact completely cross the lipid bilayer. These proteins are known as transmembrane proteins.

Transmembrane proteins are a critical component of biological membranes. They have a vast and diverse range of function ranging from transport across the bilayer, acting as receptors for signaling cascades, mediating interactions with other cells or the extracellular environment, as well as other functions. In fact, approximately 30% of the human proteome consists of transmembrane proteins and 60% of druggable targets are transmembrane proteins, further alluding to their importance and ubiquity (Overington et al. 2006, Almen et al. 2009).

Transmembrane proteins (referred to hereafter as membrane proteins), by nature of their role, have a general shared organization. They consist of a hydrophobic core that spans the bilayer in addition to hydrophilic regions on either side of the bilayer. The topology and hydrophilic regions of membrane proteins is varied but the hydrophobic core consists of 18-28 hydrophobic amino acids that form an a-helical secondary structure. For single-pass membrane proteins, a singular alpha helix suffices while for multi-pass membrane proteins, a wide number of different helices exist.

Membrane proteins are translated by cytosolic ribosomes followed by insertion into the membrane for their correct function. Due to the hydrophobic regions, membrane proteins face several challenges during their synthesis in the cytosol. First, hydrophobic regions are energetically unfavorable in the environment of the cytosol, thus leaving membrane proteins prone to aggregation (Kopito, 2000). Second, premature folding of the hydrophilic domains can prevent correct insertion into the membranes (Vabulas et al., 2010). Lastly, the cell contains a myriad variety of different membranes which further complicates the targeted insertion of membrane proteins. To solve the difficulty of synthesis and insertion, the cell has combined the two steps in a mechanism termed co-translational translocation.

In co-translational translocation, the cell can shield hydrophobic regions from the aqueous cytosol while also precluding premature folding from occurring. Yet while this solves the first two issues previously discussed, the targeting of membrane proteins to specific membranes is not overcome. Instead, the cell has simplified targeting by targeting most membrane proteins to the endoplasmic reticulum (ER). By targeting to the ER, membrane proteins arrive at a single point of biogenesis, further simplifying the process. In fact, almost all membrane proteins of the

secretory pathway are produced, folded, and assembled at the ER followed by trafficking to their final destination (Golgi, plasma membrane, lysosome, etc) (Barlowe and Miller, 2013). Thus, membrane protein insertion can be simplified into several concise steps. During translation, membrane proteins are captured by a targeting factor, targeted to the ER membrane, followed by insertion into the membrane and folding (**Figure 1**).

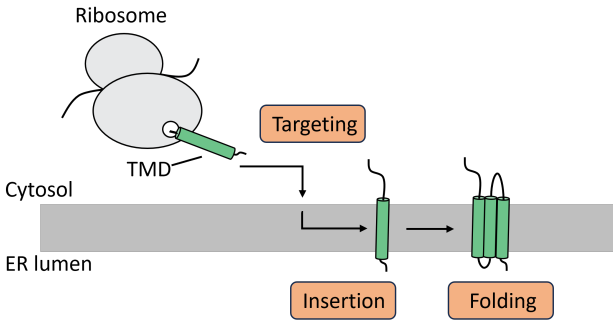

Figure 1. A general outline for membrane protein biogenesis

Nascent proteins emerge from the ribosome and are captured by targeting factors to prevent aggregation. The targeting factor brings the nascent chain to the membrane and the protein is inserted. Following insertion, the protein is able to fold and assemble with other subunits. Adapted from Hegde and Keenan *Nat Rev Mol Cell Bio* 2022

1.2. The SRP-SRP receptor pathway mediates co-translational translocation

The most widely understood and studied pathway of membrane protein biogenesis is the signal recognition particle (SRP) pathway. The SRP is a ribonucleoprotein complex that initiates co-translational translocation by recognition and binding of a stretch of 7-15 a-helical hydrophobic amino acids on a nascent polypeptide (Von Heijne, 1985). This stretch of hydrophobic residues is now known to be the N-terminal signal sequence of secretory soluble proteins and membrane proteins or the first transmembrane domain of a membrane protein (signal anchor) (Tessa et al., 2005). Binding of these hydrophobic amino acids occurs via the S-domain of SRP, in part due to a strong affinity of the methionine rich carboxy terminus of SRP54 (also known as the M-domain) (Bernstein et al., 1989, Keenan et al., 1998). Furthermore, structural work indicates that this binding domain of SRP54 is in close proximity to the ribosome

exit tunnel, allowing it to capture any nascent polypeptide chains that emerge (Voorhees and Hegde, 2015). The ability of SRP to capture the emerging nascent chain is thus the first step of targeting membrane proteins to the ER membrane. Furthermore, by directly binding these early stretches of hydrophobic amino acids, SRP can shield the nascent polypeptide from the aqueous cytosol, providing a favourable environment prior to translocation.

Previous work has shown that upon binding, elongation of the nascent polypeptide is arrested followed by docking of the ribosome-nascent chain-SRP complex to the SRP-receptor (Lipp et al., 1987, Ogg and Walter, 1995, Mason et al., 2000, Scherrer et al., 2010). Upon docking of the complex to the SRP-receptor, a handoff occurs where the SRP-receptor delivers the ribosome-nascent chain to the Sec61 channel (Halic et al., 2006). The disassociation of SRP-SRP receptor from the ribosome nascent chain has been shown to be dependent upon GTP hydrolysis from the GTPase domains of SRP and SRP receptor (Connolly and Gilmore, 1989, Powers and Walter, 1995). This mechanism serves as a failsafe where ribosome-nascent chain dissociation from the complex only occurs after the ribosome has made it to the ER membrane. The subsequent step of ribosome-nascent chain docking to the Sec61 channel, however, is poorly understood. Previous work has shown that the SRP and Sec61 cannot bind simultaneously and that the Sec61 channel undergoes significant conformational changes upon ribosome binding (Schaffitzel et al., 2006, Voorhees et al., 2014, Voorhees and Hegde, 2015)

Now that the translocating polypeptide has been brought to the Sec61 channel, the next step of biogenesis can occur: translocation. The Sec61 channel is a trimeric protein composed of 3 subunits, the a, b, and g subunits (referred to as Sec61). The central subunit is the a-subunit containing a central pore that allows the nascent polypeptide to extrude from the ribosome and

into the ER lumen (Berg et al., 2004; Kedrov et al., 2011; Park and Rapoport, 2012; Voorhees et al., 2014). This central pore contains two key features, both of which play a central role in translocation, a plug domain as well as a lateral gate. The plug domain blocks the channel in order to maintain the closed environment of the membrane while the lateral gate is involved in allowing signal sequences and transmembrane domains in entering the lipid bilayer (Junne et al., 2006).

After SRP-SRP receptor handoff, the ribosome docks to Sec61 and priming of the channel for translocation occurs. Structures of the docking step indicate that ribosome binding primes the channel for translocation by triggering conformational changes that slightly open the cytosolic side of the lateral gate (Voorhees et al., 2014). The nascent chain then samples Sec61, upon which, sufficient hydrophobic signals open the channel by destabilizing the plug of Sec61 (Gogala et al., 20114; Li et al., 2016). This is an important point to note. It is in fact, the hydrophobicity of the signal that further destabilizes the plug as well as opening the gate. Studies have shown that hydrophilic signal sequences that are efficiently targeted fail translocation, indicating that there are minimal hydrophobic requirements (Cioffi et al., 1989).

Further structures have shown that N-terminal signal sequences sit in the lateral gate of the channel, directly in contact with the lipid bilayer (Voorhees et al., 2016). While high resolution structures of transmembrane domains do not exist, lower resolution structures of the first transmembrane domain of proteins indicate that these signal anchors follow a similar pathway as signal sequences (Bischoff et al., 2014; Gogala et al., 2014). The consensus model is that the hydrophic region of signal sequences/signal anchors diffuse into the lipid bilayer followed by the remainder of the hydrophilic protein entering the ER lumen through the channel. For a multipass

membrane protein, an extrapolation of this model for the remainder of the TMD's has long been the view of the field (Blobel 1989; Matlack et al., 1998). In essence, as each TMD is synthesized, it enters the channel, contacts the lateral gate and diffuses into the lipid bilayer in a sequential manner. Thus, a unifying model of membrane protein biogenesis of SRP-SRP receptor targeting followed by Sec61 translocation emerges as the predominant pathway for insertion into the lipid bilayer **(Figure 2).**

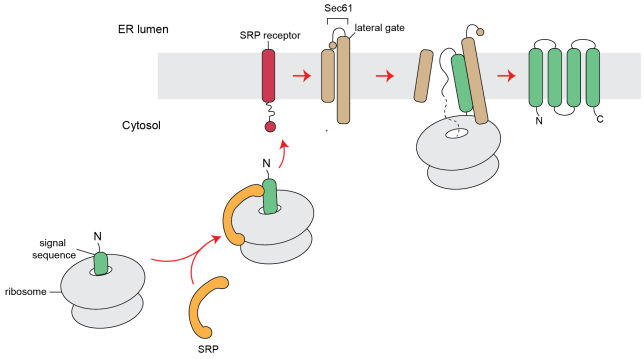

Figure 2. The SRP-SRP receptor and Sec61 pathway for protein targeting

The vast majority of secretory proteins are targeted to the ER membrane by the signal recognition particle (SRP). SRP binds both the ribosome and the signal sequence or first TMD of membrane proteins followed by targeting to the SRP receptor and the Sec61 channel. Displacement of the plug domain occurs and the membrane protein enters the bilayer via Sec61's lateral gate.

1.3. The Oxa1 Superfamily and their function in membrane protein biogenesis

While the Sec61 channel is ubiquitous and widely utilized by the vast majority of membrane proteins, insertion systems independent of this channel do exist. Several distinctions exist within these insertion systems. First is the ability of some proteins to insert into the membrane in a post-translational manner. Second is the ability of other proteins to insert into the membrane independently of Sec61 while still maintaining co-translational translocation. Unsurprisingly, the two alternative pathways utilize machinery that share features and are from a common superfamily. The Oxa1 superfamily is a superfamily of proteins that share a function to

facilitate membrane protein biogenesis (**Figure 3**). Comprised of bacterial YidC, mitochondrial Oxa1/2, chloroplast Alb3/4, and recently identified eukaryotic WRB/TMCO1/EMC3, all

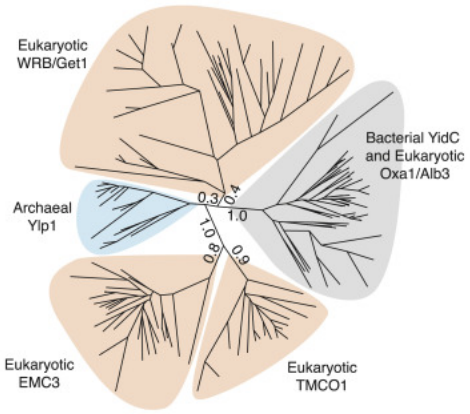

Figure 3. Phylogenetic tree of DUF106 homologs defining the Oxa1 superfamily

Maximum-likelihood tree of representative sequences of the DUF106 family of proteins. Branch lengths for the five main clades are indicated. From Anghel et al. *Cell Reports* 2017

members have been implicated in the ability to insert membrane proteins (Anghel et al., 2017). All members of the superfamily possess a shared architecture comprising of a shared topology (N-out/C-in) and core (cytosolic coiled and a three-TMD core that forms a lipid-exposed hydrophilic groove). In the following paragraphs, there will be a brief discussion on each member of the Oxa1 superfamily and its role in membrane protein biogenesis.

1.3.1. YidC functions co- and post-translationally to insert membrane proteins

The most widely studied and best understood member of the Oxa1 family is the bacterial YidC. YidC is comprised of one gene within gram-negative bacteria and 2 paralogs (YidC1 and YidC2) in gram-positive bacteria. Topologically, it has 5 TMD's, a N-out/C-in topology, and a cytosolic coiled coil, key characteristics of the Oxa1 superfamily. It's role within bacterial membrane protein biogenesis is varied. It has been shown to insert proteins both co- and post-translationally, independent of the SecYEG channel while also having been shown to function in

a SecY-dependent role where it facilitates folding and insertion of substrates (**Figure 4**) (Dalbey et al., 2014). In the SecY-independent co-translational mechanism, YidC is able to insert proteins with very short, translocated regions across the plasma membrane. In fact, YidC is able to insert the Pf3 phage coat component and the M13 Procoat protein in a SecY independent manner both in vivo and in vitro (Serek et al., 2001; Samuelson et al. 2004; Ernst et al., 2011). Additional substrates of YidC have also been identified: the F_0c subunit of the ATP Synthase, the MscL mechanosensitive channel, as well as C-terminal tail anchored proteins DjlC and Flk (Van Bloois

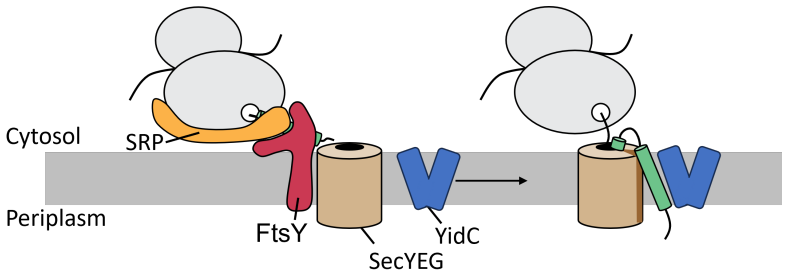

Figure 4. YidC-SecYEG insertion pathway

SRP-bound substrate is targeted to the SecYEG holotranslocon via membrane bound SRP receptor FtsY. The N-terminus of the substrate inserts between the interface of SecYEG and YidC and the second TM initiates C-terminal translocation. Adapted from Shanmugam and Dalbey *Microbiology Spectrum* 2019

et al., 2004; Facey et al., 2007; Peschke et al., 2018). Interestingly, increasing the charge of the periplasmic loop region of the MscL channel reduces its dependence on YidC, while more hydrophobic Pf3 inserted spontaneously without YidC, suggesting that basic amino acid properties may influence insertion dependence (Ernst et al., 2011; Neugebauer et al., 2012). The common feature of a short, translocated loop devoid of charge suggests that the Yid-C machinery can only handle simple domains in its SecY-independent role.

While YidC has been shown to insert these simple membrane proteins, the complete mechanism of their insertion from substrate capture to membrane remains poorly understood. For example, in the SecY pathway, the initial targeting of the ribosome to the membrane is

mediated by SRP-SRP receptor. It is currently unknown how bacterial ribosomes are able to target to the plasma membrane in a SecY-independent manner. One theory postulates that SRP handoff occurs to YidC directly. Alternatively, another hypothesis is that YidC constitutively binds ribosomes, thus bypassing the SRP pathway altogether, allowing the nascent chain to directly be captured and inserted (Seitl et al., 2014). Regardless, it is clear that somehow substrate capture does indeed occur given the dependence of the aforementioned proteins on YidC. Following substrate capture, the protein is then inserted by YidC into the lipid bilayer. How YidC is able to complete this task remains an open question. Initially, it was believed that YidC dimers functioned as a pore, akin to the SecY channel, but structures indicate that YidC monomers are competent to bind translating ribosomes (Kedrov et al., 2013; Seitl et al., 2014). Structural studies have shown that YidC contain a hydrophilic groove, a core feature that we now understand to be a defining feature of the Oxa1 superfamily (Kumazaki et al., 2014). In fact, one structural study has hypothesized a model in which the hydrophilic groove allows translocation of the substrate by binding a conserved arginine residue (Kumazaki et al., 2014).

Apart from its role in SecY independent membrane insertion, YidC has also been shown to function in a SecY dependent manner. While the base channel of the bacterial translocon is the SecYEG channel, in vivo, the translocon is composed of a larger protein complex known as the holo-translocon. The holo-translocon is comprised of the SecYEG channel, YidC, and SecDF-YajC (Schulze et al., 2014; Komar et al., 2016). YidC's role within this holo-translocon is not clear, but it is potentially thought to assist in folding of TMD's of multipass membrane proteins (Zhu et al., 2013). While the SecYEG channel maintains the role of translocating the hydrophilic regions as well as insertion of the TMD's, YidC may prime the lateral gate for the TMD's. This

is supported by work that places YidC directly at the lateral gate via in vitro and in vivo cross-linking (Neugebauer et al., 2012). In addition, it has been shown that a TMD can in fact displace YidC from this lateral gate, further implicating its role in TMD translocation (Sachelaru et al., 2013). Further work is required to elucidate the complete function of YidC in translocating these TMD's and its role in multipass membrane biogenesis.

1.3.2. Post-translational insertion by the GET pathway

While the vast majority of proteins undergo co-translation translocation, a small subset of proteins exist that undergo post-translational insertion into the ER bilayer. What are the characteristics of these proteins that do not allow them to utilize the SRP-SRP receptor pathway? For one, membrane proteins that utilize the post-translational pathway share a common feature, the presence of a TMD at the C-terminus (Hegde and Keenan, 2011). The reason for this commonality is that the SRP-SRP receptor pathway requires approximately 50-60 amino acids of the nascent chain for recognition and targeting (Walter and Blobel, 1981). Any membrane protein lacking a signal sequence that has its first or only TMD within 60 amino acids of the C-terminus would necessarily finish translation before SRP-SRP receptor is able to efficiently recognize and target the translating nascent chain-ribosome complex to the ER bilayer. (Kutay et al., 1993). This small subset of membrane proteins are aptly named "tail-anchored" (TA) proteins. Thus, a different set of machinery exists to capture the newly translated protein, target, and insert the membrane protein into the lipid bilayer. In eukaryotes, this machinery is termed the GET (Guided Entry of Tail anchored protein) pathway.

In yeast, the GET complex is comprised of 6 different proteins (Get1-5, and Sgt2) that function in conjunction to capture the substrate, target it to the membrane, and finally insert the protein into the bilayer (**Figure 5**). As translation terminates on a TA protein, it is released from the ribosome. This newly synthesized polypeptide is then captured by the Get4/Get5/Sgt2 in what is known as the "pre-targeting" phase (Bozkurt et al., 2010; Chartron et al., 2010; Wang et al., 2010). Following binding of the substrate by Get4/Get5/Sgt2 it is passed on to Get3, the targeting factor of the GET pathway. Get3 functions as a dimer and shields the substrate's TMD from the cytosol, a critical step of substrate capture and targeting, preventing aggregation of these TA proteins (Bozkurt et al., 2009; Suloway et al, 2009; Mateja et al, 2009; Mateja et al, 2015). After binding, Get3 then delivers the substrate to the ER bilayer, where handoff occurs to the Get1/Get2 receptor (Schuldiner et al., 2008). Get1 and Get2 are 2 membrane proteins that together, not only bind Get3 but also mediate insertion of the TA protein (Mariappan et al., 2011). Previous work showed that the insertion of TA proteins by Get1/2 was dependent on the

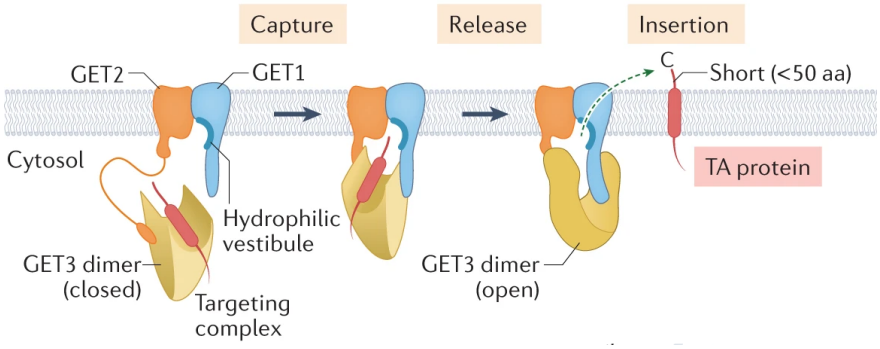

Figure 5. The GET pathway mediates post-translational insertion of tail-anchored proteins

A targeting complex comprising GET3 and a TA protein is captured by the cytosolic domain of GET2. Next, the cytosolic domain of GET1 releases the TA protein from GET3. The TMD of the TA protein then inserts into the membrane, using the hydrophilic vestibule in GET1 to facilitate translocation of the short carboxy-terminal tail. From Hegde and Keenan *Nat Rev Mol Cell Bio* 2022

TMD domains of both proteins (Mariappan et al., 2011; Stefer et al., 2011). Indeed, mutations to the TMD's of Get1/2 prevented insertion of the substrate into the bilayer and instead kept the protein bound with Get3 (Wang et al. 2015). Thus, their dual function serves as a checkpoint in which it facilitates handoff of the TA protein from Get3 while mediating the insertion of the TA protein. Get1/2 heterodimer achieves handoff of the substrate from Get3 via ATP-ase dependent interactions between Get1 and Get3 followed by insertion of the substrate (Kubota et al., 2012).

The exact mechanism of insertion by Get1/2 was not fully understood until recently. Previous in vitro work had shown that a single Get1/2 heterodimer can mediate insertion of TA proteins (Zalisko et al. 2015), but recent work has indicated that the mechanism of insertion revolves around a heterotetramer of Get1/2 which forms a dynamic aqueous channel (McDowell et al. 2020, Heo et al. 2023). While further investigation is required to definitively confirm the mechanism of insertion, it is prudent to note here that Get1 is a member of the Oxa1 superfamily. Like many members of the Oxa1 superfamily, it possesses a cytosolic facing hydrophilic vestibule. An attractive model is one where Get3 and the TA targeting complex engages Get1/2 heterodimer or heterotetramer. After engagement, a possible model is that the substrate is dislodged from Get3 and the TMD enters the membrane, with the hydrophilic vestibule lowering the penalty of translocating the hydrophilic tail.

1.3.3. Oxa1 and Alb3

While YidC and Get1 are the most well characterized and understood of the Oxa1 superfamily, other homologs within the Oxa1 superfamily exist, namely the mitochondrial homolog Oxa1 and the chloroplast homolog Alb3. Oxa1 has been shown to be involved in the co-translational insertion and translocation of cytochrome c oxidase subunit II (Cox2) (Bonnefoy

et al., 1994). Cox2 is a two-TMD protein with a N-out, C-out topology containing a leader peptide that is cleaved in the intermembrane space (IMS) of the mitochondria. Yeast strains lacking Oxa1 showed a clear defect in translocation of the N-terminus of Cox2, and further work demonstrated that Oxa1 directly interacted with nascent mitochondrial polypeptide chains in a co-translational manner (Hell et al., 2001). In fact, crosslinking of Oxa1 and topological analysis to a variety of nuclear encoded inner membrane proteins further established that Oxa1 was essential for N-terminal export and its role in membrane protein biogenesis (He and Fox, 1997). Similar to Oxa1 is the chloroplast membrane protein Alb3.

Alb3 has been similarly characterized to have a role in membrane protein biogenesis through the study of its substrate light harvesting complex protein (LHCP) (Moore et al., 2000). While the biogenesis of LHCP is post-translational, it interestingly utilizes a chloroplast specific signal recognition particle. Initially, after translation termination, the polypeptide of LHCP is recognized by chloroplast SRP (cpSRP), a homologue of SRP54, (Schuenemann et al., 1998) which then targets the polypeptide to the thylakoid membrane by binding chloroplast SRP receptor (cpFtsY), a homologue of the bacterial SRP receptor FtsY (Kogata et al., 1999). Alb3 then inserts LHCP in a SecYE independent manner (Mori et al., 1999; Moore et al., 2003). This study is interesting to note as LHCP contains 3 TMD's, providing the first inkling that members of the Oxa1 superfamily may be involved in insertion of multipass membrane proteins.

1.3.4. The ER Membrane Complex (EMC)

Of the multiple members of the Oxa1 superfamily, one member of particular interest has recently been studied extensively, the ER Membrane Complex subunit 3 (EMC3). EMC3 is a member of a larger 10 protein complex known as the ER Membrane Complex (EMC). Highly

conserved in eukaryotes, this complex was first discovered in a genetic screen in yeast for ER protein homeostasis (Jonikas et al., 2009). Initial work indicated that depletion of EMC led to a variety of phenotypes ranging in a wide range of organisms (Taylor et al., 2005; Louie et al., 2013). Further work showed that EMC was necessary for synthesis and subunit assembly for a variety of membrane proteins such as rhodopsin (Satoh et al. 2012) and acetylcholine (Richard et al. 2013) among many others (Tian et al., 2019). The first study proving the direct role of EMC in membrane protein biogenesis was on post-translational tail-anchored membrane protein insertion into the ER (Guna et al., 2018). In vivo and in vitro, EMC was shown to directly handle the insertion of moderately hydrophobic tail-anchored proteins such as squalene synthase (SQS). After synthesis, SQS was shown to bind calmodulin, followed by dynamic release and insertion into the ER by EMC. Reconstitution of purified EMC in liposomes were insertion capable and demonstrated its direct ability to function as an insertase in a post-translational function.

Aside from post-translational function, EMC has also robustly been shown to have insertase activity co-translationally. Previous work had indicated that EMC was involved in the expression of rhodopsin in Drosophila but did not distinguish between effects on translation, maturation, degradation, and trafficking (Satoh et al., 2015, Xiong et al., 2020). Further work utilizing ribosome profiling hypothesized that EMC may play a role in enhancing protein stability during translation by recognizing features such as charged residues within multipass membrane protein TMD's (Shurtleff et al., 2018). Nevertheless, the mechanistic function of EMC remained elusive until recently.

Of the multiple types of membrane protein biogenesis impacted by EMC, a particular class was investigated in depth to understand the effect of EMC on protein biogenesis.

Rhodopsin is a member of the g-protein coupled receptor (GPCR) protein family. GPCRs are 7 transmembrane domain proteins that topologically contain an N_{exo} C_{cyto} topology, belonging to the Type III family of multipass membrane proteins. It has recently emerged that the critical step that EMC functions for GPCR's is the biogenesis and insertion of the first N_{exo} TMD (Chitwood et al., 2018). In fact, it appears that GPCR's have a wide range of dependence on EMC, as measured by topogenesis and biogenesis assays. Interestingly, EMC was also shown to be sufficient to insert the N_{exo} TMD of GPCR's in the absence of Sec61 while integration of the second TMD strictly required Sec61, indicating that topogenesis and biogenesis hinge upon correct insertion of the first TMD. Thus, a model for GPCR insertion emerges where EMC may insert the first TMD followed by integration of the remaining TMD's by Sec61 (**Figure 6**). It is critical to note that for those proteins that are not fully dependent on EMC, some other pathway is sufficient to insert the first TMD. While this could be Sec61, it is not fully clear and remains an unanswered question.

Lastly, EMC has been shown to be involved in the biogenesis of Type III single pass membrane proteins. Type III single pass membrane proteins contain 1 TMD, with a defining feature being a short N_{exo} head and a C_{cyto} tail. Appreciably, this is analogous to the first TMD of a GPCR (which is in fact a Type III multipass protein). The clue that there was a separate

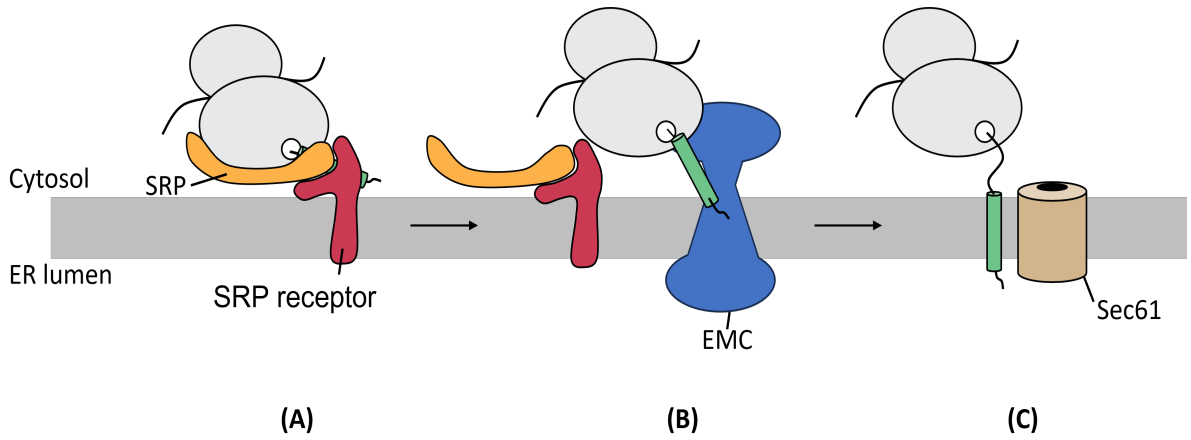

Figure 6. The ER Membrane Complex facilitates insertion of the first TMD of Type III multipass membrane proteins

(A) A ribosome translating a TMD-containing protein is targeted to the ER by SRP which then docks to its receptor.
(B) After docking, the ribosome is far enough from the membrane to allow EMC to sample the TMD. The TMD engages EMC and is then inserted into the membrane. Insertion occurs via the hydrophilic vestibule which facilitates translocation of the short N-terminus.
(C) Following insertion of the first TMD, the ribosome is brought to the membrane and docks with Sec61. The remaining TMD's of the protein are synthesized and inserted.

pathway for Type III membrane protein insertion came about when studies showed that upon addition of inhibitors that block the lateral gate of Sec61, insertion of Type III single pass membrane proteins were largely unaffected, while signal sequence and signal anchors were strongly inhibited (McKenna et al., 2017; Zong et al., 2019). Further work then showed that when EMC was depleted, various type III single pass membrane proteins were observed to be defective (O'Keefe et al., 2021). Furthermore, when Sec61 was knocked down, many of these single pass membrane proteins were still efficiently glycosylated, suggesting that EMC may be sufficient for insertion. Presumably, the mechanism of this insertion is identical to the insertion of the first TMD of a GPCR.

Recent structural work has shown that the 3 TMD's of EMC3 and 2 other TMD's of EMC form a 5 TMD hydrophilic pocket similar in nature to YidC (Bai et al., 2020; O'Donnel et al., 2020). A recent Cryo-EM structure has linked this hydrophilic vestibule to EMC's role in

both co-translational and post-translational membrane protein insertion (Pleiner et al., 2020). Highly conserved, the vestibule is positively charged and charge mutations at this interface directly affect EMC-dependent insertion of membrane proteins. Further evidence of EMC3's role in membrane protein insertion is the presence of methionine rich cytosolic loops, a feature conserved in some members of the Oxa1 superfamily and analogous to how SRP54 and Get3 interact with substrates (Borowska et al., 2015). Mutations of methionines within this loop disrupted biogenesis of both co-translational and post-translational EMC substrates, indicating that this loop may indeed play a role by interacting with the substrates. From this structure, it is postulated that EMC mediates both co- and post-translational insertion by first capturing the substrate with the methionine rich loops and guiding it to the membrane. Once within the membrane, EMC can position the hydrophilic lumenal domain in the vestibule followed by the TMD sampling the lipid bilayer. This model is attractive as it utilizes many of the conserved features of the Oxa1 superfamily. Further work will be needed to fully investigate all roles of the EMC in membrane protein biogenesis and quality control.

1.3.5. Transmembrane and coiled-coil domain 1 (TMCO1)

TMCO1, a 3 TMD membrane protein, was previously characterized as an ER load-activated calcium channel responsible for ER calcium homeostasis (Wang et al., 2016). Recent work, however, identified TMCO1 as a member of the Oxa1 superfamily via a phylogenetic search, resulting in a direct conflict with its aforementioned role as a calcium channel (Anghel et al., 2017). TMCO1 possesses many of the core structural features of the Oxa1 superfamily, with 3 TMDs, a N-in/C-out orientation, a cytosolic coiled coil, as well as a clear hydrophilic groove. In addition, TMCO1 was able to form a stable complex with the ribosome and Sec61 translocon.

This may potentially explain its previous assignment as a calcium channel as other well-characterized insertases have been known to conduct ions. Given its membership within the Oxa1 superfamily and its ability to form a stable complex with the ribosome and Sec61, it was hypothesized that TMCO1 may potentially function as an insertase or chaperone, highlighting a role in membrane protein biogenesis. Much of the work presented in this thesis will focus on the role of TMCO1 and its function.

1.4. Accessory factors of the Eukaryotic Translocon

The eukaryotic translocon is comprised of not only Sec61 but many integral membrane proteins that assemble in complexes to serve various functions in a substrate specific manner. While some of these subunits such as the Oligosaccharyl Transferase (OST) complex have well defined roles, others are poorly understood, and further study is needed to elucidate their function in membrane protein biogenesis. Here, we discuss both the more well-characterized accessory factors and ones of particular interest.

1.4.1. The Oligosaccharyl Transferase Complex (OST)

Of the various integral membrane proteins complexes that make up the translocon, the OST complex is the most characterized and possibly the most important. Comprised of 8 subunits in yeast and 7 in humans, OST catalyzes process of N-linked glycosylation, a critical post-translational modification affecting approximately 70% of secretory proteins (Zafar et al., 2011). OST is responsible for the transfer of a 14-amino acid glycan from dolichol to the asparagine in the nascent chain glycosylation sequon. This sequon is a 3 amino acid consensus sequence comprised of asparagine (N)- X- Threonine (T) where X is any amino acid (Kelleher and Gilmore, 2006). For glycosylation of this sequon to occur in membrane proteins, the

minimal distance from the TMD within the lateral gate to the sequon was shown to be approximately 12-14 amino acids and structurally derived to be approximately 6.5nm (Nilsson et al., 1993; Braunger et al., 2018)

Within metazoans, the OST complex is comprised of 2 different catalytic subunits, STT3A and STT3B. STT3A is the catalytic subunit that is responsible for co-translational glycosylation whereas STT3B is the catalytic subunit for post-translational glycosylation (Kelleher et al., 2003; Nilsson et al., 2003). It is important to differentiate the two as the STT3A subunit is known to associate with Sec61 at the translocon, while the STT3B subunit is present in the membrane, but not present at the translocon (Chavan et al., 2005; Li et al., 2008; Cherepanova et al., 2016; Shrimal et al., 2017; Braunger et al., 2018). It is hypothesized that STT3B functions as a housekeeper, glycosylating sequons that may have been skipped by STT3A as well as any proteins that are post-translationally inserted into the membrane (as they do not encounter STT3A) (Cherepanova et al., 2016).

While STT3A and STT3B are well characterized as the catalytic subunits of OST, the remaining subunits are poorly understood. It is important to note here that within the OST complex, STT3A-OST and STT3B-OST share 6 common subunits but also contain complex-specific accessory subunits. Recent structural work has implicated the common subunits of OST (Ost4, Ribophorin I, Ribophorin II, Ost48, DAD1 and TMEM258) to largely function in a stabilizing role (Pfeffer et al., 2014; Braunger et al., 2018). Of the complex-specific accessory subunits, many of these proteins function to regulate glycosylation due to the specific mechanism. For example, in the STT3B-OST complex, oxidoreductase activity of MagT1 and TUCS3 is necessary for glycosylation (Cherepanova et al., 2014). This requirement is most

likely due to the cysteine residues of MagT1 allowing disulfide bond formation between MagT1 and the glycoprotein substrate and enabling STT3B glycosylation. While the STT3A-OST complex does not contain MagT1 and TUCS3, other subunits such as DC2 and KCP2 provide a similar role in modulating interactions of STT3A to the Sec61 complex (Shrimal et al., 2017).

1.4.2. Ribosome associated membrane protein 4 (RAMP4)

RAMP4, also known as stress-associated endoplasmic reticulum protein 1 (SERP1), is a small tail-anchored protein of approximately 65 amino acids (~7 kDa) originally discovered during purification of the Sec61 complex and found to be in complex with the ribosome and Sec61 (Gorlich and Rapaport, 1993). Depletion of this protein, however, had no effect on protein translocation in vitro, leaving a puzzling question on its role within the translocon (Gorlich and Rapaport, 1993). Initial work showed that RAMP4 is able to directly crosslink to the lumenal tail of a stalled type II membrane protein and subsequent studied indicated that RAMP4 can be crosslinked to a ribosomal protein at specific lengths of a stalled substrate (Schroder et al., 1999; Pool 2009). Further work implicated RAMP4 in ER stress as addition of tunicamycin upregulated RAMP4 while deletion of RAMP4 resulted in the activation of the unfolded protein response (UPR) (Yamaguchi et al., 1999; Hori et al., 2006). Interestingly, overexpression of RAMP4 prevented aggregation and/or degradation of membrane proteins, and also facilitated subsequent glycosylation of these proteins. Curiously, another gene encoding a protein known as RAMP4-2 (SERP2) exists and possesses 88% similarity with RAMP4. Presumably a paralog of RAMP4, it has not been studied and it remains to be seen what role and function it plays within the cell. Thus, while the exact function of RAMP4 is unknown, the clear association with the

ribosome-Sec61 complex warrants further exploration of its role within the translocon and remains an interesting question worthy of further investigation.

1.4.3. Translocating chain-associating membrane protein (TRAM)

TRAM, is a multipass membrane protein first isolated as a crosslinking partner for secretory proteins that contain a signal sequence (Gorlich et al., 1992; Voight et al., 1996). Further work showed that TRAM can, in fact, be crosslinked to TMD's and that addition of TRAM stimulated translocation of soluble and membrane proteins in proteoliposomes and purified Sec61 complex (Do et al., 1996; McCormick et al., 2003). One hypothesis is that TRAM with Sec61, directly influences lipid partitioning by capturing TMD's of moderate hydrophobicity and releasing them into the bilayer (Heinrich et al., 2000). Thus, TRAM may function in response to the various hydrophilicities of TMD's and signal sequences and facilitate the entry of these hydrophobic segments into the bilayer. At the same time, however, loss-of-function studies of TRAM do not show any phenotypes in either membrane protein topology or insertion, leaving some question as to its specific role in membrane protein biogenesis (Hegde and Keenan, 2023).

1.4.4. The translocon-associated protein complex (TRAP)

The TRAP complex is a 4-unit complex comprised of three single pass membrane proteins, the a,b,d subunits and a larger, 4-TMD subunit (g) (Hartmann et al., 1993) . The TRAP complex has been shown to stoichiometrically associate with Sec61 in a 1:1 ratio and can be crosslinked to substrates at the translocon (Shibitani et al., 2005; Conti et al., 2015). Cryo-EM structures have also placed TRAP in complex with Sec61, OST, and the ribosome, indicating that it functions in a higher order complex (Pfeffer et al., 2017; Braunger et al., 2018; Gemmer et al.,

2023). The exact role of TRAP within the translocon is not fully understood. Previous studies have shown that TRAP is required for the proper translocation of certain soluble proteins, and that its dependence is the efficiency of the substrate's signal sequence role in initiating substrate translocation (Fons et al., 2003; Nguyen et al., 2018). Deletion of TRAP can lead to glycosylation defects (Ng et al., 2020), indicating that TRAP may play a role in the glycosylation of nascent chains by OST (Pfeffer et al., 2017). Recent proteomics have also implicated the role of TRAP in recognizing signal sequences with high glycine and proline content as well as signal sequences with low hydrophobicity, potentially functioning as a gatekeeper for opening of the Sec61 channel for these substrates (Nguyen et al., 2018). Furthermore, a recent Cryo-EM structure implicates the lumenal domains of TRAP in interactions with the nascent chain of translocated proteins and that TRAP may function in a chaperone-like manner (Jaskolowski et al., 2023). Lastly, for membrane proteins, some evidence indicates that TRAP may play a role in enforcing topogenesis of membrane proteins, by enforcing the "positive-inside" rule (Sommer et al., 2003).

1.4.5. Sec62 and Sec63

Like many of the eukaryotic translocon accessory factors, Sec62 and Sec63 are poorly understood members of the translocon. Topologically, Sec62 and Sec63 have 2 and 3 TMD's respectively while Sec72 is a peripheral membrane protein and Sec71 is a single pass with a C-terminal cytosolic domain. It is important to note here that Sec63 contains a lumenal Hsp40 J-domain which has been shown to activate the soluble Hsp70 chaperone, Kar2 (Brodsky et al., 1995). Previous work has shown that in yeast, Sec62 and Sec63 are able to function in conjunction with Sec61p and other factors (Sec71, Sec72, and Kar2) to post-translationally

translocate proteins with moderately hydrophobic signal sequences (DeShaies et al., 1991; Panzner et al., 1995). Deletion of any of these components adversely affects translocation and results in translocation defects in yeast (Young et al., 2001).

The mechanism of this post-translational translocation is relatively well-characterized. Initially, following termination of translation, chaperones of the Hsp70 family bind the substrate (Plath and Rapaport 2000). Substrate handoff from these Hsp70 chaperones occurs and the substrate arrives at the Sec61 complex. Sec62 and Sec61 both simultaneously then contact the signal sequence of a soluble substrate at the same time as Sec61 (Plath et al., 2004). The J-domain of Sec63 then activates the ATPase function of a HSP70 family member, Kar2, which then binds the translocating chain to prevent backwards sliding into the cytosol (Panzner et al., 1995). Furthermore, recent cryo-EM structures of the Sec61/63/71/72 complex in yeast indicate that the mechanism of this translocation occurs due to interactions between Sec63 and Sec61 that open both the lateral gate and translocation pore (Itskanov et al., 2019).

In mammals, this post-translational pathway is conserved, and recent work has shown that Sec62/Sec63 functions to translocate proteins in which the SRP is unable to efficiently target these proteins to the ER (perhaps due to their small size) (Lang et al., 2012). In mammals, however, Sec71 and Sec72 do not exist, their role is instead replaced by the protein Calmodulin (Shao and Hegde 2011). While Sec62 and Sec63 exist in the ribosome free fraction with Sec61 (Meyer et al., 2000), Sec62 has been shown to also bind the ribosome (Muller et al., 2010). This discovery has led to the possibility that these proteins thus also function in a co-translational manner.

While co-translational function of Sec62 and Sec63 is much less well understood in relation to their post-translational function but it is evident they play a role (Muller et al., 2010; Lang et al., 2012; Conti et al., 2015). In fact, very little is known about any potential mechanism and function of the role these proteins play. Previous work has shown that deletion of Sec63 definitively impaired co-translational translocation of invertase as well as leading to increased accumulation of SRP-dependent precursors (Jung et al., 2019). Recently, one study has shown that Sec62 and Sec63 are recruited to the Sec61 translocon in a substrate dependent manner (Conti et al., 2015). In essence, a stalled soluble substrate (preprolactin) with a folding domain preventing translocation was able to recruit Sec62/Sec63. Similarly, an endogenous membrane protein, prion protein with a weakly hydrophobic TM also recruited Sec62/Sec63, indicating a potential role for these proteins in co-translational membrane protein biogenesis. Interestingly, overexpression of Sec63 resulted in decreased levels of multipass membrane proteins while not affecting soluble and single pass membrane proteins (Mades et al., 2012). Furthermore, Sec62/63 can insert the C-terminal domain of membrane proteins and translocate signal anchor proteins as well as orienting the N-terminus of Type II membrane proteins (Jung et al., 2014). Given the wide variety of evidence for Sec62/Sec63 function it is clear that these proteins may play multiple roles in the cell, from co-translational to post-translational. Specifically of interest is the role that this complex may play in the biogenesis of multipass membrane proteins and further work is required to understand their exact function.

2. An ER Translocon for multi-pass membrane protein biogenesis

2.1. Overview

We previously identified TMCO1 as a eukaryotic member of the Oxa1 superfamily, whose members are linked to membrane protein biogenesis (Anghel et al., 2017). These proteins, including the EMC3 subunit of the 'ER Membrane Complex' (EMC) (Chitwood et al., 2018; Guna et al., 2018; Shurtleff et al., 2018; Volkmar et al., 2019), the Get1 subunit of the Get1/2 complex (Schuldiner et al., 2008; Mariappan et al., 2011; Wang et al., 2014), and the Oxa1/Alb3/YidC proteins (Shanmugam and Dalbey, 2019), function in different contexts as TMD insertases and/or as intramembrane chaperones to facilitate membrane protein folding and assembly (Shurtleff et al., 2018; Nagamori et al., 2004; Serdiuk et al., 2016; Klenner et al., 2008). The function of TMCO1 is not yet known, but consistent with a role in a co-translational process at the ER membrane, it can be natively isolated in association with ribosome-Sec61 complexes (Anghel et al., 2017). Here, we isolated TMCO1-ribosome complexes and utilizing mass spectrometry we were able to identify a translocon comprising multiple membrane proteins linked to quality control. Furthermore, we showed that TMCO1-bound ribosomes selectively translate multi-spanning membrane proteins, implicating TMCO1 to directly be involved in the biogenesis of membrane proteins, similar to other members of the Oxa1 superfamily.

A version of this work was published as McGilvray, P.T., Anghel, S.A., Sundaram, A.K., Zhong, F., Trnka, M.J., Fuller, J.R., Hu, H., Burlingame, A.L., and Keenan, R.J. (2020). An ER translocon for multi-pass membrane protein biogenesis eLife 9:e56889.

2.2. Contributions

In this work, I performed the construction of CRISPR cell lines and the functional analysis of TMCO1/NCLN/CCDC47 depletion on multipass substrates. A.A carried out the mass spectrometry and RNA-sequencing sample preparation. A.K.S. performed functional analysis on multipass substrates, interaction analysis of TMCO1-ribosome complexes, and RT-qPCR. RNA sequencing was performed at The University of Chicago Genomics Core Facility. Mass Spectrometry was performed at the Harvard University FAS Center for Systems Biology. R.J.K and A.A. performed the analysis of the RNA sequencing data. R.J.K. conceived the project and guided experiments.

2.3. Interaction partners of natively isolated TMCO1-ribosome complexes

To gain insight into the components of the TMCO-1 ribosome complexes we solubilized microsomes isolated from 3xFlag-TMCO1 HEK293 cells, affinity purified via the Flag tag on TMCO1, isolated the ribosome-bound fraction by sedimentation, and identified co-purifying proteins by quantitative mass spectrometry (**Figure 7A,B**). Ribosomal proteins, subunits of the Sec61 complex, and TMCO1 were enriched relative to control cells lacking the Flag tag, whereas known translocon accessory factors—including subunits of the OST and TRAP complexes, TRAM, Sec62/63 and the signal peptidase complex—were either weakly enriched or absent. We also observed strong enrichment of three poorly studied proteins: the single-pass membrane

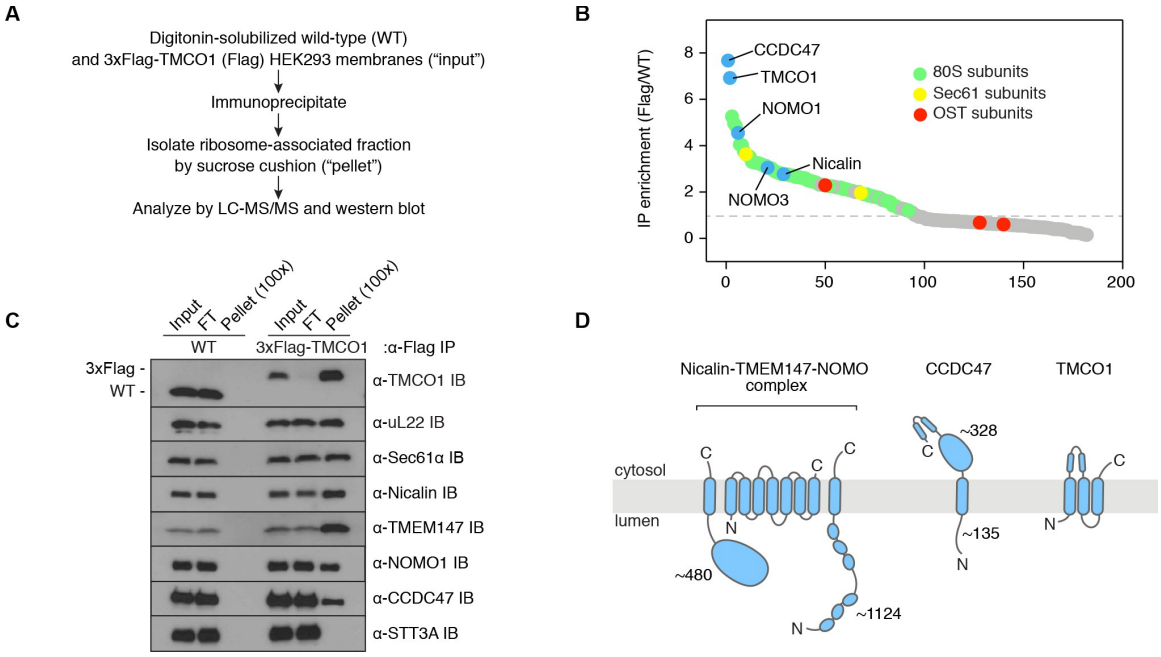

Figure 7. Natively isolated TMCO1-ribosome complexes contain multiple transmembrane components.

(A) Comparison of co-purifying components in the ribosome-bound fraction ("Pellet"), following immunoprecipitation from digitonin-solubilized microsomes isolated from HEK293 cells stably expressing 3xFlag-TMCO1 or 3xFlag-Nicalin. (B) Digitonin-solubilized microsomes from 3xFlag-TMCO1 HEK293 cells were cleared of ribosomes by sedimentation. The ribosome-free fraction ("Input") was then subjected to affinity purification using anti-Flag or anti-NOMO antibodies. Immunoprecipitation of 3xFlag-TMCO1 recovers only trace amounts of the other components, and NOMO1 immunoprecipitation fails to recover either TMCO1 or CCDC47. However, as shown previously (Dettmer et al., 2010), Nicalin is efficiently recovered by NOMO immunoprecipitation.

protein CCDC47 (calumin) and two subunits of the Nicalin-TMEM147-NOMO transmembrane complex (Dettmer et al., 2010).

We confirmed recovery of Sec61, TMCO1, Nicalin, TMEM147, NOMO and CCDC47 in the ribosome-associated fraction following 3xFlag-TMCO1 immunopreciptation (**Figure 7C,D**). Interestingly, the catalytic subunit of OST, STT3A, was not detected, consistent with the absence of OST from the TMCO1-ribosome complexes. We hypothesize that this may be due to mutual exclusion of TMCO1 and OST binding to the Sec61-ribosome complex. Affinity purification of Nicalin (via Flag tag) recovered TMCO1, CCDC47 and NOMO in the ribosome-bound fraction

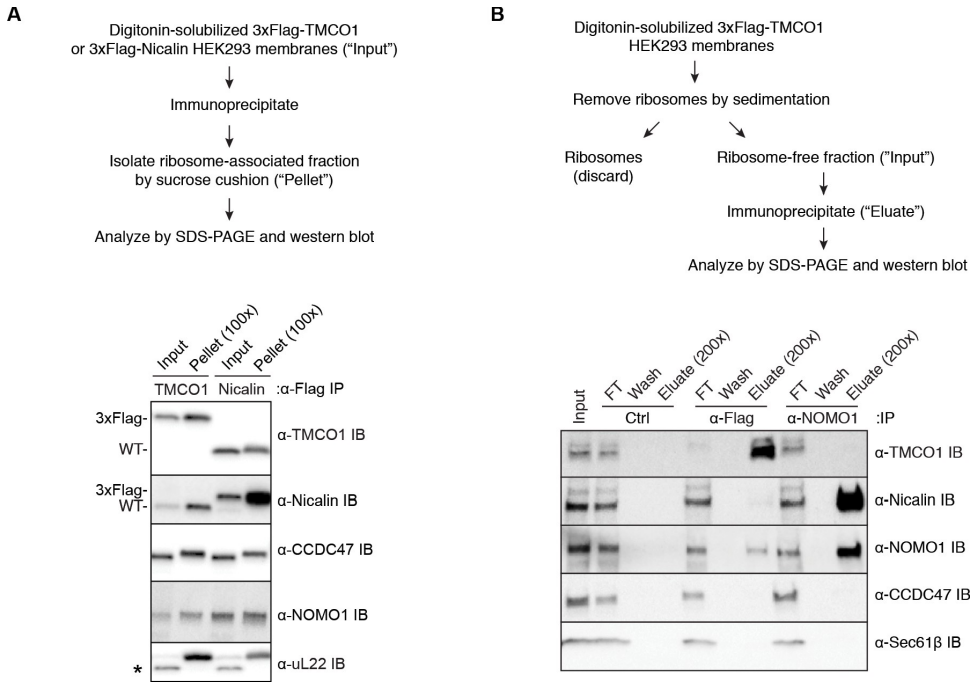

Figure 8. Additional interaction analysis of the TMCO1 translocon components.

(A) Comparison of co-purifying components in the ribosome-bound fraction ("Pellet"), following immunoprecipitation from digitonin-solubilized microsomes isolated from HEK293 cells stably expressing 3xFlag-TMCO1 or 3xFlag-Nicalin. (B) Digitonin-solubilized microsomes from 3xFlag-TMCO1 HEK293 cells were cleared of ribosomes by sedimentation. The ribosome-free fraction ("Input") was then subjected to affinity purification using anti-Flag or anti-NOMO antibodies. Immunoprecipitation of 3xFlag-TMCO1 recovers only trace amounts of the other components, and NOMO1 immunoprecipitation fails to recover either TMCO1 or CCDC47. However, as shown previously (Dettmer et al., 2010), Nicalin is efficiently recovered by NOMO immunoprecipitation.

(**Figure 8A**), indicating that these proteins can be isolated as a single, ribosome-associated complex. In the absence of ribosomes, however, only components of the Nicalin-TMEM147-NOMO complex remained intact (**Figure 8B**), suggesting that TMCO1, CCDC47 and the pre-formed Nicalin-TMEM147-NOMO complex assemble in the context of the ribosome.

CCDC47, Nicalin, TMEM147 and NOMO are abundant ER-localized proteins, conserved across eukaryotes, widely expressed in human tissues, and associated with several human diseases (Itzhak et al., 2016; Burdon et al., 2011; Sharma et al., 2012; Xin et al., 2010; Caglayan et al., 2013; Alanay et al., 2014; Li et al., 2019; Reuter et al., 2017; Morimoto et al., 2018). Although their functions remain obscure, CCDC47 has been linked to various membrane-associated processes (Morimoto et al., 2018; Zhang et al., 2007; Konno et al., 2012; Thapa et al., 2018; Yamamoto et al., 2014), and the Nicalin-TMEM147-NOMO complex has been proposed to regulate subunit assembly and localization of several cell surface receptors and ion channels (Almedom et al., 2009; Gottschalk et al., 2005; Kamat et al., 2014; Rosemond et al., 2011). More recently, all four genes were identified in a genome-wide screen for factors that impair surface expression of a mutant TRP channel (Talbot et al., 2019). That these proteins can be stably isolated with TMCO1-bound ribosome-Sec61 complexes suggests a link between these observations and a co-translational process at the ER.

Although their functions remain obscure, CCDC47 has been linked to various membrane-associated processes (Morimoto et al., 2018; Zhang et al., 2007; Konno et al., 2012; Thapa et al., 2018; Yamamoto et al., 2014), and the Nicalin-TMEM147-NOMO complex has been proposed to regulate subunit assembly and localization of several cell surface receptors and ion channels (Almedom et al., 2009; Gottschalk et al., 2005; Kamat et al., 2014; Rosemond et al., 2011). More

recently, all four genes were identified in a genome-wide screen for factors that impair surface expression of a mutant TRP channel (Talbot et al., 2019). That these proteins can be stably isolated with TMCO1-bound ribosome-Sec61 complexes suggests a link between these observations and a co-translational process at the ER.

2.4. The TMCO1 translocon functions in multi-pass membrane protein biogenesis

We sought to test this possibility by sequencing the mRNAs associated with ribosomes recovered after affinity purification via the Flag tag on TMCO1 (RIP-seq). Remarkably, we

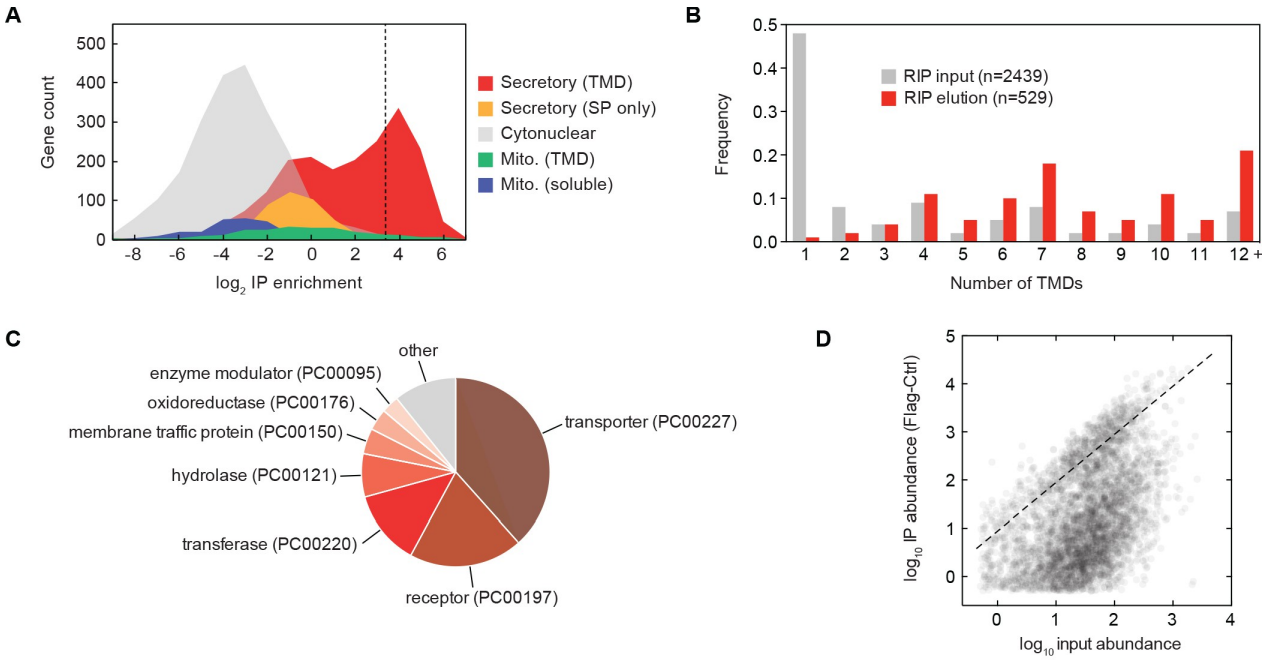

Figure 9. The TMCO1 translocon acts on multi-pass membrane proteins.

(A) Log2 enrichment of transcripts encoding proteins of the indicated categories according to Uniprot annotation. Enrichment was calculated as (Flag IP - Ctrl IP)/Input, where "Flag IP" and "Ctrl IP" are the average transcript levels in the ribosome fraction following anti-Flag immunoprecipitation from digitonin-solubilized wild-type (Ctrl) or 3xFlag-TMCO1 (Flag) HEK293 membranes (n=3), and "Input" is the average transcript abundance in the total membrane fraction (n=2). More than 98% of the most enriched transcripts (right of the dashed line) encode secretory pathway transmembrane proteins. (B) Proportion of secretory pathway transmembrane proteins containing the indicated number of Uniprot-predicted TMDs in the input (gray), and in the 529 most enriched membrane-protein encoding transcripts from the elution (red). (C) PANTHER classification for the enriched set of membrane proteins. (D) Transcript levels in the TMCO1 immunoprecipitated sample ("IP abundance") plotted against transcript levels in total HEK293 membranes ("input abundance"). Enrichment (above the dashed line) is seen across three orders of magnitude of input mRNA abundance.

observed strong enrichment for transcripts encoding secretory pathway transmembrane proteins (Figure 9A). Of these, single-pass proteins—by far the most abundant type of membrane protein in the human genome—were strongly depleted (**Figure 9B**). By contrast, transcripts encoding multi-pass membrane proteins with four or more TMDs were enriched (**Figure 9B**). These include numerous transporters, receptors, transferases and hydrolases (**Figure 9C**). Consistent with selective enrichment of TMCO1-linked transcripts, we observed enrichment across three orders of magnitude of transcript abundance in the input sample (**Figure 9D**), and this was independent of protein length (**Figure 11A**). These data directly link the TMCO1 translocon to a co-translational process involving hundreds of different multi-pass clients.

To evaluate the role of the TMCO1 translocon in biogenesis, we monitored the endogenous protein levels of the 'Excitatory amino acid transporter 1' (EAAT1; SLC1A3; GLAST-1) in HEK293 cells lacking different accessory components. EAAT1 is a member of the

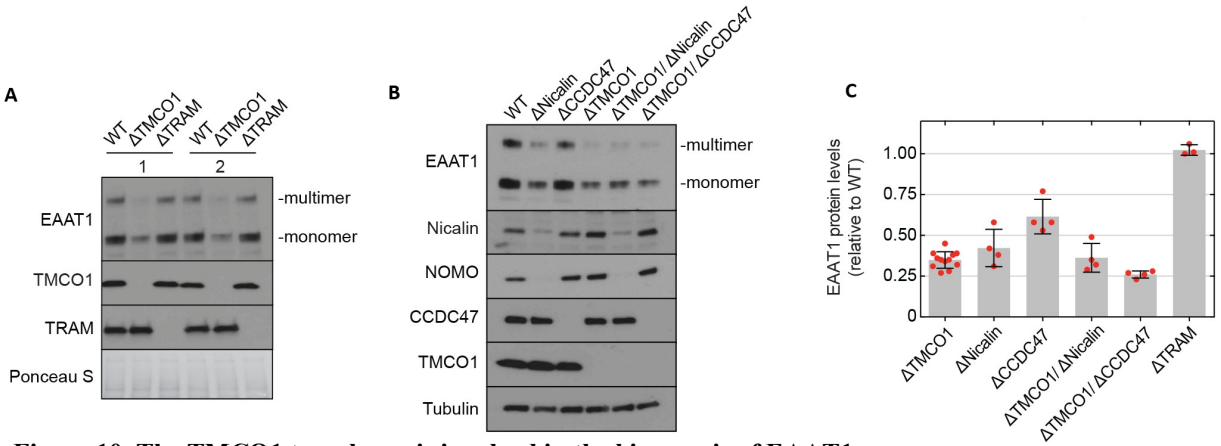

Figure 10. The TMCO1 translocon is involved in the biogenesis of EAAT1

(A) Representative western blot of total HEK293 lysate from wild-type (WT) and knockout (ΔTMCO1 and ΔTRAM) cells, in duplicate. Expression of the multi-pass membrane protein EAAT1, is decreased in the TMCO1 knockout cells, but is unaffected by deletion of the unrelated Sec61 accessory factor, TRAM. Note that the EAAT1 "multimer" band is from SDS-induced aggregation. (B) As in (A), for the indicated single- and double-knockout cells. Tubulin serves as a loading control. Note that disruption of Nicalin reduces the expression levels of its binding partner, NOMO, as shown previously (Dettmer et al., 2010). The faint band migrating just above Nicalin in the ΔNicalin cells is a cross-reacting band. (C) Quantification of protein expression levels for EAAT1 (monomer and multimer), showing mean and S.D., relative to WT cells.

large solute carrier (SLC) transporter superfamily, more than one-third of which were enriched by RIP-seq. EAAT1 functions as a homotrimer, and its structure contains multiple TMDs of marginal hydrophobicity and re-entrant helical loops on both sides of the membrane, all of which are required for function (Canul-Tec et al., 2017). Compared to wild-type cells, the steady-state expression level of EAAT1 was reduced by ~3 fold in TMCO1 knockout cells, but was unaffected in cells lacking the auxiliary translocon component TRAM (**Figure 10A**). Similar reductions were observed in Nicalin (2.4-fold), TMCO1/Nicalin (2.8-fold) and TMCO1/CCDC47 (3.8-fold) single- and double-knockout cells, while a single CCDC47 (1.6-fold) knockout showed only a modest reduction (**Figure 10A,B,C**). By contrast, the steady-state

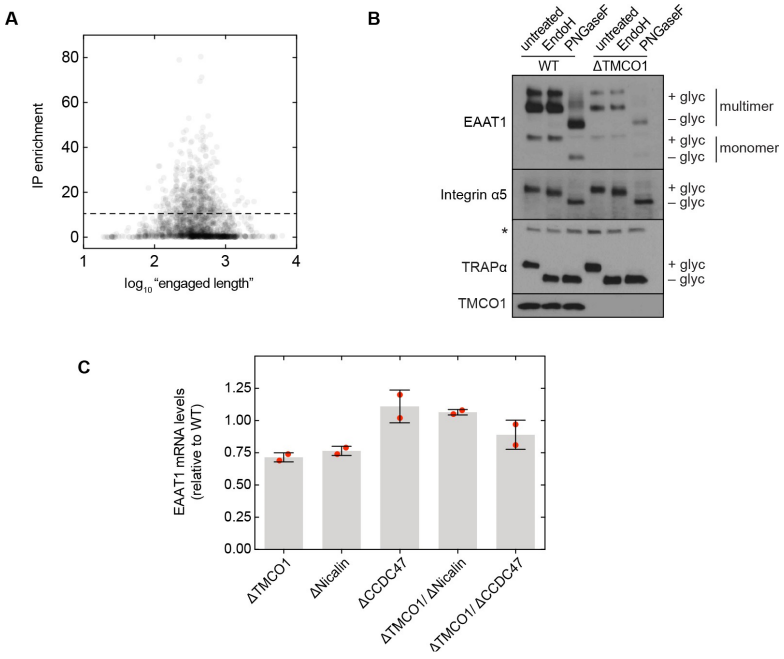

Figure 11. Additional functional analysis

(A) Plot of RIP-seq transcript enrichment ("IP enrichment") vs. protein "engaged length" for all observed secretory pathway transmembrane proteins. Here, "engaged length" is defined as the number of residues following the signal peptide or first transmembrane domain. No correlation is observed between the engaged length and enrichment. (B) Steady-state expression levels and glycosylation patterns of the multi-pass protein EAAT1, and two single-pass proteins, integrin α5 and TRAPα. EAAT1 and integrin α5 are plasma membrane proteins, and TRAPα is an ER membrane protein. The asterisk indicates a cross-reactive band. (C) Quantification of EAAT1 mRNA levels by qRT PCR analysis. GAPDH-normalized EAAT1 mRNA levels (mean, S.D.) in the indicated cell lines, relative to wild-type cells. In each case, EAAT1 mRNA levels change by less than 1.5-fold.

expression levels and glycosylation patterns of two single-pass membrane proteins, integrin α5 and TRAPα, were unchanged, demonstrating that TMCO1 disruption does not lead to a general defect in membrane protein biogenesis (**Figure 11B**). We also observed little change in EAAT1 mRNA levels in TMCO1, Nicalin and CCDC47 single- and double-knockout cells (**Figure 11C**). Together with the structural analysis, these data implicate the TMCO1 translocon in multi-pass membrane protein biogenesis.

2.5. Discussion

Our data identify TMCO1, CCDC47 and the Nicalin-TMEM147-NOMO complex as conserved components of an ER translocon that functions co-translationally with Sec61 during biogenesis of multi-pass membrane proteins. The biochemical function of the TMCO1 translocon is currently unclear. Although we do not formally exclude a role in client-specific targeting to the ER, we propose that the TMCO1 translocon functions as an insertase and intramembrane chaperone.

A general role for the TMCO1 translocon in multi-pass membrane protein biogenesis is consistent with the wide expression and conservation of its subunits, and the numerous cellular and organismal phenotypes associated with their dysfunction. In humans, TMCO1 has been linked to glaucoma (Burdon et al., 2011; Sharma et al., 2012), and loss of either TMCO1 (Xin et al., 2010; Caglayan et al., 2013; Alanay et al., 2014) or CCDC47 (Morimoto et al., 2018) causes rare autosomal recessive developmental disorders. Similarly, a mutation in TMEM147 has been linked to a rare neurodevelopmental disorder manifesting with severe intellectual disability and impaired vision (Reuter et al., 2017). Interestingly, repeated polymorphisms in the non-coding region of the TMCO1 gene lead to significant increases in risks of glaucoma as well as colorectal

cancer (Mukamel et al. 2023). Clearly, TMCO1 plays a critical role in developmental function and its loss is substantive in human physiology.

At the cellular level, disrupting TMCO1, CCDC47, Nicalin, TMEM147 or NOMO leads to reduced fitness (Wang et al., 2015). Cells lacking CCDC47 show attenuated ERAD (Yamamoto et al., 2014) and impaired Ca2+ signaling (Zhang et al., 2007; Konno et al., 2012), while the Nicalin-TMEM147-NOMO complex is linked to Nodal signaling (Haffner et al., 2004) and altered localization and subunit composition of some multi-pass membrane proteins (Almedom et al., 2009; Kamat et al., 2014; Rosemond et al., 2011). Cells lacking TMCO1 show defects in Ca2+ handling, which has led to the proposal that TMCO1 functions as a Ca2+-channel (Wang et al., 2016). Our data reconcile these different observations, which likely result from biogenesis defects in hundreds of different multi-pass proteins.

As the folding capacity of the cell must be robust to mutations and other stresses that affect folding efficiency, it is likely that other ER chaperones and accessory factors can partially compensate for loss of TMCO1 translocon components. In this regard, it will be important to define the functional relationship between the TMCO1 translocon and the ER membrane complex (EMC), each of which harbors a subunit belonging to the Oxa1 superfamily (Anghel et al., 2017) and facilitates multi-pass membrane protein biogenesis (Chitwood et al., 2018; Guna et al., 2018; Shurtleff et al., 2018; Volkmar et al., 2019; Tian et al., 2019).

3. Substrate-driven assembly of a translocon for multipass membrane proteins

3.1. Overview

We previously established that affinity purification of TMCO1 strongly enriches for ribosome-Sec61 complexes that are translating multipass membrane proteins (McGilvray et al. elife 2020). This 'multipass translocon' also contains CCDC47 and a three-protein complex comprising TMEM147, Nicalin and NOMO13 (hereafter termed the BOS complex). Using cryogenic electron microscopy, these factors were visualized behind Sec61, where the oligosaccharyl transferase complex (OST) ordinarily resides (Pfeffer et al., 2014). How the multipass translocon is recruited to this site in place of OST, why it is selective for multipass membrane proteins, and what its functions are during protein biogenesis are all poorly defined.

Here, we identify the composition, function, and assembly of a translocon specialized for multipass membrane protein biogenesis. We analysed insertion intermediates of multipass substrates to examine how features of the nascent chain trigger multipass translocon assembly. Lastly, we utilized in vitro and in vivo topogenesis and biogenesis assays to demonstrate a role for multipass translocon components in multipass membrane synthesis. These results establish the mechanism by which nascent multipass proteins selectively recruit the multipass translocon to facilitate their biogenesis. More broadly, they define the ER translocon as a dynamic assembly whose subunit composition adjusts co-translationally to accommodate the biosynthetic needs of its diverse range of substrates.

A version of this work was published as Sundaram, A.K.S., Yamsek, M., Zhong, F., Hooda, Y., Hegde, R.S., and Keenan, R.J. (2012). Substrate-driven assembly of a translocon for multipass membrane proteins. Nature 611, 167–172 (2022).

3.2. Contributions

In this work, I performed the interaction analysis in cells, in vitro analyses for substrate recruitment, and flow cytometry experiments. A.K.S. performed interaction analysis in cells and in vitro analyses for substrate recruitment and glycosylation assays. M.Y. performed in vitro analyses for substrate recruitment and glycosylation assays as well as the cell-based glycosylation assays. Y.H. contributed to the flow cytometry assays. R.S.H. and R.J.K. provided funding and guidance. R.J.K. conceived the study and wrote the manuscript with input from all authors.

3.3. Organization of the multipass translocon

As previously shown, affinity purification of epitope-tagged TMCO1 from cells co-purified ribosomes that contained the Sec61 complex, CCDC47, and the BOS complex (**Figure 12a,b**) (McGilvray et al., 2020). These ribosomes also contained Asterix, the partner of CCDC47 in the recently defined "protein associated with translocon" (PAT) complex (Meacock et al., 2002; Chitwood et al., 2020), and C20Orf24, a recently hypothesized binding partner of TMCO1 (Lewis and Hegde 2021). Like the PAT and BOS complex subunits, TMCO1 and C20Orf24 were mutually dependent on each other, so we named the latter OPTI for "obligate partner of TMCO1 insertase" (**Figure 12b and Figure 13a**). OPTI is homologous to Get2 and EMC6, binding partners of the Oxa1 superfamily members Get1 and EMC3, respectively (Bai et al., 2020; McDowell et al., 2020; Pleiner et al., 2020; O'Donnel et al., 2020; Lewis and Hegde

2021). TMCO1 and OPTI are hereafter termed the GEL complex for “GET- and EMC-like” (**Figure 13b**).

TMCO1-purified ribosomes contained the TRAP complex but did not contain OST (**Figure 12b**). This is consistent with the observation that the PAT, GEL, and BOS complexes occupy positions that overlap with OST, but on a different side of Sec61 than the TRAP complex (Pfeffer et al., 2014; McGilvray et al., 2020). Affinity purification via tagged subunits of the PAT or BOS complexes similarly recovered ribosomes that contain the PAT, GEL, BOS, Sec61, and TRAP complexes, but not OST. Strikingly, the co-purification of all of these complexes is only seen in the ribosome fraction, with little or no association observed in the ribosome-free fraction (**Figure 12b**). Although the subunits within each multipass translocon complex are mutually dependent on each other, loss of any one complex does not impact the overall abundance of the others (**Figure 12c**). However, because they make (limited) contact with each other at the translocon (**Figure 13b**), recruitment of each complex to the ribosome is partially

dependent on the other two, as discussed later. Thus, the multipass translocon contains the PAT, GEL, and BOS complexes co-assembled on ribosomes containing the Sec61 and TRAP complexes, but lacking OST (**Figure 12d**). Earlier work analyzing ER membranes engaged in protein secretion defined a "core translocon" containing only the Sec61 and TRAP complexes, and a "secretory translocon" that additionally contains the OST complex (Pfeffer et al., 2014).

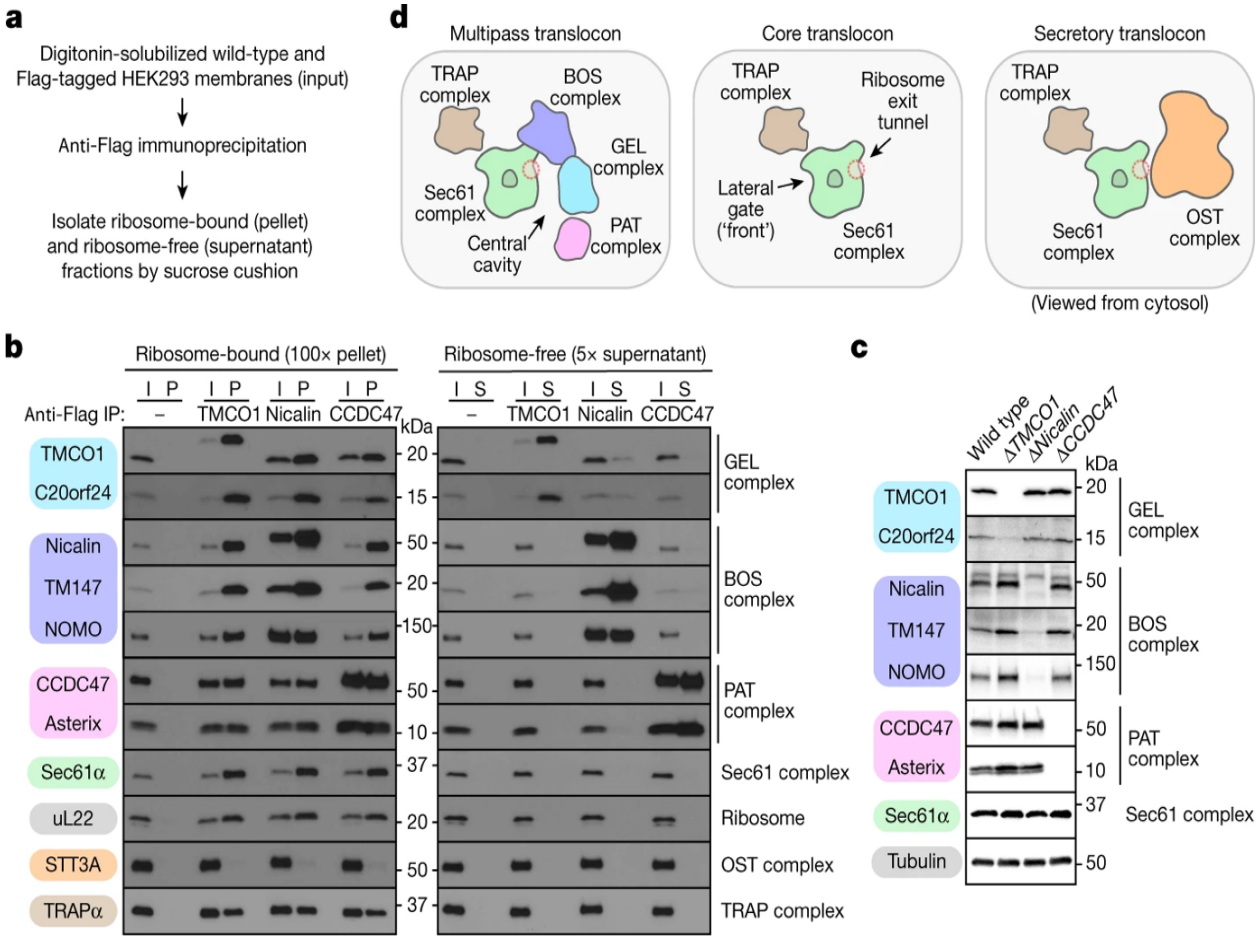

Figure 12. The multipass translocon is distinguished by three obligate heterocomplexes.

(a) Experimental strategy. Nuclease-treated membranes from wild-type or stably integrated Flag-tagged (TMCO1, Nicalin (also known as NCLN) and CCDC47) HEK293 cells were digitonin-solubilized, immunoprecipitated and sedimented through a sucrose cushion to isolate the ribosome-bound and ribosome-free fractions for analysis. (b) Analysis of input (I), ribosome-bound (pellet (P)) and ribosome-free (supernatant (S)) fractions by SDS–PAGE and immunoblotting. uL22 and STT3A are used here as markers for the ribosome and OST, respectively. IP, immunoprecipitation. (c) Whole-cell lysates from the indicated wild-type and knockout HEK293 cell lines were analysed by SDS–PAGE and immunoblotting. (d) Subunit organization and key architectural features of the compositionally distinct multipass, core and secretory translocons, viewed from the cytosol.

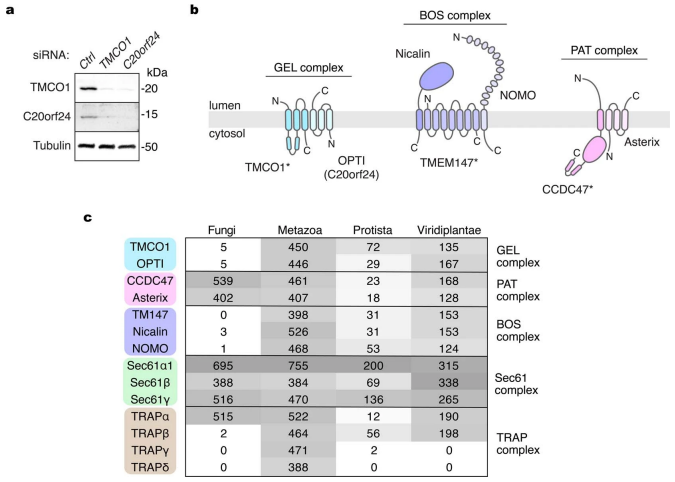

Figure 13. Three obligate complexes of the multipass translocon.

(a) Whole cell lysates from siRNA depleted HEK293 cells were analysed by SDS-PAGE and immunoblotting; 'Ctrl' is a non-targeting control siRNA. (b) Nomenclature, subunit topology and number of transmembrane domains for three obligate heterocomplexes of the multipass translocon. Subunits that directly contact the ribosome in the assembled state are indicated with an asterisk. Within the translocon, CCDC47 and TMEM147 contact different regions of Sec61, while interactions between the PAT, GEL and BOS complexes are limited to small portions of TMCO1 that contact CCDC47, TMEM147 and Nicalin. (c) Distribution of the multipass translocon components in eukaryotes (OrthoDB v10.1).

3.4. The multipass translocon assembles in response to defined signals

To understand the relationship between these translocons, we analysed a series of translocation intermediates assembled at ER membranes by in vitro translation (**Figure 14a**). Both early and late intermediates of the single-spanning membrane protein ASGR1 were associated with the secretory translocon, but not the multipass translocon (**Figure 14b**). The five-

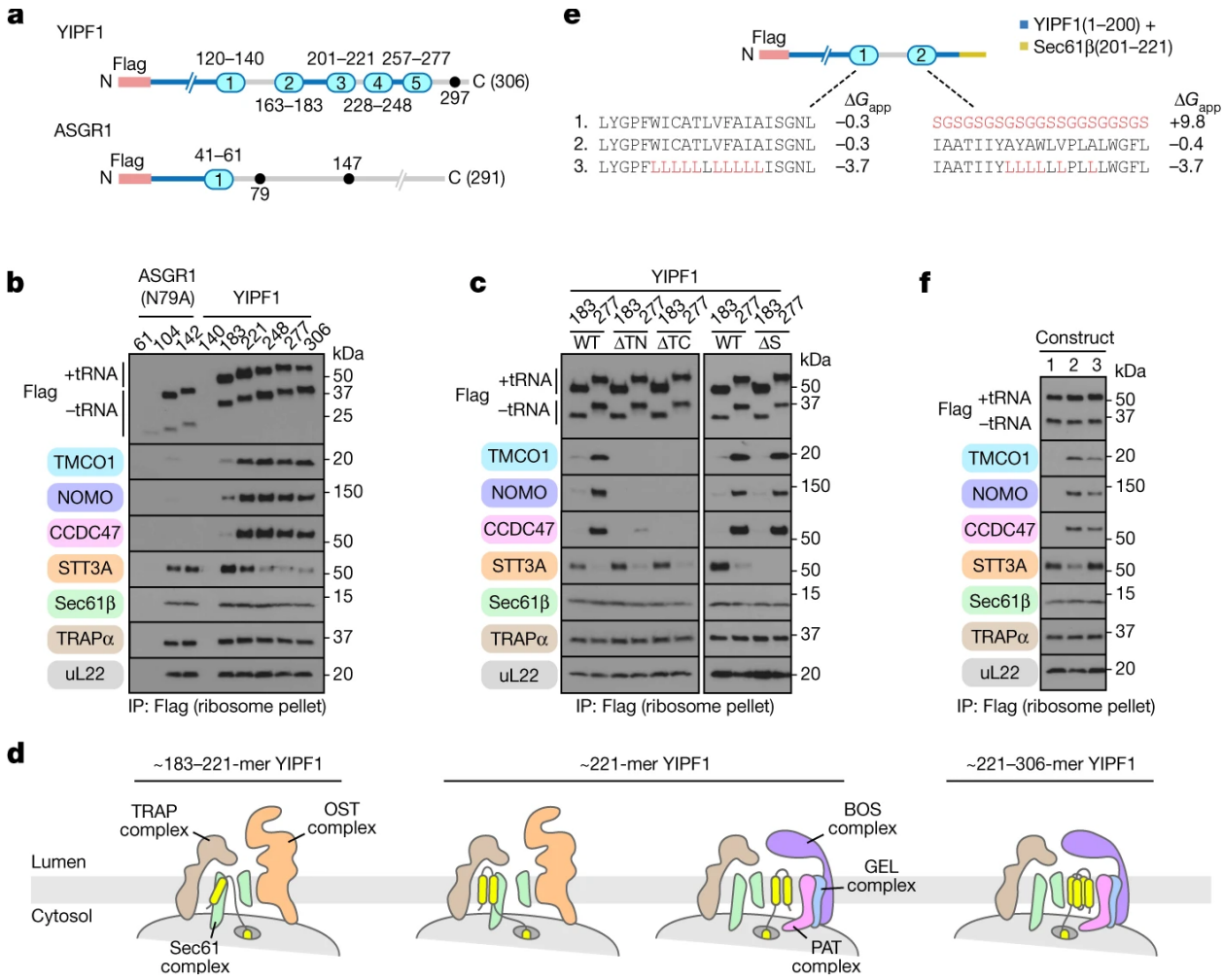

Figure 14. Substrate-directed assembly of the multipass translocon.

(a) Templates used to generate truncated, Flag-tagged constructs for affinity purification of stalled (no stop codon) ribosome–nascent chain complexes. All stalled intermediates are appended with Met-Leu-Lys-Val. Luminal loops (grey) and native N-glycosylation acceptor sites (black circles) are indicated. (b) Stalled, Flag-tagged ASGR1(N79A) and YIPF1 constructs truncated at the indicated positions were translated in rabbit reticulocyte lysate (RRL) in the presence of wild-type HEK293 rough microsomes, and the membrane-associated fraction was isolated by sedimentation. Following anti-Flag immunoprecipitation of the digitonin-solubilized membranes, stalled ribosome–nascent chain complexes were isolated by sedimentation and analysed by SDS–PAGE and immunoblotting. Note the earliest intermediates (ASGR1 61-mer and YIPF1 140-mer) do not target to the membrane as their first TMD remains buried inside the ribosome exit tunnel, thus serving as a control for nonspecific binding. (c) Stalled, Flag-tagged YIPF1 constructs truncated at positions 183 and 277 were translated in RRL in the presence of wild-type (WT), double-knockout (TMCO1/Nicalin (ΔTN) and TMCO1/CCDC47 (ΔTC)) or STT3A-knockout (ΔS) rough microsomes, and analysed as in b. (d) Diagram of translocon composition at different stages of YIPF1 synthesis, based on data in b,c. (e), Series of two-TMD YIPF1 templates containing different TMD1 and TMD2 sequences. The calculated apparent free energy of membrane insertion48 (ΔGapp) for each TMD is indicated. (f) Stalled, Flag-tagged YIPF1 constructs as in e were analysed as in b; quantification for n = 5 biological replicates is shown in Extended Data Fig. 4b.

TMD protein YIPF1 (Shakoori et al., 2003), chosen because its mRNA is enriched with the affinity-purified multipass translocon, behaved differently. Although early intermediates of YIPF1 contained the secretory translocon, this was markedly reduced with concomitant gain of multipass complexes at later stages (**Figure 14b**). A similar result was observed using a series of intermediates of the eight-TMD protein TRAM2 (**Figure 15a,b**). The key step when this switch begins corresponds to the point when two TMDs have been membrane inserted and the third is inside the ribosome exit tunnel. Thus, OST is exchanged for the PAT, GEL and BOS complexes

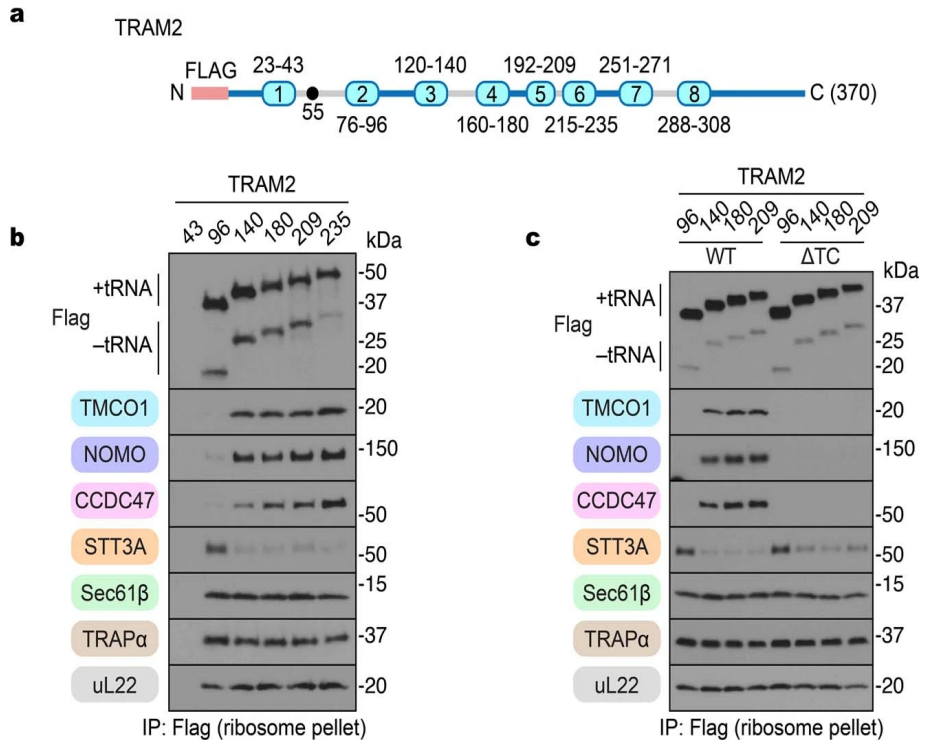

Figure 15. Translocon dynamics during TRAM2 synthesis

(a) Template used to generate truncated, Flag-tagged TRAM2 constructs, as in Fig. 2A. (b) Stalled, Flag-tagged TRAM2 constructs truncated at the indicated positions were analysed as in Fig. 2B. Note that the 140-mer intermediate (and beyond) is glycosylated at position 55. (c) Stalled, Flag-tagged TRAM2 constructs truncated at the indicated positions were translated in RRL in the presence of WT and double knockout (TMCO1/CCDC47, 'ΔTC') rough microsomes, and analysed as in (b).

specifically at the point when the substrate can be minimally defined as a multipass membrane protein.

Unexpectedly, the PAT, GEL and BOS complexes were not required for substrate-triggered displacement of OST from the translocon. Even in ER membranes lacking the complexes, OST was effectively displaced by YIPF1 and TRAM2 intermediates with at least two membrane-inserted TMDs (**Figure 14c and Figure 15c**). These results indicate that the presence of multiple TMDs in the membrane impairs OST binding to its site behind Sec61. This might be explained by a shift in the position of the inserted TMDs relative to Sec61 (Sadlish et al., 2005). Notably, the ribosome exit tunnel is offset from the central channel of Sec61 towards its back side **(Figure 12d**). As a consequence, an insertion intermediate ending with a TMD whose N terminus faces the lumen (N(exo)) TMD and a 30–40-amino-acid downstream tether to the truncation point might favour the back side of Sec61 due to tension in the nascent chain (**Figure 14d**). If such a TMD associates with preceding TMDs (such as TMDs linked by short loops), the presence of multiple TMDs behind Sec61 would hinder OST binding.

Consistent with this idea, an earlier structural analysis provisionally assigned an N(exo) TMD (followed by a 32-amino-acid tether) to a site behind Sec61 adjacent to OST (Braunger et al., 2018). As additional TMDs cannot be accommodated at the OST–Sec61 interface, a multipass insertion intermediate ending in this TMD–tether configuration would not be compatible with OST binding. However, the multipass complexes would be able to bind such an intermediate because there is more space between Sec61 and the multipass components3 (**Figure 12d**). Indeed, structural and photocrosslinking analysis of a rhodopsin intermediate with three membrane-inserted TMDs in the multipass translocon revealed the third TMD in its N(exo)

topology behind Sec61 and connected to the downstream tether inside the ribosome exit tunnel (see Smalintskie et al., 2023). YIPF1 and TRAM2 intermediates with two membrane-inserted TMDs are probably in the same configuration, albeit with one fewer N-terminal TMD.

Similar behaviour was observed with KDELR1, a seven-TMD N(exo) protein with the opposite topology to YIPF1 and TRAM2, whose N termini face the cytosol (N(cyt)) (**Figure 16a**). The first targeted intermediate of KDELR1 engaged the core translocon (Extended Data **Figure 16b**). Further elongation resulted in a mixture of secretory and multipass translocons until TMD2 and TMD3 were inserted. At this point, OST binding was reduced, with a concomitant increase in recruitment of the multipass components. OST displacement was largely independent of the multipass components (**Figure 16c**). Thus, N(cyt) and N(exo) substrates trigger displacement of OST from the translocon by a similar mechanism, except offset by one TMD.

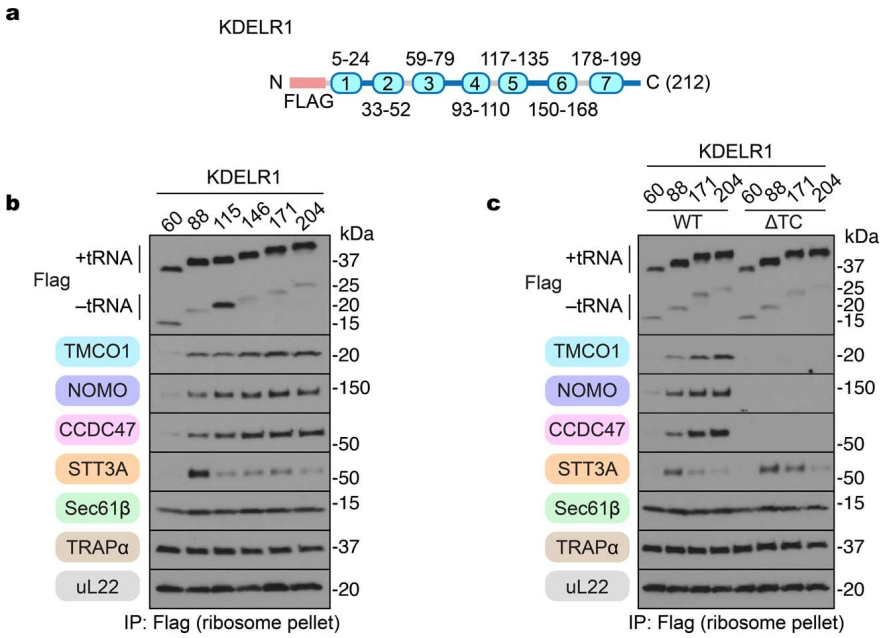

Figure 16. Translocon dynamics during KDELR1 synthesis.

(a) Template used to generate truncated, Flag-tagged KDELR1 constructs, as in Fig. 2a. (b) Stalled, Flag-tagged KDELR1 constructs truncated at the indicated positions were analysed as in Fig. 2b. (c) Stalled, Flag-tagged KDELR1 constructs truncated at the indicated positions were translated in RRL in the presence of WT and double knockout (TMCO1/CCDC47, 'ΔTC') rough microsomes, and analysed as in (b).

Surprisingly, displacement of OST was insufficient for assembly of the multipass translocon, because an early YIPF1 intermediate did not recruit the multipass components even in ER membranes lacking OST (**Figure 14c**). To further define the trigger(s) for multipass translocon assembly, we analysed variants of the minimal recruitment intermediate containing only the first two TMDs of YIPF1 followed by a 42-amino-acid downstream tether (**Figure 14e**). At this length, a mixture of secretory and multipass translocons are observed, making it a sensitive reporter of changes to this balance. The second TMD proved to be strictly required because its replacement with a hydrophilic linker abolished multipass translocon assembly (**Figure 14f**). Conversely, introducing TMD2 of YIPF1 downstream of the native ASGR1 TMD was sufficient to trigger recruitment of the multipass translocon complexes (**Figure 17a**). In the

two-TMD YIPF1 intermediate, increasing the hydrophobicity of both TMDs slightly (but reproducibly) reduced multipass translocon assembly in favour of secretory translocon retention (**Figure 14f and Figure 17b**). This is consistent with the finding that TMD hydrophilicity is a key requirement for interaction with the PAT complex (Chitwood et al., 2020), and perhaps other multipass translocon components. Thus, a shift in translocon composition can be triggered in two non-mutually exclusive ways: accumulation of multiple TMDs behind Sec61 to disfavour OST binding and direct TMD engagement of the multipass complexes to favour their recruitment and retention.

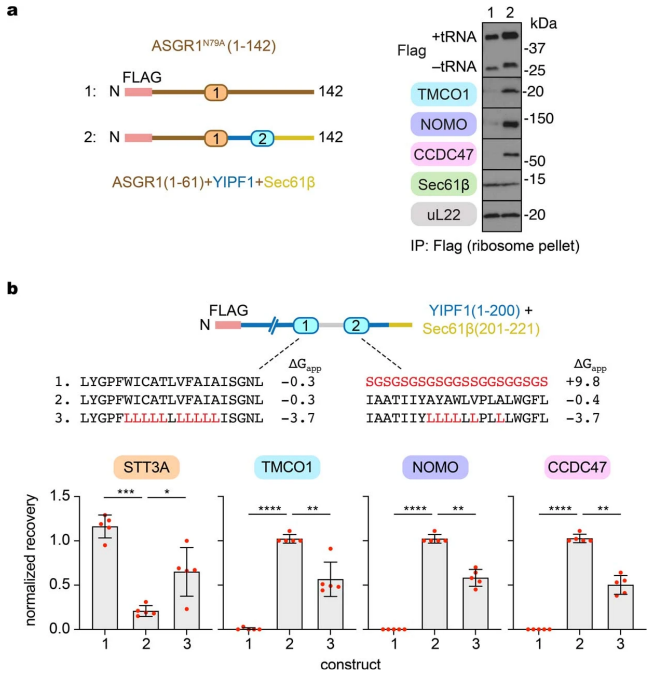

Figure 17. Additional characterization of substrate features that direct assembly of the multipass translocon.

(a) The indicated ASGR1-derived intermediates were translated in RRL in the presence of wild-type HEK293 rough microsomes, and the membrane-associated fraction was isolated by sedimentation. Following anti-Flag immunoprecipitation of the digitonin-solubilized membranes, stalled RNCs were isolated by sedimentation and analysed by SDS-PAGE and immunoblotting. (b) Quantification of STT3A, TMCO1, CCDC47 and NOMO recruitment to stalled 2-TMD YIPF1 constructs as in Fig. 2f, for n = 5 biological replicates. Data are mean ± S.D. Analysis was performed using an RM one-way ANOVA with the Geisser-Greenhouse correction and Tukey's multiple comparisons test as implemented in GraphPad Prism 9.4.0. *, $p < 0.0332$; **, $p < 0.0021$; ***, $p < 0.0002$; ****, $p < 0.0001$.

3.5. The translocon is dynamic and responsive to the needs of substrates

Although most co-translationally modified glycosylation sites in multipass membrane proteins occur early, at a point when OST would still be at the translocon, at least some sites occur in long loops translocated after multiple TMDs have been inserted (Cherepenova et al., 2019). These loops presumably begin translocating through the Sec61 complex when the preceding TMD engages the lateral gate of Sec61 in the N(cyt) orientation. To test whether internal loop translocation occurs at the secretory translocon, we analysed biogenesis intermediates of EAAT1, an eight-TMD protein (Canul-Tec et al., 2017) with a glycosylated luminal loop after TMD3 (**Figure 18a**). As with YIPF1 and TRAM2, the earliest targeted insertion intermediate is part of the secretory translocon, after which OST is displaced when TMD2 is inserted (**Figure 18b**). This EAAT1 153-mer intermediate is largely associated with the core translocon presumably because its tether length or TMD hydrophobicity limits binding to the multipass components. With elongation to a point when TMD3 has emerged from the ribosome exit tunnel, a mixture of secretory and multipass translocons are observed. Notably, the reappearance of OST at the translocon coincides with the onset of glycosylation (**Figure 18b**). At later lengths OST again departs, concomitant with increased recruitment of the multipass translocon components (**Figure 18b**). At each point, OST displacement occurs independently of the multipass components (**Figure 18c**). We posit that TMD3 engagement of the lateral gate favours repositioning of the preceding TMDs to the front side of Sec61, allowing OST to rebind at the back side (**Figure 18d**). Thus, translocon subunit composition is responsive to the nascent chain and is influenced by both the positions (relative to Sec61) and interactions of preceding TMDs.

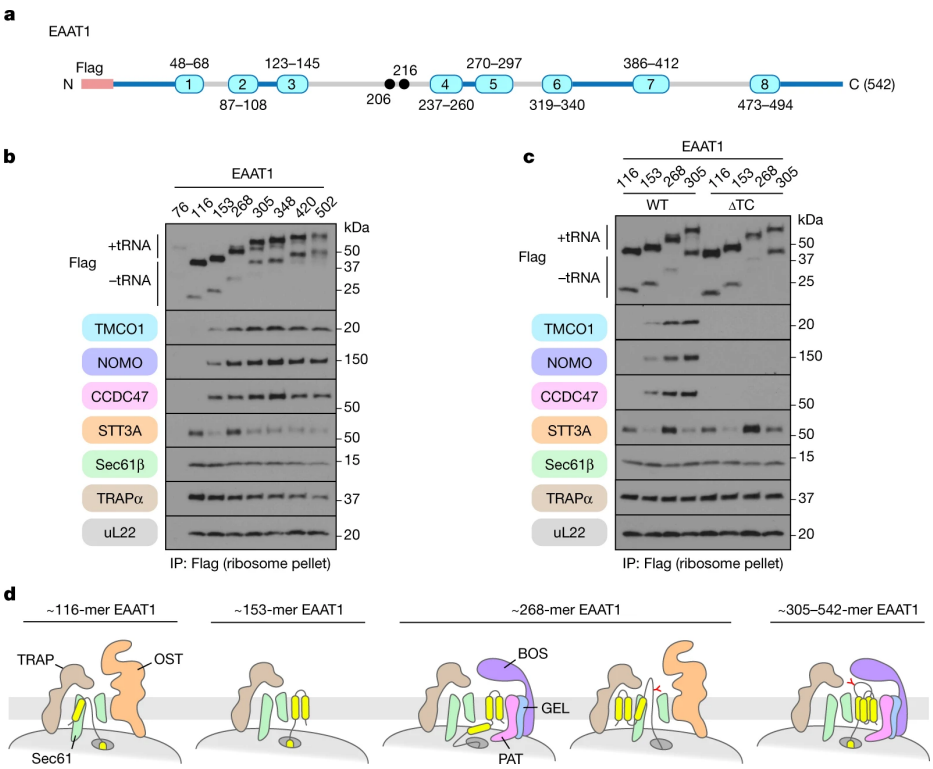

Figure 18. Internal loop translocation at the secretory translocon.

(a) The template used to generate truncated, Flag-tagged EAAT1 constructs, as in Fig. 2A. (b) Stalled, Flag-tagged EAAT1 constructs truncated at the indicated positions were analysed as in Fig. 2B. The appearance of additional EAAT1 bands in later intermediates (EAAT1(268) onwards) is due to glycosylation in the TM3–TM4 luminal loop. (c), Stalled, Flag-tagged EAAT1 constructs truncated at the indicated positions were translated in RRL in the presence of wild-type and double-knockout (TMCO1/CCDC47 (ΔTC)) rough microsomes, and analysed as in b. (d) Diagram of translocon composition at different stages of EAAT1 synthesis, based on data in B,C. Glycosylation of the EAAT1 acceptor site(s) is indicated.

3.6. The multipass translocon facilitates the biogenesis of multipass membrane proteins

To analyse the consequence of multipass translocon assembly for membrane protein biogenesis, we examined the insertion of YIPF1. The single N-linked glycosylation site in this substrate is close to the carboxy terminus and is necessarily modified post-translationally (**Figure 19a**). It therefore serves as a reporter of topogenesis errors occurring anywhere preceding it. The fraction of glycosylated YIPF1 was substantially reduced when it was inserted into ΔTMCO1 microsomes compared to microsomes from wild-type cells (**Figure 19b**). Notably, equal percentages of YIPF1 were recovered from these two reactions after carbonate

extraction, indicating comparable levels of membrane insertion. As glycosylation itself is unimpaired in these microsomes (see below), the defect in YIPF1 glycosylation is likely to be a consequence of altered topology. Consistent with this idea, protease protection analysis of YIPF1 showed a reduction of around 40% of protected fragments in ΔTMCO1 microsomes (**Figure 19c**).

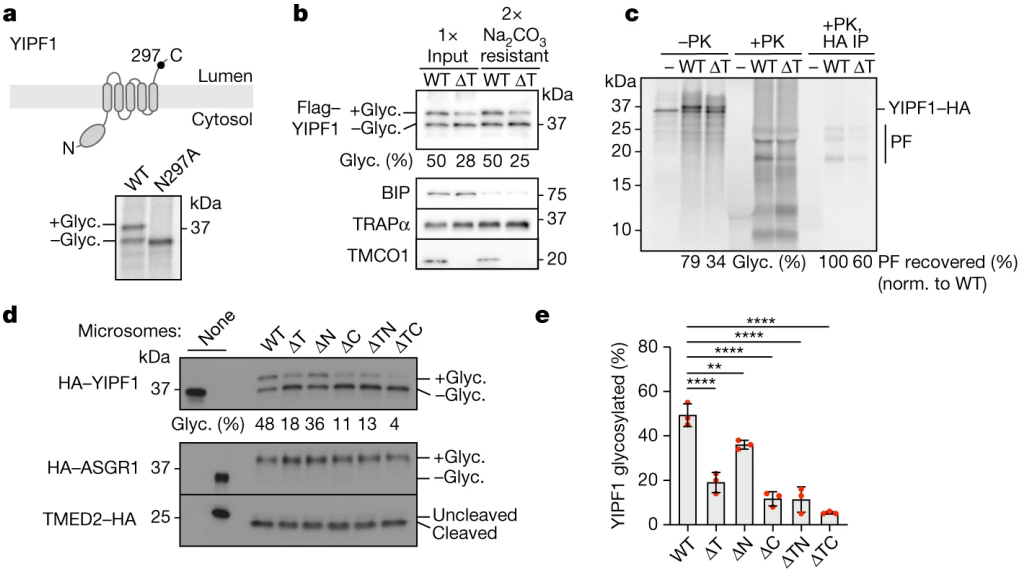

Figure 19. Multipass-translocon-dependent topogenesis in vitro

(a) Top: YIPF1 harbours a single N-glycosylation site (black circle) near its C terminus. Bottom: [35S]methionine-labelled wild-type and mutant (N297A) YIPF1 were translated in RRL in the presence of rough microsomes, isolated by sedimentation, and analysed by autoradiography. (b) Flag–YIPF1 was translated in RRL with wild-type or TMCO1-knockout (ΔT) rough microsomes, isolated by sedimentation, and analysed either directly (input) or after alkaline sodium carbonate extraction. YIPF1, TMCO1, BIP (ER luminal) and TRAPα (ER integral) were visualized by immunoblotting. The proportion of glycosylated (Glyc.) YIPF1 is indicated. (c) [35S]methionine-labelled, C-terminally haemagglutinin (HA)-tagged YIPF1 was translated in RRL with wild-type or ΔT rough microsomes, isolated by sedimentation, and analysed by autoradiography before (−PK) or after (+PK) proteinase K treatment. The PK-treated sample was also analysed after immunoprecipitation using the HA tag. Full-length YIPF1–HA, its protease-protected fragments (PF), and the proportion of recovered PF are indicated. (d) HA–YIPF1, HA–ASGR1 and TMED2–HA were translated in RRL with wild-type, single-knockout (TMCO1 (ΔT), Nicalin, (ΔN) or CCDC47 (ΔC)) or double-knockout (TMCO1/Nicalin (ΔTN) or TMCO1/CCDC47 (ΔTC)) rough microsomes, isolated by sedimentation, and analysed by immunoblotting. (e) Quantification of YIPF1 glycosylation for n = 3 biological replicates, as in D. The data are shown as the mean ± s.d.

Using glycosylation as a proxy for proper YIPF1 topogenesis, we observed similarly strong defects in microsomes lacking the PAT, GEL or BOS complexes, and even stronger effects in double-knockout microsomes (**Figure 19d,e**). The YIPF1 defects could not be overcome by adding more microsomes to the reaction, consistent with an intrinsic biogenesis

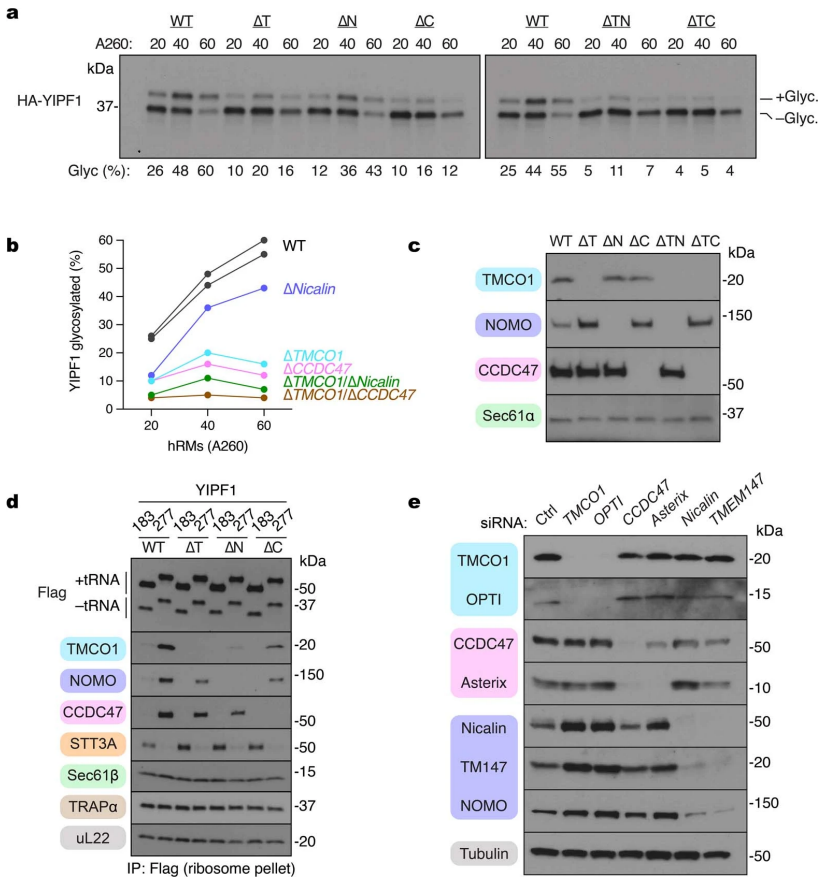

Figure 20. Additional characterization of the in vitro system and validation of siRNA knockdowns.

(a) HA-YIPF1 was translated in RRL in the presence of WT, single- (TMCO1, ΔT; Nicalin, ΔN; CCDC47, ΔC) or double-knockout (TMCO1/Nicalin, ΔTN; TMCO1/CCDC47, ΔTC) rough microsomes at different concentrations (determined by absorbance at 260 nm), isolated by sedimentation, and analysed by SDS-PAGE and immunoblotting. The percentage of glycosylated YIPF1 is indicated below the gel. (b) Plot of the data in (A). (c) Membranes prepared from the indicated wild-type, single- or double-knockout HEK293 cell lines were analysed by SDS-PAGE and immunoblotting. (d) Stalled, Flag-tagged YIPF1 constructs truncated at position 183 and 277 were translated in RRL in the presence of wild-type (WT) or single knockout rough microsomes, and the membrane-associated fraction was isolated by sedimentation. Following anti-Flag immunoprecipitation of the digitonin-solubilized membranes, stalled RNCs were isolated by sedimentation and analysed by SDS-PAGE and immunoblotting. (e) Whole cell lysates from HEK293 cells treated with the indicated siRNAs were analysed by SDS-PAGE and immunoblotting; 'Ctrl' is a non-targeting control siRNA.

defect (**Figure 20a,b**). ASGR1 biogenesis (as judged by glycosylation) and translocation of another single-spanning membrane protein TMED2 (as judged by signal peptide cleavage) were unaffected in the same set of knockout microsomes (**Figure 19d**). Thus, loss of the multipass translocon components impairs YIPF1 topogenesis without affecting SRP-dependent targeting, Sec61-mediated translocation and insertion, OST-mediated glycosylation or signal peptidase-dependent signal peptide cleavage. It is noteworthy that loss of any one multipass translocon complex reduces ribosome recruitment of the others (**Figure 20d**). For this reason, it is difficult from these data to assign the YIPF1 topogenesis defect to any one factor. Nonetheless, it is clear that the multipass translocon is functionally important for biogenesis of the multipass protein YIPF1.

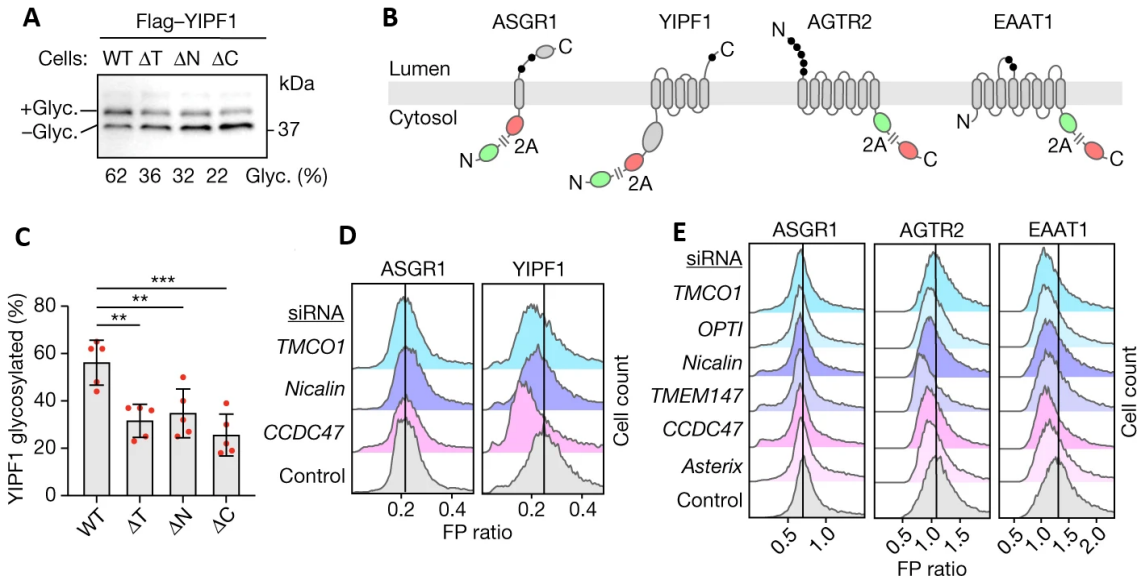

Figure 21. Multipass-translocon is required for optimal topogenesis and biogenesis in cells

(a) Flag-YIPF1 was transiently transfected into wild-type or knockout cells, and total lysates were analysed by immunoblotting. (b), Quantification of YIPF1 glycosylation for n = 5 biological replicates. The data are shown as the mean ± s.d. (c), Reporter constructs to monitor protein stability in cells. (d,e) Stably integrated HEK293 reporter lines were treated with the indicated short interfering RNA (siRNAs), induced with doxycycline, and analysed by flow cytometry. The histograms show FP ratios for each siRNA–reporter pair; the vertical black line indicates the mode of the control population.

Analysis of YIPF1 in cultured cells showed glycosylation defects in multipass translocon mutants similar to the in vitro results, indicating similar topogenesis defects in both systems (**Figure 21a,b**). The consequence of this defect is promiscuous degradation of YIPF1 tagged with red fluorescent protein (RFP) as determined using a flow cytometry assay (**Figure 21c**). In this setup, RFP–YIPF1 is translated in tandem with green fluorescent protein (GFP) but separated by the ribosome-skipping viral 2A sequence. Instability of newly made YIPF1 can be monitored as a reduction in RFP signal relative to the signal from GFP, which is necessarily translated at equal levels. The fluorescence ratio for the YIPF1 reporter was reduced in cells on knockdown of genes encoding components of the PAT, GEL or BOS complexes, consistent with impaired biogenesis (**Figure 21d**). A similar effect was seen for reporters of two unrelated multipass membrane proteins (EAAT1 and the G-protein-coupled receptor AGTR2), but not for ASGR1 (**Figure 21e**). Thus, the multipass translocon is not only recruited to nascent multipass membrane proteins as monitored in vitro, but also facilitates their biogenesis in cells.

3.7. Discussion

We have defined the modular composition of the multipass translocon, established its role in multipass protein topogenesis, and revealed how nascent substrates drive translocon remodelling to facilitate their successful maturation. The multipass translocon components are most broadly distributed in metazoans. This mirrors the marked increase in membrane proteome complexity that accompanied evolution of multicellular organisms (Attwood et al., 2017). The most notable example of this expansion is seen with the seven-TMD G-protein-coupled receptors, with about nine hundred family members encoded in the human genome but only three

in Saccharomyces cerevisiae (Frederiksson et al., 2005). The multipass translocon may have evolved to increase the efficiency of multipass protein biogenesis, particularly in metazoans.

Demand for multipass protein synthesis in other organisms might be satisfied by more broadly conserved components of the biogenesis machinery. In eukaryotes lacking some or all of the multipass components, the widely conserved EMC31 may play a more central role in multipass protein biogenesis (Chitwood et al., 2018; Shurtleff et al., 2018; Tian et al. 2019). Fungi, which lack recognizable homologues of the GEL and BOS complexes, may use their conserved PAT complex components during multipass protein synthesis at Sec61. Prokaryotes lack PAT and BOS components, but GEL complex homologues in archaea (Borowska et al., 2015; Lewis and Hegde, 2021) and the Oxa1 superfamily insertase YidC (Zhu et al., 2013; Serdiuk et al., 2019) in bacteria may facilitate multipass protein biogenesis with SecY. In other cases, the TMD chaperone and insertase functions of the multipass components may be encoded by still unknown membrane factors.

Accommodating the diversity of secretory and membrane proteins during biogenesis requires the ER translocon to coordinate multiple transmembrane factors that operate on the nascent chain. These factors include TRAM family members (Gorlich et al., 1992; Voight et al., 1996), RAMP4 (Gorlich and Rapaport, 1993; Pool et al., 2009), signal peptidase (Evans et al., 1986; Liaci et al., 2021), chaperones (Chevet et al., 1999; Dudek et al., 2005), putative RNA-binding proteins (Cui et al., 2012) and others. For multipass membrane proteins, the signals directing translocon composition proved to be multifactorial, and included negative selection (for example, by disfavouring the binding of OST on the basis of TMD number and position) and positive selection (for example, by binding to specific factors such as the PAT complex). This is

analogous to the interplay between cytosolic factors at the ribosome exit tunnel during synthesis of soluble proteins. Our findings provide a framework for dissecting how other biogenesis factors are coordinated at the ER translocon.

4. RAMP4 and its role in protein translocation

4.1. Overview

While little is known about RAMP4, previous work has shown that RAMP4 co-purifies with Sec61 and can be found in complex with the ribosome and Sec61 (Gorlich and Rapaport, 1993). Beyond this, no definitive function has been assigned to RAMP4. Indeed, even how RAMP4 interacts with the ribosome and Sec61 complex was unclear. RAMP4 is a 65 amino acid tail-anchored protein with a predicted (via Alphafold) single TMD and a more structured N-terminal region thought to bind the ribosome. No known structure exists and where that TMD is in relation to Sec61 and the ribosome during protein synthesis is unknown. Recent work, however, from our collaborators in the Hegde lab indicated that the TMD of RAMP4 is in fact positioned within the lateral gate of Sec61 (unpublished). This naturally piqued our interest given its unknown function and position in a critical region important to protein translocation. Previous evidence has indicated that the protein itself is most likely unessential to protein translocation as only very small quantities are shown to copurify with Sec61. Furthermore, addition of RAMP4 did not improve translocation activity to any degree (Gorlich and Rapaport 1993). Thus, our hypothesis was that RAMP4 is recruited to Sec61 to occupy the lateral gate in replacement of a SS or TMD. Here we show that RAMP4 is indeed a part of the secretory translocon and able to stably associate with the ribosome and Sec61. We show that RAMP4 recruitment to the translocon is in response to defined signals such as hairpin inversion of a type II TMD, departure of a signal sequence, as well as translocation of long internal lumenal loops. We further show that when a protein does not utilize the Sec61 channel, RAMP4 is not recruited. While this work

is not complete, we hope to continue with further experiments to truly confirm the function of RAMP4 and the clients that utilize RAMP4 during synthesis.

4.2. Contributions

In this work, I performed the interaction analysis in cells, in vitro analyses for substrate recruitment, flow cytometry experiments, and in vitro analyses utilizing Sec61 inhibitors. A.K.S. performed interaction analysis in cells and in vitro analyses for substrate recruitment and glycosylation assays. J.T. performed in vitro analyses for substrate recruitment. R.J.K. provided funding and guidance.

4.3. RAMP4 forms a complex with the ribosome and Sec61

To understand RAMP4's role in the translocon, we sought to understand at what stage of synthesis of a membrane protein RAMP4 is required. Given that the translocon remodels itself based on substrate needs, we sought to understand whether RAMP4 was functioning as part of the multipass translocon or the secretory translocon. While previous work had implicated RAMP4 in the biogenesis of single-pass membrane proteins, no work had strictly ruled out a role for RAMP4 synthesis during multipass protein biogenesis. We engineered a 3xFlag-RAMP4 cell line in a RAMP4 KO background and performed a Flag pulldown in order to isolate RAMP4/Ribosome/Sec61 complexes (**Figure 22**). We observed a complete depletion of multipass components yet a strong enrichment for STT3A as well as TRAPα. Similarly, a reciprocal pulldown on 3xFlag-TMCO1 showed little to no RAMP4, implicating its role in the secretory and core translocon and not the multipass. From our previous work, we had shown that both the secretory and core translocon functioned strongly at the beginning of multipass membrane proteins before translocon remodeling induced recruitment of multipass components.

We thus reasoned that studying early-stage synthesis of membrane proteins may elucidate the timing of RAMP4 recruitment and function. As the first TMD of a multipass protein is functionally similar to a single pass membrane protein, we initially examined RAMP4 recruitment in a model substrate, a type II single pass membrane protein, ASGR1.

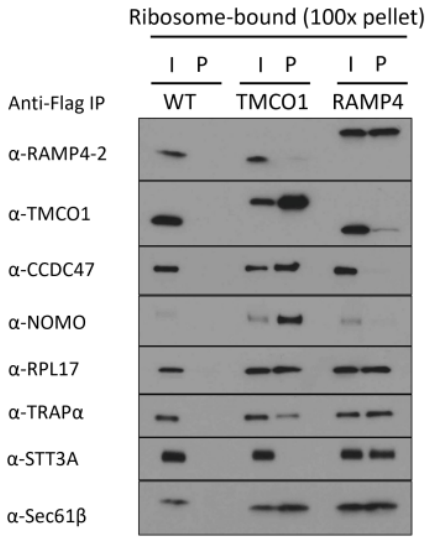

Figure 22. RAMP4 is a component of the secretory translocon

Nuclease-treated membranes from wild-type or stably integrated Flag-tagged (TMCO1, RAMP4) HEK293 cells were digitonin-solubilized, immunoprecipitated and sedimented through a sucrose cushion to isolate the ribosome-bound and ribosome-free fractions for analysis. Analysis of input (I) and ribosome-bound (pellet (P)) fractions by SDS–PAGE and immunoblotting. RPL17 and STT3A are used here as markers for the ribosome and OST, respectively. IP, immunoprecipitation.

4.4. Translocation of lumenal loops recruits RAMP4

We first examined ASGR1, a type II single-pass membrane protein. Previous work has shown that RAMP4 can be crosslinked to the lumenal domain of a synthetic Type II membrane protein construct. While this cross-linking was at a significantly later length than expected (approximately 115 amino acids after the TMD), we reasoned that this cross-linking was most likely indicative of the recruitment of RAMP4 to these type II proteins. Given our hypothesis of RAMP4 being recruited to the lateral gate as a replacement for the TMD/SS, we reasoned that the recruitment would occur rapidly after TMD/SS departure from the lateral gate. Previous

structural studies have shown that the SS of pre-prolactin is engaged with the lateral gate when 56 amino acids have been synthesized after the SS (Voorhees et al. 2016). Similarly, Type II membrane protein TMD hairpin inversion occurs approximately as the nascent chain after the TMD is extended to 60-70 amino acids (aa) (Devaraneni et al. 2013). Combining these previous observations, we constructed a series of intermediates of ASGR1 (Figure 23a) by extending the nascent chain in a series of 10 aa. Interestingly, at nascent chain lengths of 45 and 55 aa after the TMD, we observed no RAMP4 at the translocon (**Figure 23b**). As the nascent chain was

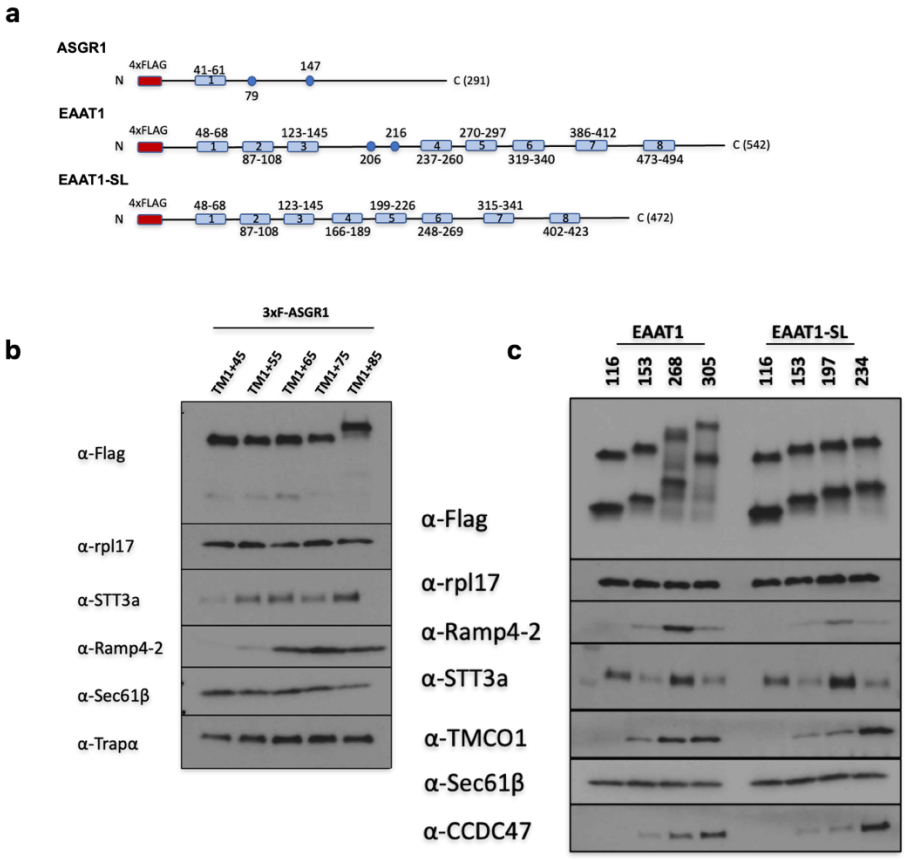

Figure 23. RAMP4 is recruited during translocation of lumenal loops

(a) The template used to generate truncated, Flag-tagged ASGR1 and EAAT1 constructs. (b) Stalled, Flag-tagged ASGR1 constructs truncated at the indicated positions were analysed (c) Stalled, Flag-tagged EAAT1 constructs truncated at the indicated positions were translated in RRL in the presence of wild-type microsomes

lengthened to 65 aa, we observed a sharp increase in the recruitment of RAMP4. While OST is in fact recruited to the translocon at a nascent chain of 55 aa, with little RAMP4, the recruitment of RAMP4 and STT3A are relatively strongly correlated throughout the rest of the intermediates. Given that hairpin inversion occurs at nascent chain lengths of 60-70 aa after the TMD, we hypothesized that this recruitment was correlated with the ability of RAMP4 to replace the TMD.

While early synthesis is a natural point to study TMD replacement with RAMP4, it was unclear whether this phenomenon would occur at later stages where many of the TMD's are inserted via the multipass translocon (Sundaram, Yamsek, Zhong al., 2022 Smalintskie et al., 2022). Thus, we looked at multipass membrane proteins with long lumenal loops that are associated with the secretory translocon. From our previous work, we had characterised EAAT1, a type II membrane protein with a long lumenal loop that strongly associates with the secretory translocon. Indeed, the same intermediate EAAT1-268 showed strong levels of RAMP4 recruitment (**Figure 23c**). Mutation of the lumenal loop between TMD 3 and TMD 4 to a loop of 20 amino acids strongly depleted RAMP4 levels without reducing STT3A levels, a puzzling observation. Similarly, in a type III multipass membrane protein with a long loop, C3AR1, a long lumenal loop engages RAMP4 as well as the secretory translocon (**Figure 24a**). Unlike EAAT1, however, mutation of the long lumenal loop to a 20 aa shortened loop completely abolished both RAMP4 and STT3A recruitment while concomitantly increasing multipass translocon engagement (**Figure 24b**). This lack of engagement with the secretory translocon can be explained by the fact that a shorter loop does not strictly require Sec61 and may in fact be inserted by the multipass translocon. The increased recruitment of RAMP4 during intralumenal loop synthesis, where the loop most likely transits the Sec61 channel, is in strong agreement with

the hypothesis of TMD replacement at the lateral gate. A model that emerges is that as the lumenal loop transits Sec61, the preceding TMD engages Sec61 and as the TMD leaves the lateral gate, RAMP4 is thus recruited to the translocon.

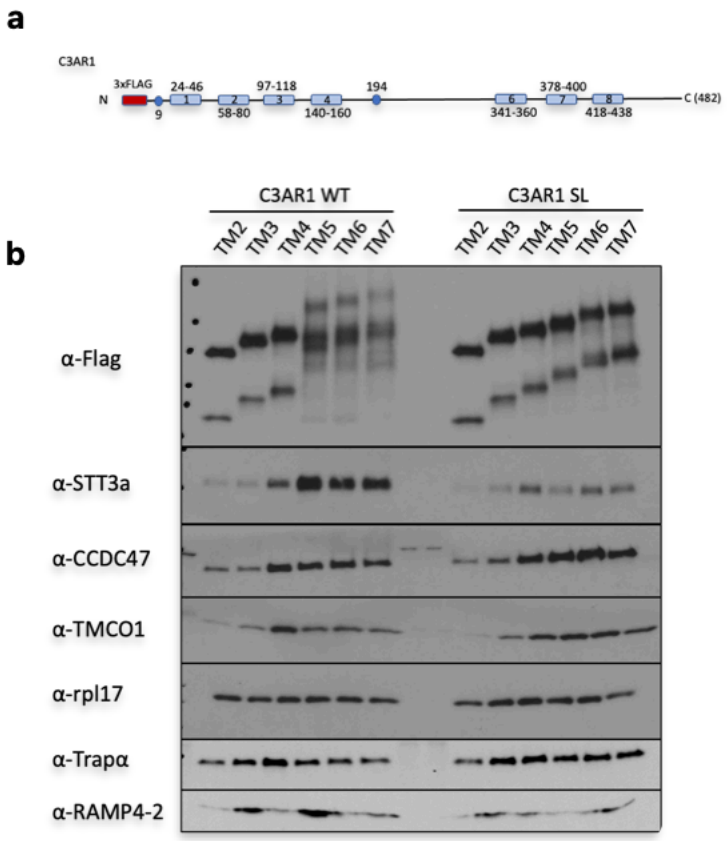

Figure 24. Translation dynamics during C3AR1 synthesis

(a) Template used to generate truncated, Flag-tagged C3AR1 constructs (b) Stalled, Flag-tagged C3AR1 WT and SL constructs truncated at the indicated positions were analysed. Note that the TM5 intermediate (and beyond) is glycosylated at position 194.

With the data that RAMP4 is recruited to the translocon at various stages during protein biogenesis, we sought to understand the functional consequences of RAMP4 depletion within the cell. Utilizing in vitro translation, we examined the glycosylation efficiency of ASGR1, EAAT1, and Yipf1 in cells lacking RAMP4 (**Figure 25a**). Glycosylation efficiency serves as a marker for correct topogenesis of these proteins. We observed no defects in glycosylation or overall protein

synthesis. In vitro analysis of TMED2, a single pass protein containing a signal sequence also showed no defect in signal peptide cleavage, confirming correct topogenesis (**Figure 25b).** We then turned our attention to an in vivo characterization utilizing a dual-colour flow cytometry assay (**Figure 25c**). In this assay, the N-terminus of ASGR1 is appended with a green fluorescent protein (GFP) and red fluorescent protein (RFP) separated by a viral 2A-peptide skipping sequence. Any translated ASGR1 mRNA generates two products in a one-to-one ratio so that any change in GFP:RFP ratio following siRNA depletion necessarily reflects a post-translational change in ASGR1 stability. SQS, a known substrate of EMC, showed significantly reduced levels of RFP:GFP in ΔEMC6 cells relative to WT cells, consistent with what has previously been reported (Guna et al. 2018, Chitwood et al. 2018). Within ΔRAMP4 cells, however, we observed no significant difference in the RFP:GFP or GFP:RFP levels of ASGR1 relative to WT cells. While this does not rule out a potential function of RAMP4 in protein biogenesis, it reinforces the notion that the function of RAMP4 is not essential to the synthesis of these

proteins. Further work will be required to understand the full function and mechanism of RAMP4 in protein biogenesis.

4.5. Discussion

We have shown that RAMP4 can bind ribosome-translocon complexes, specifically those of the secretory and core translocons. Furthermore, we show specific and dynamic recruitment of RAMP4 to the translocon, dependent on defined signals such as translocation of lumenal loops. These observations, hint that RAMP4 plays a role in protein biogenesis. Furthermore, while we have not shown definitively that TMD/SS disengagement is the signal for RAMP4 recruitment to the translocon, unpublished structural data in combination with in vitro translation data currently suggests that this may be the case. Coupling our observations to the structure of the RAMP4 TMD in the lateral gate, it emerges that a potential function of RAMP4 could be to function as a

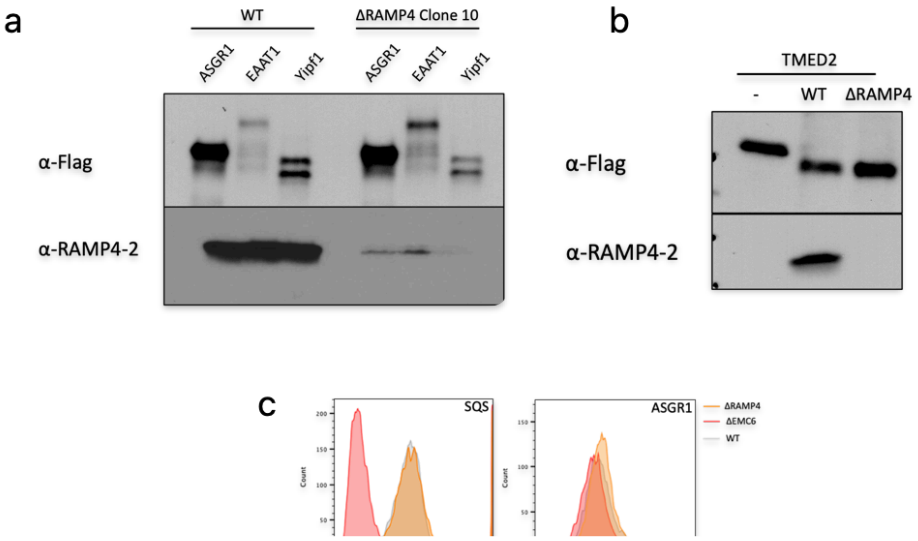

Figure 25. In vitro and In vivo characterization of RAMP4 substrates

(a) 3xF-ASGR1, 3xF-EAAT1, and 3xFlag-Yipf1 were translated in RRL with wild-type and single-knockout RAMP4 (ΔRAMP4), isolated by sedimentation, and analysed by immunoblotting. (b) 3xFlag-TMED2 were translated in RRL with wiltd-type and single-knockout RAMP4 (ΔRAMP4), isolated by sedimentation, and analysed by immunoblotting. (c) WT and ΔRAMP4 cells were transfected with the indicated reporter induced with doxycycline, and analysed by flow cytometry. The histograms show FP ratios for each reporter in a particular cell line.

"doorstop" for the lateral gate. In essence, as TMDs and SSs traverse the lateral gate and slide into the bilayer (Martoglio et al. 1995, Mothes et al. 1995, Voorhees et al. 2016), RAMP4 would prevent movement of the lateral gate helices and allow further translocation of lumenal domains downstream of the TMD. Further characterization to define this interaction will be required.

As assays characterizing functional consequences of RAMP4 depletion showed no defects in protein biogenesis or topogenesis, we hypothesize that other proteins or pathways in the cell can facilitate biogenesis in the place of RAMP4. In fact, multipass membrane proteins are known to be inserted into membranes even when Sec61 is inhibited (Mckenna et al. 2017, Smalintskie et al., 2022, unpublished data). There may yet remain an alternative pathway into the cell for single-pass membrane proteins that remains yet undiscovered. Alternatively, it is possible that RAMP4 acts in a catalytic fashion and its depletion, while affecting the kinetics of protein biogenesis, do not affect the steady state level in cells. The assays we use are not kinetic in nature and thus we may not be able to visualize any slowing of insertion of these membrane proteins. Further investigation into the role of RAMP4 is required.

5. FKBP11 facilitates protein biogenesis at the ER translocon

5.1. Overview

While many accessory factors of the eukaryotic translocon are well known (OST, TRAP, TRAM) albeit not fully understood, there remains a high possibility that other eukaryotic translocon accessory factors exist but have not been discovered. Here we show that a FKBP11 is a novel translocon accessory factor and functions in membrane protein biogenesis.

Previously, in a quantitative mass spectrometry experiment examining the proteome of ΔTMCO1 cells, we observed a protein that was highly upregulated relative to WT HEK293 cells

(data not shown). This protein, FKBP11, belongs to the FK 506 binding protein (FKBP) family, so named as they bind the drugs FK506 and rapamycin. The proteins in this family generally function as cis/trans peptidyl prolyl isomerases (PPIases) and are ER resident soluble proteins (Tong and Jiang, 2015). FKBP11, however, possesses a single TMD and its strong upregulation led us to believe that it may function as a translocon accessory factor. Our reasoning was that as one accessory factor was depleted, other accessory factors would be upregulated to maintain cellular homeostasis. Here, we show that FKBP11 binds to ribosome-translocon complexes, and in fact can stably associate as part of the secretory translocon. Furthermore, we confirmed a role for FKBP11 in biogenesis of membrane proteins with long translocated regions. Depletion of FKBP11 resulted in impairment of both secretory and transmembrane proteins.

A version of this work is in preparation for submission as Diguilio, A., Cheng, B., Zhong, F., Keenan,. R.J. to Molecular Biology of the Cell.

5.2. Contributions

In this work, I performed flow cytometry experiments, ribosome pelleting experiments, and in vitro recruitment. A.D. performed interaction analysis in cells, mass spectrometry, and RNA-seq sample preparation. B.C. performed sucrose gradients, siRNA knockdown, and flow cytometry experiments. RNA sequencing was performed at The University of Chicago Genomics Core Facility. Mass spectrometry was performed at the University of Wisconsin Madison. R.J.K and A.D. performed the analysis of the RNA sequencing data and mass spectrometry data. R.J.K. conceived the project and guided experiments.

5.3. FKBP11 binds to ribosome-translocon complexes

While FKBP11 is part of the larger FKBP family of proteins, it is relatively unique as it contains a single TMD in contrast to the other soluble FKBP members which contain ER-retention signals (**Figure 26a**). To confirm that FKBP11 is a ribosome-bound protein, we pelleted ribosomes from HEK293 digitonin-solubilized membranes and examined the pellet for FKBP11. In fact, FKBP11 is present in the ribosome pellet in contrast to the soluble protein FKBP2 (**Figure 26b**).

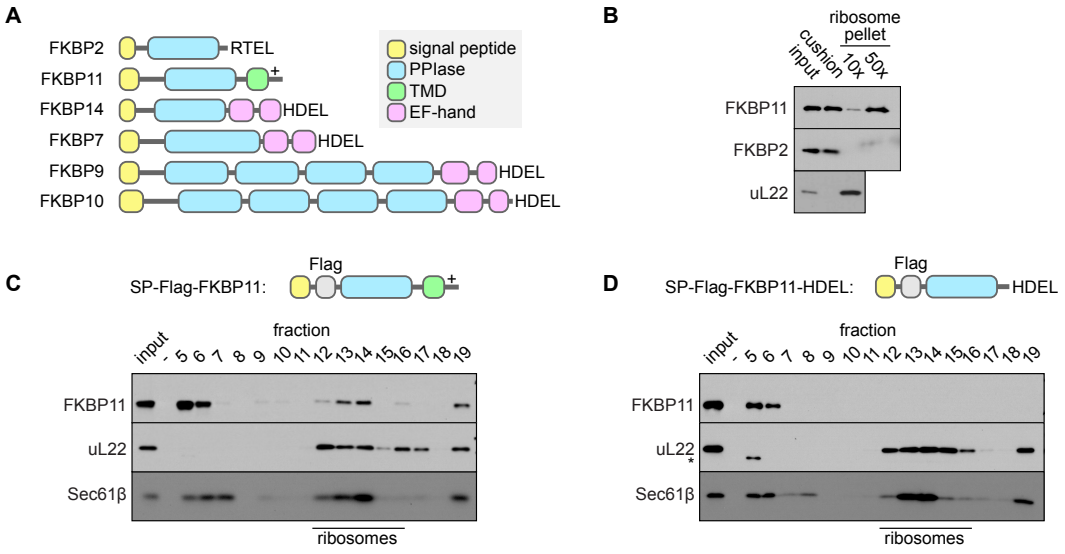

Figure 26. FKBP11 forms a complex with the Sec61 Translocon and RNCS

(a) ER phylogeny of FK-506 binding protein members, note that FKBP11 alone has a TMD among family members (b) Microsomes from wild-type (WT) HEK293 cells were digitonin-solubilized and pelleted over a sucrose cusion. Note that FKBP11 is in the ribosome pellet while FKBP2, an er lumenal protein, is not. (c) Digitonin-solubilized microsomes from 3xFlag-FKBP11 cells were separated by high-resolution sucrose cushion and analysed by western blotting. Note that FKBP11 co-fractionates with the 80s ribosome and Sec61 translocon. (d) Digitonin-solubilized microsomes from 3xFlag-FKBP11-HDEL cells were separated by high-resolution sucrose cushion and analysed by western blotting. Note that the 3xFlag-FKBP11-HDEL does not fractionate with the 80s ribosome and Sec61 translocon.

To identify interaction partners of FKBP11 we engineered an HEK293 cell line for expression of 3xFlag-tagged FKBP11 at near-physiologic levels (**Figure 27**). When digitonin-solubilized membranes prepared from these cells were fractionated by sucrose gradient, FKBP11 and Sec61 were present in the 80S ribosome fraction (**Figure 26c**). This was dependent on the single transmembrane domain (TMD) and positively charged C-terminus of FKBP11, since replacing this region with an HDEL ER-retention signal abolished co-migration with 80S ribosomes and Sec61 (**Figure 26d**).

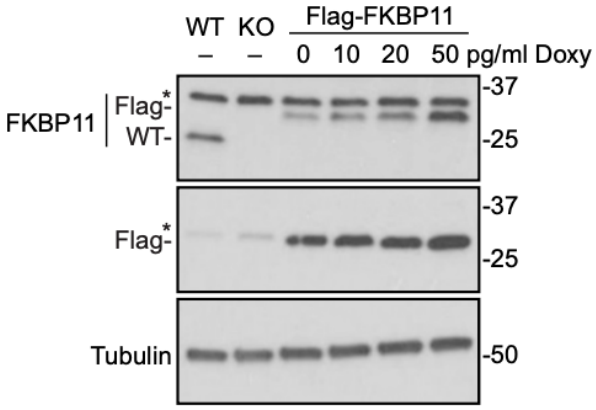

Figure 27. Titration of 3xFlag-FKBP11

3xFlag-FKBP11 was engineered into a HEK293cell line using the Flp/FRT system and titrated to near physiological levels by doxycycline induction for analysis.

Next, we affinity purified epitope-tagged FKBP11 from cells and identified co-purifying proteins present in the ribosome-bound fraction by mass spectrometry (**Figure 28**). Multiple subunits of the Sec61 complex, the TRAP complex and OST were enriched relative to controls. Other components of the biogenesis machinery, including subunits of the ER-membrane complex (EMC), the multipass translocon (MPT) (Sundaram, Yamsek, Zhong et al., 2022;

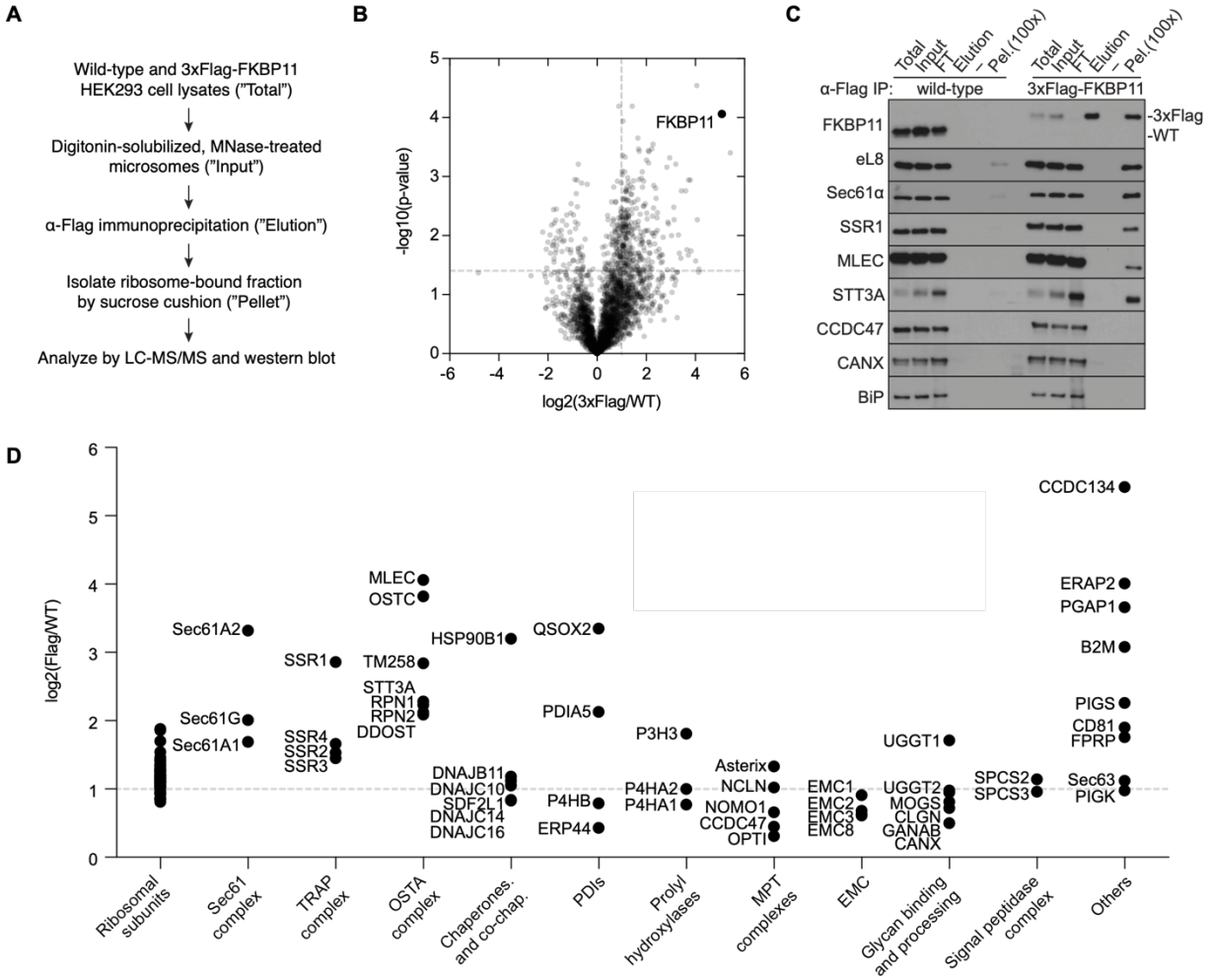

Figure 28. FKBP11 engages OST-bound translocons

(a) Experimental strategy. Nuclease-treated membranes from wild-type or stably integrated Flag-tagged FKBP11 HEK293 cells were digitonin-solubilized, immunoprecipitated and sedimented through a sucrose cushion to isolate the ribosome-bound and ribosome-free fractions for analysis. (b) Volcano plot of the LC-MS/MS, FKBP11 is marked (c) Western blots of the indicated components are shown as confirmation of the hits from the LC-MS/MS (d) Hits from the mass spectrometry data are grouped by complex, note that there is significant enrichment for OST components as well as Sec61 and TRAP

Smalinskaite et al., 2022; McGilvray et al., 2020) and the signal peptidase complex were either poorly enriched or absent. With several exceptions (e.g., CCDC134, HSP90B1 and QSOX2), lumenal ER chaperones, lectin chaperones, protein disulfide isomerases (PDI), prolyl hydroxylases and other peptidyl-prolyl isomerases (PPIases) were also not enriched in the FKBP11-purified ribosomes. These observations suggest that FKBP11 engages ribosome-bound translocons comprising the Sec61-, TRAP- and OST complexes.

5.4. FKBP11-bound ribosomes synthesize proteins with long translocated regions

To identify potential clients of FKBP11 we sequenced ribosome-bound mRNAs recovered after affinity purification via the Flag tag on FKBP11 (RIP-seq). We observed strong enrichment for transcripts encoding signal peptide-containing soluble proteins (**Figure 29b**). Transmembrane proteins were also enriched, but showed a broad, bimodal distribution. By contrast, transcripts encoding cytonuclear and mitochondrial proteins were not enriched. Consistent with specificity of the experiment, enrichment was independent of transcript abundance in the input sample, and of protein length.

Analysis of the enrichment of transcripts encoding different classes of transmembrane proteins revealed a preference of FKBP11 for proteins containing long lumenal regions (**Figure 29c,d**). Thus, type I and type II single-pass proteins, which generally possess long N- and C-terminal lumenal domains (respectively), were strongly enriched, while type III single-pass proteins, which possess short lumenal N-tails, were not. Type I multipass proteins, which have long N-terminal lumenal regions were enriched, albeit more modestly than type I single-pass proteins. Type II multipass proteins were poorly enriched, consistent with generally short lumenal loops between their first two TMDs, as were type III multipass proteins, which possess

short lumenal N-tails. Thus, FKBP11 associates with ribosomes that are translating a broad range of secretory and transmembrane proteins, a distinguishing feature of which is the presence of long lumenal segments.

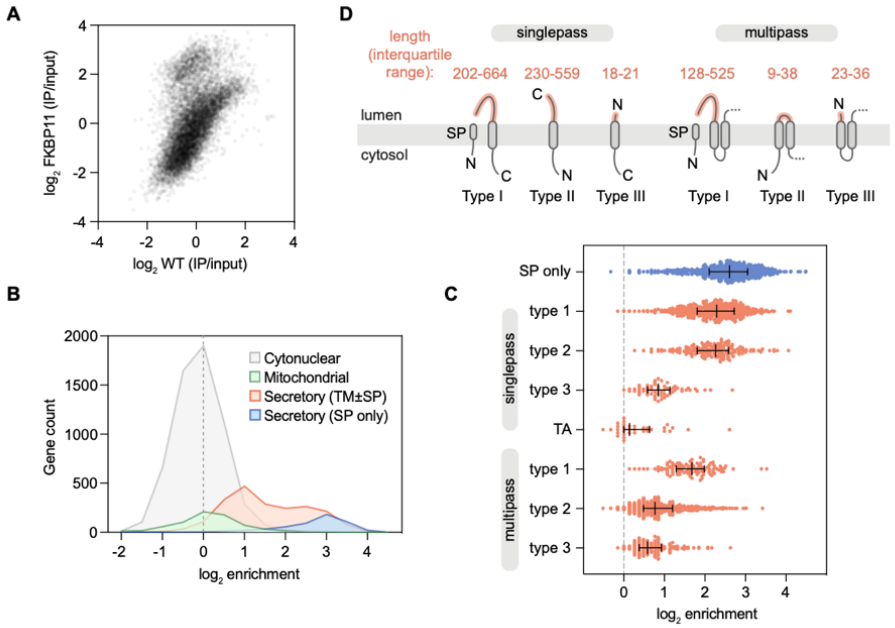

Figure 29. FKBP11-bound translocons are selectively enriched at ribosomes translating signal- peptide containing proteins

(a) Scatterplot of FKBP11 bound ribosomes against WT ribosomes shows significant enrichment of a subset of proteins (b) Log2 enrichment of transcripts encoding proteins of the indicated categories according to Uniprot annotation. Enrichment was calculated as (Flag IP - Ctrl IP)/Input (c) Analysis of classes of membrane proteins in the RIP-seq dataset (d) Classes of membrane proteins and the annotated interquartile range of translocated region lengths for these classes

Given the enrichment that we have seen for FKBP11 with long lumenal segments, we sought to understand the recruitment dynamics of FKBP11 for these clients. To that end, we examined insertion intermediates of ASGR1, a Type II single pass membrane protein (**Figure 30a**). We observed significant enrichment of FKBP11 coinciding with STT3A, with an insertion intermediate approximately 55 amino acids after the TMD (**Figure 30b**). This length corresponds roughly with engagement of a TMD with the lateral gate (Deveraneni et al., 2011)

and further validates the fact that FKBP11 translocons most likely belong to a sub-class of the "secretory translocon". We posit that the association of FKBP11 at this length, in direct correlation with OST, indicates that FKBP11 may play a role in glycosylation of proteins. Further investigation into this hypothesis is required.

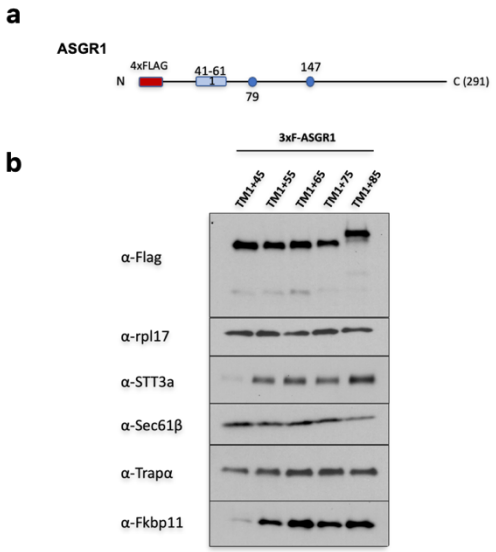

Figure 30. FKBP11 recruitment dynamics of ASGR1

(a) The template used to generate truncated, Flag-tagged ASGR1 (b) Stalled, Flag-tagged ASGR1 constructs truncated at the indicated positions were analysed by SDS-PAGE and immunoblot

5.5. FKBP11 promotes secretory and transmembrane protein biogenesis

To explore the role of FKBP11 in biogenesis we monitored the endogenous protein levels of the epithelial cell adhesion molecule (EpCAM) and cathepsin Z (CTSZ) in HEK293 cells following small interfering RNA (siRNA) depletion of FKBP11. EpCAM, a type I single-pass membrane protein, and CTSZ, a soluble secretory protein, were selected as representative strong hits in the FKBP11 RIP-seq experiment. Compared to cells treated with a scrambled siRNA control, the steady-state expression levels of EpCAM and CTSZ were both reduced following FKBP11 depletion with any of three independent siRNAs (**Figure 31a**). By contrast, siRNA

depletion of FKBP2, a soluble FKBP family member in the ER that shares ~52% sequence identity with FKBP11, had no effect on the steady-state levels of either EpCAM or CTSZ.

To investigate whether the reduction of EpCAM levels following FKBP11 depletion was due to increased degradation, we employed a flow cytometry assay for protein stability. For this EpCAM was appended at its C-terminus with green- (GFP) and red fluorescent protein (RFP) separated by a ribosome-skipping viral 2A sequence (**Figure 31b**). Translation of this mRNA generates two products in a one-to-one ratio so that any change in GFP:RFP ratio following siRNA depletion necessarily reflects a post-translational change in EpCAM stability.

We found that depletion of FKBP11 reduced the GFP:RFP fluorescence ratio for the EpCAM reporter relative to a scrambled siRNA control, consistent with reduced stability (**Figure 31c**). By contrast, siRNA depletion of FKBP2 had no effect on the GFP:RFP ratio. Similarly, a reporter cell line for the plasma membrane type III multi-pass membrane protein

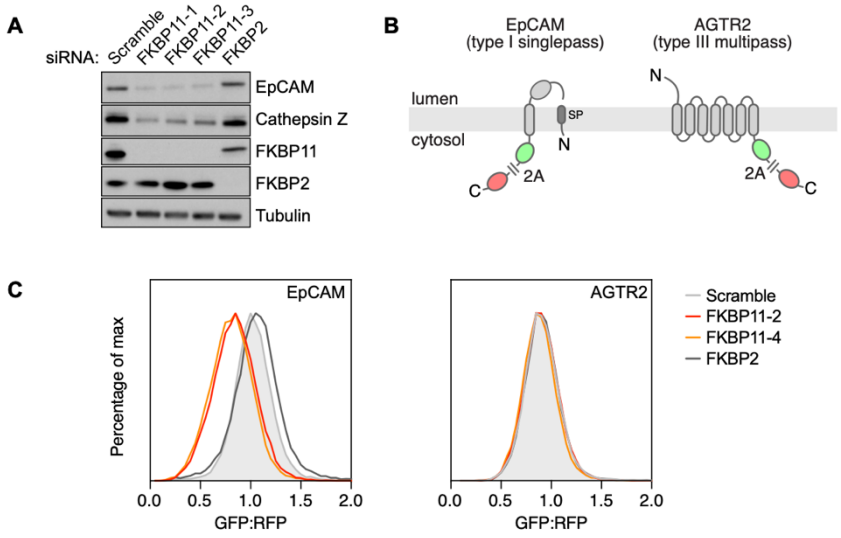

Figure 31. FKBP11 depletion impairs protein biogenesis

(a) HEK293 cells were treated with the indicated short interfering RNA (siRNA). Total lysates were then analysed by SDS-PAGE and immunoblotting (b) Reporter constructs to monitor protein stability in cells. (c) Stably integrated HEK293 reporter lines were treated with the indicated siRNA, induced with doxycycline, and analysed by flow cytometry. The histograms show FP ratios for each siRNA–reporter pair.

angiotensin II receptor (AGTR2) showed no effect upon FKBP11 depletion. These data suggest that FKBP11 disruption of EpCAM biogenesis is specific and not a result of Sec61-mediated translocation or TMD integration. These data suggest that loss of FKBP11 leads to increased EpCAM misfolding, the result of which is destabilization and degradation.

5.6. Discussion

Our results provide a number of insights into the function of FKBP11. First, we show that it binds to ribosome-translocon complexes (RTCs) and that this interaction is dependent on FKBP11's conserved TMD and positively charged C-terminus. Second, we show that this interaction is selective for ribosomes that are translating soluble and transmembrane proteins with long translocated segments. Finally, we demonstrate that biogenesis of two different proteins, the soluble secretory protein CTSZ and the type I single-pass membrane protein EpCAM, is disrupted in the absence of FKBP11. These observations lead us to propose FKBP11 as a previously unrecognized translocon accessory factor that acts on a broad range of secretory and transmembrane proteins during their synthesis at the ER.

The preference of FKBP11 for proteins with long translocated regions likely reflects its association with translocons comprising the Sec61, TRAP and OST complexes. These "core" and "secretory" translocons (Sundaram, Yamsek, Zhong et al., 2022; Gemmer et al., 2023) mediate translocation of long segments across the membrane via the Sec61 channel (REF classic papers). In most cases these substrates are either fully translocated soluble proteins or membrane proteins harboring long lumenal segments immediately following the first signal peptide or TMD (**Figure 29d**). By associating with these translocons, FKBP11 would be positioned to act on the nascent chain as it enters the lumen.

By contrast, proteins with short, translocated regions may only access the Sec61 channel transiently, if at all. For example, the short N-tails of type III single-pass membrane proteins are translocated by EMC (O'Keefe et al., 2021). Similarly, those of type III multipass proteins can be translocated by EMC (Chitwood et al., 2018) before the protein is handed off to the multipass translocon for integration of downstream TMDs (McGilvray et al, 2020; Smalinskaite et al. 2022; Sundaram, Yamsek, Zhong et al., 2022). As evidenced by insensitivity to Sec61 inhibitors, these proteins do not require the Sec61 channel for translocation of their lumenal segments (O'Keefe et al., 2021; Smalinskaite et al., 2022). These simple considerations likely explain why FKBP11 does not robustly engage with proteins containing only short translocated regions.

How FKBP11 engages with the ER translocon remains unclear. Recruitment based solely on the FKBP11 lumenal domain seems unlikely, since a truncated construct lacking the TMD does not bind to RTCs (**Figure 26**). More likely, assembly involves a combination of ribosome binding by the conserved, positively charged C-terminus of FKBP11, and interaction of its TMD with other translocon components. Consistent with the robust co-purification of multiple components of OST (**Figure 26**) and in situ structural analysis of the secretory translocon (Gemmer et al., 2023), additional interactions between the FKBP11 and OST lumenal domains would position FKBP11 near the translocating nascent chain as it exits the Sec61 channel. Future work is necessary to test this hypothesis.

6. Future Directions

6.1. Relating to the multipass translocon

The work presented here provides insight into a fundamental question of membrane protein biology, how multipass membrane proteins are synthesized and inserted into the ER bilayer. Previously, the long-standing paradigm of multipass TMD insertion was a model of sequential-TMD insertion mediated by Sec61 (Blobel 1980, Matlack et al. 1998). We show that a novel translocon, termed the multipass translocon, is comprised of 3 distinct sub-complexes (GEL, BOS, PAT) and mediates the insertion of multipass membrane proteins. We define the signal required for recruitment of these sub-complexes to Sec61 and show that depletion of any of these sub-complexes results in impaired topogenesis and biogenesis. Work from both our lab and a collaborator also have shown high-resolution structures of this translocon, including substrate TMD density in the lipid-filled cavity (McGilvray et al. 2020, Smalinskaite et al. 2022). Nevertheless, many questions remain both on both the mechanism of multipass mediated TMD insertion as well as the physiological function of this translocon.

Our identification of the multipass translocon has raised many questions on the mechanistic functions of this translocon. For example, while we show that the multipass translocon is assembled on various types of multipass membrane proteins (Type II and Type III), a question that remains is the timing of component assembly. Does the multipass translocon assemble on all membrane proteins in response to the synthesis of a second TMD? Is there differential assembly of the multipass translocon dependent on substrate features such as TMD hydrophobicity or internal loop lengths? Do different sub-complexes have differential assembly on substrates, i.e. do certain substrates require only one of the sub-complexes (PAT)? While our

in vitro stalled recruitment assays suggest that certain features affect assembly (such as synthesis of a second TMD), a global examination of multipass membrane proteins would provide conclusive evidence of how the multipass translocon assembles. We are well-positioned to conduct this work utilizing the techniques we have established. For example, utilizing our RNA-seq immunoprecipitation strategy, we can take this a step further and perform ribosome footprinting on the associated mRNA's of the multipass translocon complex. In fact, we can perform ribosome footprinting on ribosome-translocon complexes (RTC) from different sub-complexes by tagging members of each sub-complex (TMCO1, Nicalin, CCDC47) with a 3x-Flag tag and isolating the RTC's. Utilizing such a strategy, we would then be able to examine the position of the multipass translocon on various substrates and whether there is differential assembly of sub-complexes or the translocon itself based on the sub-complex member that we pull down upon. This would provide a global overview of multipass translocon assembly and positioning on a vast majority of membrane proteins, further validating our initial observations.

Another question that remains is the insertase function of the multipass translocon. While inhibitor experiments have shown that multipass membrane proteins are in fact inserted while Sec61 is blocked (Smalinskaite et al. 2022, unpublished data), no definitive insertase function of the multipass components has been shown. Reconstitution of PAT, GEL, BOS complexes in proteo-liposomes with the minimal machinery required for protein translation would provide conclusive evidence that the multipass translocon functions as an insertase. Previous work has shown that immunoaffinity purification of EMC followed by proteo-liposome reconstitution is feasible for EMC (Guna et al., 2018). Analagous to this, reconstitution of the multipass translocon with Sec61 should be possible. Furthermore, selective depletion of various

components of the PAT, GEL, BOS complex will allow for identification of the absolute minimal machinery required for multipass membrane protein biogenesis.

Finally, one of the remaining questions is that if TMCO1 functions as an insertase, what domain is responsible for this insertase function. Recent work has shown that EMC functions as an insertase and that this insertion is dependent on the hydrophilic vestibule formed by EMC3 and EMC6 (Chitwood et al., 2018, Pleiner et al., 2020, Pleiner, Hazu et al., 2023). Similar to EMC3, TMCO1 is part of the larger Oxa1 superfamily and also contains a large lipid-filled hydrophilic groove as well as forming a larger lipid filled cavity (Anghel et al., 2017, McGilvray et al., 2020). Previous mutagenesis analysis in the hydrophilic vestibule of EMC3 resulted in significant defects in insertion for both post- and co-translational substrates. Experiments utilizing mutagenesis of amino acids within the hydrophilic groove of TMCO1 would allow us to then test the insertase activity of TMCO1 and pinpoint the specific catalytic domains of TMCO1. Furthermore, once specific amino acids have been identified, cross-linking experiments can be done with the substrate in order to understand the mechanism of insertion.

6.2. Relating to RAMP4

The work we present here implicates RAMP4 directly in membrane protein biogenesis. While previous work has shown that RAMP4 co-purifies with Sec61 as well as being present at the translocon during protein synthesis, we are able to unequivocally show that RAMP4 is able to pull down with ribosome-Sec61 translocon complex. Furthermore, we show that RAMP4 is dynamically recruited to the translocon in response to the translocation of lumenal loops. As RAMP4 depletion did not lead to any clear functional defects either in vitro or in vivo, we hypothesize 2 potential possibilities that explain this phenomenon. The first is one catalytic in

nature, which enhances protein translocation, possibly quickening translocation as it keeps the lateral gate open. The second is that RAMP4 opening of the lateral gate can be compensated by the existence of other proteins in the cell. Perhaps other proteins within the cell exist that can intercalate within the lateral gate and allow translocation to continue. Further investigation into these possibilities is required to understand the function of RAMP4.

Several other questions remain as to the recruitment dynamics of RAMP4. First, an interesting observation that was presented is that RAMP4 recruitment was abolished when long lumenal loops were truncated to short lumenal loops, yet OST remained bound (**Figure 23c**). Most likely, this indicates that the secretory translocon itself is dynamic and has different signals to recruit transient factors such as RAMP4. Second, we have established that RAMP4 is recruited when lumenal loops are translocated through the Sec61 channel. Previous work has established that certain Type III membrane proteins (both single and multipass) are strictly Sec61 insensitive and inserted by EMC (McKenna et al., 2017, Chitwood et al., 2020, O'Keefe et al., 2021). By definition, these substrates would not translocate through Sec61. An interesting question thus is, during synthesis of Type III membrane proteins that utilize the EMC pathway, would RAMP4 be recruited? We hypothesize that as the Type III membrane proteins do not translocate through Sec61, there would be a complete absence of RAMP4 recruitment. Utilizing our in vitro stalled substrate recruitment assay, we are in the process of conducting this experiment. Lastly, does the ribosome binding domain of RAMP4 affect recruitment? Our data suggests that RAMP4 is recruited, even as a second TMD inserts into the bilayer and RAMP4 is not displaced during this process (unpublished data). One explanation is that the positively charged N-terminus of RAMP4, which we hypothesize to be the ribosome binding domain

(unpublished data), remains bound to the ribosome even as RAMP4 has left the lateral gate (**Figure 32**). In fact, cryo-EM density as well as Alphafold modeling indicates that this positively charged regions packs tightly against the ribosome (unpublished data). Mutations to this domain followed by ribosome binding assays would allow us to examine if the recruitment we see during the insertion of successive TMD's is due to the presence of RAMP4-bound ribosomes that are not intercalated in the lateral gate.

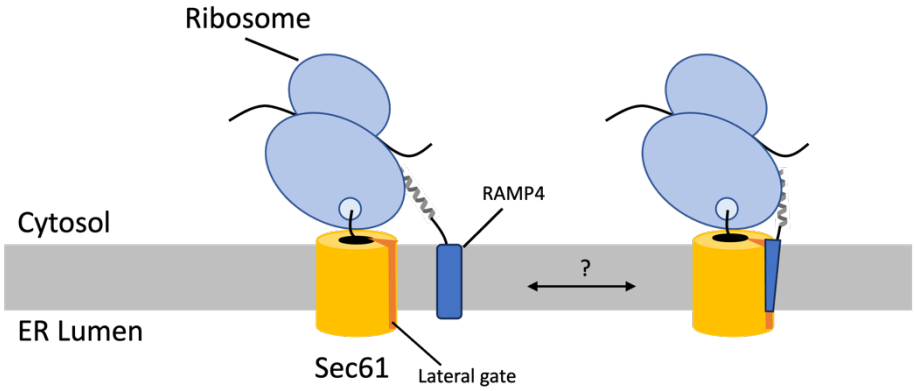

Figure 32. Two differential binding possibilities of RAMP4

The two different potential binding states of RAMP4. On the left RAMP4's N-terminus is bound to the ribosome but the TMD is not in the lateral gate. On the right, the N-terminus is still bound to the ribosome but the TMD is now intercalated in the lateral gate.

6.3. Relating to FKBP11

The work presented here indicates that FKBP11 is a bona fide member of the secretory translocon. Furthermore, we are able to demonstrate that these secretory translocons are selective for ribosomes that translate soluble and transmembrane proteins with long translocated segments. We then show that depletion of FKBP11 disrupts synthesis, specifically, of EpCam and Cathepsin Z, implicating a biogenesis function. We propose that FKBP11 acts as a translocon accessory factor involved in the biogenesis of a variety of membrane proteins at the ER.

While we have established a basic role for FKBP11 at the translocon, many questions remain on its function and mechanism. First, what are the binding domains of FKBP11 with the Sec61 complex or OST? From previous work (unpublished) it is clear that FKBP11 is not constitutively associated with Sec61 and thus must necessarily be recruited to the translocon. Second, what is the mechanism of FKBP11 depletion that results in decreased protein biogenesis in vivo? While, we have shown that a biogenesis defect occurs, a natural question is why that is. Is it a defect in glycosylation that leads to degradation or alternativcely a topogenesis defect? Third, what is the signal for the recruitment of FKBP11? Lastly, the identification of FKBP11 in engagement with the secretory translocon begs the question of differing classes of OST-bound translocons. Previously, we have shown that RAMP4 is associated with OST-bound translocons, yet the vast majority of these OST-translocons do not contain FKBP11. Thus, it appears that there are differing secretory translocons that must necessarily require different signals to recruit these accessory factors.

We are well positioned to answer these questions with the techniques we have utilized before. To understand FKBP11 recruitment, utilizing our in vitro stalled-substrate recruitment strategy, we can examine the timing of recruitment. EpCam, a proven substrate, of FKBP11 can be stalled at various lengths after the signal sequence, immunoprecipitated, and then utilizing SDS-PAGE and immunoblot, translocon components can be identified. By examining the dynamics of translocon recruitment, defining features that lead to FKBP11 recruitment can be determined. Similarly, utilizing EpCam as a model substrate, we can conduct in vitro glycosylation assays to examine differential glycosylation between WT and FKBP11 KO cells.

Further substrates can also be screened using this assay, allowing us to elucidate the exact defect that leads to in vivo degradation of EpCam in cells lacking FKBP11.

To answer the question of FKBP11 interaction with OST and Sec61, selective depletion of OST components may provide insights into FKBP11 interactions. Depletion of components followed by ribosome pelleting would provide clues into the binding of FKBP11 and how FKBP11 is able to associate with Sec61. One interesting possibility is the binding of FKBP11's lumenal domain to a protein that functions as an intermediary to interact with OST and Sec61. Alternatively, utilizing our native flag tagged immunoprecipitation strategy, we can perform single particle cryo-electron microscopy to determine a high-resolution structure of the FKBP11-bound translocon. Indeed, previous work has shown that OST-bound translocons contain unassigned density of multiple lumenal proteins (Gemmer et al. 2023) providing evidence that such a translocon should exist. This would provide definitive evidence of the position of FKBP11 and its interaction partners. Further cryo-EM structural studies of programmed ribosomes with stalled substrate intermediates would potentially provide us with mechanistic detail to then determine the function of FKBP11 and its role in membrane protein biogenesis.

7. Materials and Methods

7.1. Methods related to McGilvray et al. eLife (2020)

7.1.1. Antibodies

Antibodies against human TMCO1, Sec61β and TRAPα were characterized previously (Fons et al., 2003; Anghel et al., 2017; Görlich et al., 1992). Additional antibodies were obtained from the following sources: anti-EAAT1 (Santa Cruz, sc-515839), anti-Sec61α (Thermo Fisher, PA5-21773), anti-uL22 (Abgent, AP9892b), anti-STT3A (Novus, H00003703-M02), anti-Tubulin (Abcam, ab7291), anti-Integrin α5 (Cell signaling, 4705) anti-Nicalin (Bethyl, A305-623A-M), anti-TMEM147 (Thermo Fisher, PA5-95876), anti-NOMO (Thermo Fisher, PA5-47534), anti-CCDC47 (Bethyl, A305-100A), anti-TRAM1 (Abcam, ab190982), anti-Mouse rabbit HRP (Abcam, ab6708), anti-Rabbit donkey HRP (Sigma, SAB3700863), anti-Goat rabbit HRP (Sigma, A5420).

7.1.2. Isolation of TMCO1-ribosome complexes for interaction analysis

For mass spectrometry, approximately 2 × 108 of wild-type (control) and 3xFlag-TMCO1 cells were pelleted, resuspended in ice cold hypotonic lysis buffer (10 mM Hepes pH 7.4, 10 mM potassium acetate, 1 mM magnesium chloride) and incubated on ice for 15 min. Unless otherwise noted, all buffers included emetine at a final concentration of 50 µg/ml. Cells were lysed with 25 strokes of a pre-chilled dounce tissue grinder with a tight-fitting pestle, then 250 mM sucrose and 1 mM PMSF was added to the lysate. Nuclei were pelleted by centrifugation at 700 x g for 3 min. The membrane-containing supernatant was removed and put on ice. The pellet was washed with 1 ml ice cold assay buffer (50 mM Hepes pH 7.4, 250 mM sucrose, 250 mM potassium acetate, 10 mM magnesium chloride) and centrifuged again, and the

supernatant combined with the membrane fraction. Membranes were sedimented at 10,000 x g for 10 min at 4°C and resuspended in assay buffer to an A260 of ~50.

Monosomes were generated by treating the resuspended membranes with 1 mM calcium acetate and 10,000 U of micrococcal nuclease (NEB, M0247S), and incubating at 25°C for 10 min. Nuclease activity was stopped by adding EGTA to a final concentration of 2 mM. Membranes were solubilized in ice cold assay buffer supplemented with 2.5% digitonin (Calbiochem 11024-24-1) for 15 min on ice, and insoluble material was removed by centrifugation at 10,000 x g for 10 min at 4°C.

TMCO1-ribosome complexes were affinity purified by incubating solubilized material with M2 Flag affinity gel (Sigma, A2220) for 1 hr at 4°C with gentle end-over-end mixing. Unbound material was removed by centrifugation, the resin was washed twice with five bed volumes of ice-cold wash buffer (50 mM Hepes pH 7.4, 250 mM sucrose, 350 mM potassium acetate, 10 mM magnesium chloride, 0.25% digitonin), and twice with five bed volumes of assay buffer supplemented with 0.25% digitonin. Bound material was eluted in two successive 30 min incubations with two bed volumes of ice-cold assay buffer supplemented with 0.25% digitonin and 0.5 mg/ml 3xFlag peptide, at 4°C with gentle end-over-end mixing. The ribosome containing fraction was obtained by sedimenting the IP elutions through a 1 mL sucrose cushion (1 M sucrose, 150 mM potassium chloride, 50 mM Tris pH 7.5, 5 mM magnesium chloride, 0.1% digitonin) at 250,000 x g for 2 hr in a TLA100.3 rotor.

Ribosome pellets were resuspended in 50 mM Hepes pH 7.4, 100 mM sodium chloride, 1% SDS. Proteins were then methanol-chloroform extracted, FASP trypsin-digested, TMT-labeled and analysed in a single 180 min LC-MS/MS run at the Proteomics and Mass

Spectrometry Facility at Harvard University. Enrichment ratios were calculated as Flag IP/control IP for all peptides identified more than once.

Small-scale IPs were performed similarly, using microsomes isolated from stably integrated 3xFlag-TMCO1 or 3xFlag-Nicalin HEK293 cells.

7.1.3. RNA-seq immunoprecipitation analysis

Affinity purified TMCO1-ribosome complexes were isolated as described above ('Isolation of TMCO1-ribosome complexes for interaction analysis'), with the following changes. ~ 108 cells were processed for each of three biological replicates. All buffers were made using DEPC-treated RNase free water. Solubilized membranes were incubated with M2 Flag affinity gel (Sigma, A2220) for 2 hr at 4°C with end-over-end mixing. To remove contaminating DNA, 1 U RNase-Free DNase (Promega, M6101) was added to the sample during resin binding. Unbound material was removed and the resin was washed four times with five column volumes of wash buffer to remove contaminating ribosomes. TMCO1-ribosome complexes were isolated by centrifugation as before. After centrifugation, the final pellet was resuspended in 250 mM sucrose, 300 mM potassium acetate, 50 mM Hepes pH 7.4, 5 mM magnesium acetate, 50 µg/mL emetine and 0.1% digitonin, flash frozen and stored at −80°C until ready for sequencing.

All mRNA sequencing was performed at the University of Chicago Genomics Facility. For each of three biological replicates, RNA was extracted, ribosomal RNA was removed by RiboZero and cDNA libraries were prepared. Fragment sizes were determined by Bioanalyzer, and samples were pooled for sequencing on an Illumina HiSeq 4000. 50 bp single-end sequence reads were aligned to the human GRCh38 reference transcriptome using STAR (v2.6.1) (Dobin

et al., 2013) and gene transcript abundance was quantified by featureCounts using the Subread package (v1.6.3) (Liao et al., 2013). Possible batch effects were adjusted using the SVA package (Leek et al., 2012) in R. An IP enrichment score was calculated as follows: IP enrichment = (Flag IP abundance - Control IP abundance)/Total membrane abundance, where 'Total membrane abundance' was determined by mRNA sequencing the total membrane fraction in HEK293 TRex cells, as described below. Only genes with mean CPM higher than 0.5 were considered confidently identified and used in the analysis.

For mRNA sequencing of total membrane-associated mRNAs, membrane suspensions from three biological replicates of parental HEK293 TRex cells were prepared as above, with the inclusion of 1 U/mL SuperaseIn and 50 µg/mL emetine at all times. Membranes were washed twice with 250 mM sucrose, 150 mM potassium acetate, 50 mM Hepes pH 7.4, 5 mM magnesium acetate, 50 µg/mL emetine, and then RNA was Trizol extracted. For each biological replicate, ribosomal RNA was removed by Oligo-dT affinity purification and cDNA libraries were prepared, sequenced, and analysed as described above.

7.1.4. Cell culture

Flp-In T-REx 293 cells containing a 3xFlag-Cas9 construct were maintained in DMEM supplemented with 10% FBS (Gemini Foundation) and penicillin/streptomycin mixture (Invitrogen). TMCO1 knockout and 3xFlag-TMCO1 HEK293 cell lines have been described and characterized previously (Anghel et al., 2017). Nicalin and CCDC47 knockout cell lines were generated using the CRISPR/Cas9 system, in both parental and TMCO1 knockout backgrounds. Cas9 expression was induced by addition of 10 ng/mL doxycycline followed by transfection of sgRNAs targeting either Nicalin (ACGGAATGCAGTGCTGAACA) or CCDC47

(TCAGTGATTATGACCCGTT). Cells were grown for 48 hr, followed by single cell sorting into 96 well plates for clonal isolation. Nicalin and CCDC47 knockouts in parental and TMCO1 knockout backgrounds were verified by western blot and genomic DNA sequencing.

A TRAM1 knockout cell line was generated using the CRISPR/Cas9 system in Flp-In T-Rex 293 cells (Thermo Fisher) by transfecting a modified pX330 plasmid (Addgene) expressing human codon-optimized Cas9 and an sgRNA targeting TRAM1 (TTTGATGCCATAGTAATAAA). Single cells were isolated by sorting and allowed to grow clonally. The final TRAM1 knockout was verified by western blot and genomic DNA sequencing.

Stable cell lines overexpressing N-terminally 3xFlag tagged TMCO1 and Nicalin were generated by transfecting the respective knockout cell lines with a modified pEGFP-n1 plasmid (Addgene) encoding N-terminally 3xFlag-tagged TMCO1 or Nicalin (tag inserted after the signal peptide), under the control of a CMV promoter. Cells were transfected using the TransIT-293 transfection reagent (Mirus) and selected for 14 days by treatment with 0.7 mg/ml G418 (Invitrogen), with selection media changed every 3 days. Selected cells were maintained in DMEM supplemented with 10% FBS, penicillin/streptomycin, and 0.3 mg/ml G418. Expression was verified by western blot.

Cells were checked approximately every three months for mycoplasma contamination using the Universal Mycoplasma Detection Kit (ATCC), and were found to be negative.

7.1.5. Analysis of membrane protein expression levels and glycosylation patterns

For each replicate of the expression analysis, 750,000 cells were plated on poly-L-lysine coated plates and grown overnight. Cells were harvested by centrifugation, lysed using RIPA

buffer (1% triton, 0.5% deoxycholate, 0.1% SDS and 1X protease inhibitor cocktail), and EAAT1 protein levels analysed by SDS-PAGE and western blotting. Immunoblots were quantified using ImageJ (Schneider et al., 2012).

For EAAT1, Integrin α5 and TRAPα glycosylation analysis, RIPA cell lysates were reduced with 2% β−mercaptoethanol and denatured by heating for 10 min at 65°C. Samples were then incubated with EndoH (NEB) or PNGaseF (Promega) for 7 hr at 37°C, and analysed by SDS-PAGE and western blotting.

For mRNA quantitation, total RNA was Trizol extracted (Ambion). cDNA (1000 ng) was synthesized using gDNA Clear cDNA Synthesis Kit (Bio-rad). qPCR was performed using iTaq Universal SYBR Green Supermix (Bio-rad) via CFX96 Touch Real-Time PCR Detection System (Bio-rad). Primers used for mRNA quantification were: EAAT1 fwd 5'-TTCCTGGGGAACTTCTGATG-3', EAAT1 rev 5'-CCATCTTCCCTGATGCCTTA-3', GAPDH fwd 5'-ACAACTTTGGTATCGTGGAAGG-3', and GAPDH rev 5'-GCCATCACGCCACAGTTTC-3'.

7.2. Methods related to Sundaram, Yamsek, Zhong et al. Nature (2022)

7.2.1. Antibodies

Antibodies to human Sec61β (1:10,000 dilution), TRAPα (ref. 49; 1:5,000) and TMCO1 (ref. 9; 1:5,000) were described previously. Other antibodies were obtained from the following commercial sources: rabbit anti-nicalin (A305-623A-M; 1:1,000) and rabbit anti-CCDC47 (A305-100A; 1:2,000) from Bethyl Laboratories; mouse anti-HA (326700; 1:1,000), goat anti-NOMO (PA5-47534; 1:1,000), rabbit anti-TMEM147 (PA5-95876; 1:1,000), rabbit anti-Asterix (PA5-66788; 1:5,000), rabbit anti-C20Orf24 (PA5-43332; 1:1,000) and rabbit anti-Sec61α (PA5-

21773; 1:1,000) from Invitrogen; rabbit anti-uL22 from Abgent (AP9892b; 1:1,000); mouse anti-tubulin (ab11304; 1:1,000) and mouse anti-HRP (ab6728; 1:1,000) from Abcam; mouse anti-Flag (F1804; 1:1,000), rabbit anti-Flag (F7425; 1:1,000), rabbit anti-peroxidase (SAB3700863; 1:10,000) and goat anti-peroxidase (A5420; 1:20,000) from Sigma; mouse anti-STT3A (H00003703-M02; 1:1,000) from Novus Biologicals; mouse anti-BiP/GRP78 (610979; 1:1,000) from BD Biosciences. siRNAs were purchased from Thermo Fisher: negative control (4390843), TMCO1 (s29085), C20Orf24 (s31821), Asterix (s28089), CCDC47 (s32576), Nicalin (s32411) and TMEM147 (s20404).

7.2.2. Constructs

pcDNA5 GFP–P2A–RFP–ASGR1 and pcDNA5 AGTR2–GFP–P2A–RFP fluorescent reporter constructs were described previously (Chitwood et al. 2020). pcDNA5 EAAT1–GFP–P2A–RFP was constructed by Gibson cloning full-length human EAAT1 (amplified from a HEK293 cDNA library) into a modified pcDNA5/FRT/TO vector encoding a C-terminal GFP–P2A–RFP tag. pcDNA5 GFP–P2A–RFP–YIPF1 was generated by Gibson cloning a gBlock (IDT) into a modified pcDNA5/FRT/TO vector encoding an N-terminal GFP–P2A–RFP tag. Full-length constructs for in vitro translation (IVT) were generated by Gibson cloning gBlock (IDT) (YIPF1, ASGR1 and TMED2) or PCR fragments (EAAT1, KDELR1 and TRAM2) into a modified pSP64 vector encoding the desired N- or C-terminal Flag or HA tags. The 221-residue Flag–YIPF1(1–200)–Sec61β series was generated by Gibson cloning DNA fragments (Twist Biosciences) into a Flag–YIPF1 SP64 vector. The 142-residue Flag–ASGR1(1–61)–YIPF1(TM2)–Sec61β construct was generated by Gibson cloning into the parent Flag-ASGR1 SP64 vector. ASGR1(N79A) and YIPF1(N297A) substitutions were introduced using the

QuikChange II Site-Directed Mutagenesis Kits (Agilent). A full-length Flag–YIPF1 construct was Gibson cloned into a pcDNA5/FRT/TO vector for in vivo glycosylation assays. All constructs were confirmed by DNA sequencing.

7.2.3. Cell culture

Flp-In T-Rex 293 cells (Invitrogen) were maintained in DMEM supplemented with 10% FBS (Gemini Foundation), and 10,000 U ml−1 penicillin and 10 mg ml−1 streptomycin mixture (Invitrogen and Gemini). Cells were checked approximately every 6 months for mycoplasma contamination using the Universal Mycoplasma Detection Kit (ATCC), and were found to be negative. Single- and double-knockout (TMCO1, Nicalin and CCDC47) HEK293 cell lines were generated by CRISPR–Cas9 as previously described (McGilvray et al. 2020, Anghel et al. 2017). An STT3A-knockout cell line was generated similarly. Briefly, Cas9 expression was induced by addition of 10 ng ml−1 doxycycline followed by transfection of single guide RNA targeting STT3A (5'-TCGACATTCGGAATGTCTGT-3'). Cells were grown for 48 h, followed by single-cell sorting into 96-well plates for clonal isolation. Clones were verified by both western blot and genomic sequencing. Stable cell lines expressing N-terminally Flag-tagged TMCO1 and nicalin in the corresponding knockout background were described previously (McGilvray et al. 2020). A stable cell line expressing N-terminally Flag-tagged CCDC47 was generated similarly. Briefly, a CCDC47-knockout cell line was transfected with a modified pEGFP-n1 plasmid (Addgene) encoding N-terminally Flag-tagged CCDC47 (tag inserted after the signal peptide), under the control of a CMV promoter. Cells were transfected using TransIT-293 (Mirus) and selected in 0.7 mg ml−1 G418 (Invitrogen) for 2 weeks, changing the medium every 3 days. After selection, cells were maintained in medium supplemented with 0.3 mg ml−1 G418. Expression was verified

by western blot. Stably integrated doxycycline-inducible ASGR1 and AGTR2 reporter lines for flow cytometry analysis were described previously (Chitwood et al. 2020). Other reporter lines were generated similarly. Briefly, pcDNA5-based reporter constructs were co-transfected with pOG44 into Flp-In T-Rex 293 cells with TransIT-293, according to the manufacturer's protocol (Invitrogen), and cells were selected in 100 μg ml−1 hygromycin B for 2 weeks.

7.2.4. Preparation of rough microsomes

HEK293 cells were grown to about 80% confluency in 15-cm dishes, washed once with 5 ml ice-cold PBS (per plate) and collected by scraping in 2 × 5 ml of PBS. Cells were collected by centrifugation for 5 min at 500g and lysed in three volumes of hypotonic homogenization buffer (10 mM HEPES-KOH pH 7.5, 10 mM KOAc, 1 mM MgCl2) for 15 min on ice, with gentle agitation every few minutes. Cells were then homogenized by 15 strokes (up and down) in a chilled dounce tissue grinder. Sucrose was added to a final concentration of 250 mM and mixed gently. Nuclei and cell debris were removed by centrifugation at 700g for 3 min at 4 °C and the supernatant was collected. The pellet was resuspended in 5 ml of insertion buffer (50 mM HEPES-KOH pH 7.5, 250 mM sucrose, 250 mM KOAc, 10 mM MgCl2) and centrifuged again. The pooled supernatant fractions were centrifuged at 10,000g for 10 min at 4 °C. The supernatant was discarded, and the resulting membrane pellet was resuspended in insertion buffer (approximately 1 ml for about four plates). Microsomes (1-ml aliquots) were treated for 10 min at 37 °C with 4,000 U micrococcal nuclease (NEB), 2 U RNase-Free DNase (Promega), 1 mM CaCl2 and 0.5 mM phenylmethylsulfonyl fluoride (PMSF), followed by quenching with 2 mM EGTA. Microsomes were pelleted at 10,000g for 10 min at 4 °C and resuspended in 1 ml insertion buffer, 40 U SUPERaseIn and 0.1 mM EGTA, followed by centrifugation at 10,000g

for 10 min at 4 °C. The supernatant was discarded, and the membrane pellet was resuspended in insertion buffer supplemented with 50 U SUPERaseIn (per four plates). The preparation was finally adjusted with insertion buffer to an absorbance at 260 nm (A260nm) of about 50, and 50-µl aliquots were flash frozen in liquid nitrogen and stored at −80 °C for further use.

7.2.5. Interaction analysis in stably-integrated cells

Microsomes from wild-type cells and cells encoding Flag-tagged versions of TMCO1, CCDC47 or Nicalin were prepared as above, except that the micrococcal nuclease digestion was performed with 10,000 U of micrococcal nuclease (NEB), 3 U DNAse (Promega), 1 mM CaCl2 and 0.6 mM PMSF, and incubated at room temperature for 20 min before quenching with 2.5 mM EGTA. Microsomes (1 ml at A260nm = 50) were solubilized in insertion buffer supplemented with 2.5% digitonin and 1× protease inhibitor cocktail (Roche, 11836170001) for 45 min on ice and then diluted twice with 150 mM KOAc insertion buffer. Digitonin-solubilized microsomes were cleared by centrifugation at 12,500g for 15 min at 4 °C. The cleared supernatant (A260nm of about 3.5) was immunoprecipitated in batch format using 50 µl M2 Flag affinity beads (Sigma, A2220) and gentle agitation overnight at 4 °C. Flow-through was removed and beads were washed three times with eight column volumes of insertion buffer supplemented with 0.4% digitonin. Bound material was eluted twice, for 30 min on ice, with two column volumes of 200 mM KOAc insertion buffer supplemented with 0.5 mg ml−1 Flag peptide (ApexBio, A6001) and 0.4% digitonin. The eluate was collected using a pre-equilibrated spin filter column (Thermo Fisher, 69725). Ribosome-free and ribosome-bound fractions were obtained by pelleting the eluate through a 300-µl sucrose cushion (50 mM HEPES pH 7.4,

10 mM MgCl2, 150 mM KCl, 500 mM sucrose and 0.4% digitonin) at 355,000g for 1 h at 4 °C in a TLA120.1 rotor.

7.2.6. In vitro transcription and translation

In vitro transcription reactions utilized PCR-based templates containing an SP6 promoter, and were carried out at 40 °C for 1 h (Sharma et al. 2010). Unless otherwise noted, reactions contained 5–10 ng µl−1 PCR product, 40 mM HEPES pH 7.6, 6 mM MgCl2, 2 mM spermidine, 10 mM dithiothreitol, 500 µM ATP, 500 µM UTP, 500 µM CTP, 100 µM GTP, 0.5 mM m7G(5′)ppp(5′)G RNA Cap, 0.4 U µl−1 SUPERaseIn and 0.4 U µl−1 SP6 RNA Polymerase. IVT reactions were performed using a RRL system (Green Hectares). Translation reactions contained 20% (v/v) of the unpurified transcription reaction, 33% (v/v) haemin- and micrococcal nuclease-treated RRL, 0.2 µCi µl−1 [35S]methionine (or 40 µM methionine for non-radioactive IVT reactions), 0.1 mg ml−1 bovine liver transfer RNA, 13 mM HEPES, 10 mM creatine phosphate, 1 mM ATP, 1 mM GTP, 9 mM KOH, 25 mM KOAc, 1 mM MgCl2, 40 µM of the remaining 19 amino acids and 10% (v/v) HEK293-derived microsomes (typically A260nm about 50). Translation reactions were carried out for 45 min at 32 °C, unless otherwise noted.

7.2.7. Interaction analysis of stalled ribosome–nascent chain complexes in vitro

Templates for the synthesis of stalled N-terminally Flag-tagged substrates were PCR amplified using reverse primers encoding a terminal Met-Leu-Lys-Val (5'-CACCTTGAGCAT-3') sequence and lacking a stop codon. In vitro transcription and translation reactions were performed essentially as described above. Briefly, 100 µl of in vitro transcription mix containing 500 ng of purified PCR template was incubated for 1 h at 40 °C. Translation reactions of 500 µl contained 60 µl microsomes (A260nm of about 50) and 100 µl of the unpurified transcription

reaction, and were carried out for 50 min at 32 °C. The translation reactions were stopped by diluting them with 500 µl IVT stop buffer, and microsomes were pelleted at 12,500g for 10 min. Microsomes were washed again with 1 ml IVT stop buffer, centrifuged at 12,500g for 10 min, and resuspended with 500 µl IVT stop buffer. The resuspension was then treated with 5,000 U micrococcal nuclease (NEB), 1 mM CaCl2 and 0.6 mM PMSF at room temperature for 20 min. The reaction was stopped with 2.5 mM EGTA, and centrifuged at 12,500g for 10 min. The resulting membrane pellet was solubilized with 200 µl insertion buffer supplemented with 2.5% digitonin and 1× Protease Inhibitor for 45 min on ice, then diluted 2× with 150 mM KOAc insertion buffer, and cleared by centrifugation at 12,500g for 15 min. The cleared supernatant (A260nm of about 1.0) was incubated overnight at 4 °C with 20 µl M2 Flag affinity beads. Flow-through was removed and beads were washed 3 times with 18 column volumes of insertion buffer containing 0.4% digitonin and 200 mM KOAc. Bound material was eluted twice with two column volumes of 200 mM KOAc insertion buffer supplemented with 0.5 mg ml−1 Flag peptide and 0.4% digitonin, by incubating for 30 min each on ice. The eluate was collected using a pre-equilibrated spin filter column. Eluted material was layered over a 300-µl sucrose cushion (50 mM HEPES pH 7.4, 10 mM MgCl2, 150 mM KCl, 500 mM sucrose and 0.4% digitonin) and pelleted at 355,000g for 1 h at 4 °C in a TLA120.1 rotor. The ribosomal pellet was resuspended in a 35-µl sucrose cushion buffer, normalized by A260nm, and then analysed by SDS–PAGE and immunoblotting.

7.2.8. Carbonate extraction

IVT reactions (150 µl) synthesizing Flag–YIPF1 were diluted tenfold with IVT stop buffer and membranes were centrifuged for 10 min at 10,000g. The membrane pellets were

resuspended with 150 µl IVT stop buffer, and one-third of the reaction was reserved as the input fraction. The remaining material was incubated with 100 volumes of 100 mM Na2CO3 (pH 11.5) for 30 min on ice. The sample was centrifuged at 214,000g for 40 min in a TLA100.3 rotor to isolate membranes, and the supernatant was discarded. This was repeated once to remove contaminating proteins. The resulting carbonate-extracted membranes were resuspended with 1× LDS sample buffer for analysis.

7.2.9. Protease protection assays

YIPF1–HA was synthesized in three 150-µl IVT reactions either lacking or containing microsomes. Immediately following synthesis, the samples were diluted with ten volumes of IVT stop buffer. Microsome-containing samples were centrifuged at 10,000g for 10 min to pellet membranes and remove haemoglobin, and then resuspended to 150 µl with IVT stop buffer. All three samples were then split into three equal fractions for PK analysis. The untreated fractions (−PK) were set aside, and PK was added to the other samples (+PK) to a final concentration of 0.5 mg ml^{-1} and incubated on ice for 45 min. The digestion was quenched with 5 mM PMSF and incubated on ice for 5 min, followed by addition of ten volumes of boiling 1% SDS, 100 mM Tris pH 8 and 1× Roche cOmplete Protease inhibitor cocktail. For analysis of the total PK-treated fraction, samples containing microsomes were TCA-precipitated to concentrate membranes before SDS–PAGE analysis. For HA immunoprecipitations, samples were diluted tenfold with immunoprecipitation buffer (1× PBS, 250 mM NaCl, 0.5% (v/v) Triton X-100) and 30 µl HA agarose resin (Pierce, 26181) was added. Samples were incubated for 2 h at 4 °C with gentle agitation, washed three times with 1 ml of immunoprecipitation buffer, and eluted by adding 50 µl 1× LDS sample buffer and incubating at 70 °C for 10 min.

7.2.10. Glycosylation analysis in vitro

IVT reactions (35 µl) synthesizing HA–YIPF1, HA–ASGR1 or TMED2–HA were carried out for 50 min at 32 °C. Immediately following translation, microsomes were washed twice with 15 volumes of IVT stop buffer (50 mM HEPES pH 7.5, 200 mM NaCl, 10 mM $MgCl_2$) and then collected by centrifugation at 13,000g for 10 min. Membrane pellets were lysed with 35 µl IVT stop buffer containing 1.5% DDM for 30 min on ice, and centrifuged at 13,000g for 10 min. A 30 µl volume of lysed material was diluted with 75 µl of 3× LDS sample buffer containing 2% β-ME, heated at 65 °C for 10 min, and then analysed by SDS–PAGE and immunoblotting. Reactions without microsomes (30 µl) were supplemented with 1.5% DDM, diluted with 100 µl of 3× LDS sample buffer containing 2% β-ME, and loaded at one-tenth the amount relative to the microsome samples.

7.2.11. Glycosylation analysis in cells

At 24 h before transfection, wild-type, ΔTMCO1, Δnicalin and ΔCCDC47 HEK293 cells were seeded at 400,000 cells per well onto a poly-lysine-coated 6-well plate, in triplicate. A transfection mixture containing 1 µg pcDNA5 Flag–YIPF1, 150 µl Opti-MEM and 3 µl TransIT-293 was incubated at room temperature for 25 min before being added dropwise to each well. A final concentration of 1 ng ml−1 doxycycline was added to induce Flag–YIPF1. Following 12 h of induction, cells were collected by scraping with chilled 1× PBS. Cells were pelleted at 500g for 5 min and resuspended in 100 µl RIPA buffer (50 mM Tris pH 7.4, 150 mM NaCl, 1% NP-40, 0.5% sodium deoxycholate, 0.1% SDS, 1 mM PMSF, 1× Roche cOmplete Protease Inhibitor Cocktail). RIPA lysis samples were incubated on ice for 15 min and gently vortexed every 5 min.

The samples were centrifuged at 15,000g for 10 min, and the supernatant was collected for SDS–PAGE and western blot analysis.

7.2.12. Flow cytometry analysis of reporter cell lines

The effect of different siRNAs on stably expressed reporter cell lines was analysed using flow cytometry as described previously (Chitwood et al. 2020). siRNA depletion was performed over a period of about 72 h using the Lipofectamine RNAiMAX reagent (Thermo Fisher) according to the manufacturer's instructions. Briefly, a first round of siRNA treatment was performed in the presence of DMEM and 10% tetracycline-free FCS. Cells were incubated for 48 h, and then a second round of siRNA treatment was performed. After a second incubation of about 24 h, expression of fluorescent reporter constructs was induced with 1,000 ng/mL doxycycline for 6 h before analysis by flow cytometry. In all experiments the cells were collected by trypsinization, washed once in ice-cold PBS, and then resuspended 1 ml of PBS. Cells were passed through a 70-μm filter before flow cytometry analysis using a Becton Dickinson LSRII instrument. Live cells were gated by forward and side scatter. Additional gating for relatively high levels of the soluble fluorescent protein reporter was used to focus on the population of cells with productive translation of reporter constructs. Between 15,000 and 30,000 GFP-positive (EAAT1 and AGTR2) or RFP-positive (ASGR1 and YIPF1) cells were collected. Data were analysed using FlowJo (version 10.8).

7.3. Methods relating to RAMP4

7.3.1. Construction of RAMP4 KO and 3xFlag-Tagged RAMP4 cells

Flp-In T-Rex 293 cells (Invitrogen) were maintained in DMEM supplemented with 10% FBS (Gemini Foundation), and 10,000 U ml−1 penicillin and 10 mg ml−1 streptomycin mixture (Invitrogen and Gemini). A RAMP4-knockout cell line was generated similar to previous CRISPR KO's (McGilvray et al. 2020). Briefly, transfection of px459 plasmid containing a guide RNA targeting RAMP4 (5'-AGCAAAGGATCCGTATGGCC-3') and Cas9 was done according to manufacturer's instructions. Cells were selected for 1 week in 1 ug/mL puromycin followed by single-cell sorting into 96-well plates for clonal isolation. Clones were verified by both western blot and genomic sequencing. Stably integrated doxycycline-inducible 3xFlag-TMCO1 and 3xFlag-RAMP4 cell lines were generated utilizing the FRT-Flp In system as described previously (Sundaram, Yamsek, Zhong, et al., 2022). Briefly, pcDNA5-based 3xFlag-TMCO1 and 3xFlag-RAMP4 constructs were co-transfected with pOG44 into Flp-In T-Rex 293 cells with TransIT-293, according to the manufacturer's protocol (Invitrogen), and cells were selected in 100 μg ml−1 hygromycin B for 2 weeks.

7.3.2. Preparation of rough microsomes

Microsomes were prepared identically as described in section 10.2.4.

7.3.3. Interaction analysis in cells

Analysis was done as previously described in section 10.2.5. with the exception of 3xFlag-tagged TMCO1 and RAMP4 cells.

7.3.4. In vitro transcription and translation

Experiments were done as previously described in section 10.2.6.

7.3.5. Interaction analysis of stalled ribosome-nascent chain complexes in vitro

Analysis was done as previously described in section 10.2.7.

7.3.6. Flow cytometry analysis

The effect of RAMP4 knockout cells on transiently transfected reporter constructs using flow cytometry is as described previously (Guna et al., 2018; Chitwood et al., 2018). Briefly, 300,000 cells were plated for transfection per well in a 6-well plate. After 24 hours, transfection of reporter constructs was conducted according to manufacturer's instructions. 200 ng of reporter plasmid, 4 uL Trans-IT 293 (Mirus Bio), and 250 uL of Opti-Mem (Life Technologies) was transfected. Cells were incubated for 24 hours, split 1:2 and induced with 100 ng of doxycycline.

In all experiments the cells were collected by trypsinization, washed once in ice-cold PBS, and then resuspended 1 ml of PBS. Cells were passed through a 70-μm filter before flow cytometry analysis using a Becton Dickinson LSRII instrument. Live cells were gated by forward and side scatter. Additional gating for relatively high levels of the soluble fluorescent protein reporter was used to focus on the population of cells with productive translation of reporter constructs. Between 15,000 and 30,000 RFP-positive (ASGR1 and SQS) cells were collected. Data were analysed using FlowJo (version 10.8).

7.4. Methods related to DiGuilio, et al. (in submission)

7.4.1. Cell culture

Flp-In T-Rex 293 cells (Invitrogen) were maintained in DMEM supplemented with 10% FBS (Gemini Foundation), and 10,000 U/ml penicillin and 10 mg/ml streptomycin mixture (Invitrogen and Gemini). Cells were checked approximately every 6 months for mycoplasma contamination using the Universal Mycoplasma Detection Kit (ATCC) and were found to be negative.

An FKBP11 knockout cell line was generated using the CRISPR/Cas9 system in Flp-In T-Rex 293 cells (Thermo Fisher) by transfecting a modified pX330 plasmid (Addgene) expressing human codon-optimized Cas9 and an sgRNA targeting FKBP11. Single cells were isolated by sorting and allowed to grow clonally. The final FKBP11 knockout was verified by western blot and genomic DNA sequencing. A STT3A-knockout cell line has previously been characterized (Sundaram, Yamsek, Zhong et al., 2022).

A doxycycline-inducible 3xFlag-FKBP11 cell line was generated in the FKBP11 knockout background by co-transfection of pOG44 and pcDNA5/FRT/TO/3xFlag-FKBP11 in a 9:2 ratio with TransIT-293 (Mirus Bio). After 24 hrs, cells were selected 100 ug/mL hygromycin for at least 2 weeks until transfection control cells cultured in parallel were dead. Doxycycline induction was optimized to obtain near-endogenous 3xFlag-FKBP11 levels after 24 hrs of treatment.

7.4.2. Preparation of rough microsomes

Rough microsomes (RMs) were isolated from wild-type (WT) and 3xFlag-FKBP11 cells treated with 0.05 ng/ml doxycycline for 24 hr prior to harvest. Cells were harvested in ice-cold

PBS and centrifuged at 500g for 5 min. The cell pellet was resuspended in 3.5 volumes of hypotonic lysis buffer (10 mM HEPES pH 7.4, 10 mM potassium acetate, 1 mM magnesium chloride), incubated on ice for 20 minutes with occasional shaking and dounce homogenized (pestle tightness B) for 18 strokes. Lysates were centrifuged twice at 700g for 3 min at 4 °C to remove nuclei. Supernatant was centrifuged at 10000g for 10 min at 4 °C. The RM pellet was resuspended in assay buffer (50 mM HEPES pH 7.4, 250 mM potassium acetate, 10 mM magnesium chloride and 250 mM sucrose) and centrifuged at 10000g for 10 min at 4 °C. The RM pellet was resuspended with assay buffer supplemented with additional aprotinin and leupeptin, 1 mM CaCl2, 4,000 U micrococcal nuclease (NEB), 2 U RNase-Free DNase (Promega), and incubated at 37 °C for 40 min. Digestion was quenched with a 2-fold molar excess of EGTA. RMs were centrifuged at 10000g for 10 min, washed 1x in AB, resuspended in 4x RM pellet volume of AB supplemented with 250 mM sucrose, and then snap frozen for further analysis. For RIP-seq, RMs were prepared as above except that no MNase was used.

7.4.3. Ribosome pelleting

Rough microsomes isolated from WT or ΔSTT3A cells (1 mL at A260 = 50) were solubilized in solubilization buffer (50 mM HEPES pH 7.4, 250 mM sucrose, 250 mM potassium acetate, 10 mM magnesium chloride, 2.5% digitonin) for 1 hour on ice with gentle mixing and then diluted twice with 150 mM KOAc buffer (50 mM HEPES pH 7.4, 250 mM sucrose, 150 mM potassium acetate, 10 mM magnesium chloride). After removing insoluble material by centrifugation for 15 min at 13,000g, the cleared supernatant was layered over a 1-mL sucrose cushion (50 mM HEPES pH 7.4, 10 mM MgCl2, 150 mM KCl, 500 mM sucrose and 0.4% digitonin) and pelleted at 355,000g for 1 h at 4 °C in a TLA 100.3 rotor. The ribosomal pellet

was resuspended in a 500-µl sucrose cushion buffer (50 mM HEPES pH 7.4, 10 mM MgCl2, 150 mM KCl, 500 mM sucrose and 0.4% digitonin), normalized by A260nm, and then analysed by SDS–PAGE and immunoblotting.

7.4.4. Sucrose gradient fractionation

Micrococcal nuclease treated microsomes from doxycycline-induced 3xFlag-FKBP11 (0.05 ng/mL) and doxycycline induced 3xFlag-FKBP11-ΔTMD-HDEL (0.1 ng/mL) cells were solubilized in solubilization buffer (50 mM HEPES pH 7.4, 250 mM sucrose, 150 mM potassium acetate, 10 mM magnesium chloride, 2.5% digitonin) for 40 min on ice with gentle mixing. After removing insoluble material by centrifugation for 15 min at 10,000g, the cleared supernatant was overlaid on a 10-40% sucrose gradient and centrifuged at 28,000 rpm in a SW28.1 rotor for 8 hours at 4 °C. Nineteen ~900 µL fractions were collected, TCA precipitated, resuspended in sample loading buffer and analysed by SDS- PAGE and immunoblotting.

7.4.5. Affinity purification of FKBP11-ribosome complexes

Microsomes from WT and doxycycline-induced 3xFlag-FKBP11 cells were solubilized in Solubilization Buffer for 40 min on ice with gentle mixing. Insoluble material was removed by centrifugation for 10 min at 10000g, and the cleared supernatant was immunoprecipitated in batch format using M2 Flag affinity beads (Sigma, A2220). After incubating with gentle end-over-end rotation for 1 hr at 4 °C and 30 min at room temperature (with freshly added protease inhibitors), beads were washed three times with 18 column volumes of Wash Buffer (50 mM HEPES pH 7.4, 250 mM sucrose, 350 mM potassium acetate, 10 mM magnesium chloride, 0.2% digitonin). Bound material was eluted twice, for 30 min at 4 °C with gentle end-over-end rotation, using 2 column volumes of Wash Buffer supplemented with 0.5 mg/ml Flag peptide.

The eluate was collected using a pre-equilibrated spin filter column. To isolate the ribosome-bound fraction, the eluate was layered over a 1 ml sucrose cushion (1 M sucrose, 150 mM potassium chloride, 50 mM Tris pH 7.5, 5 mM magnesium chloride, 0.2% digitonin) and centrifuged at 250,000g in a TLA100.3 rotor for 2 hr at 4°C. Pellets were resuspended in Resuspension Buffer (50 mM HEPES pH 7.4, 150 mM potassium acetate, 5 mM magnesium chloride, 0.2% digitonin) and normalized by absorbance at 260 nm.

7.4.6. Mass Spectrometry

Affinity-purified FKB11-ribosome complexes were prepared from WT and doxycycline-induced 3xFlag-FKBP11 cells as described above, in three biological replicates. Samples were spiked with 20 µL 10x stock of TCEP and chloroacetamide to reach final concentrations of the chemicals of 10 and 40 mM, respectively. The mixtures were vortexed for 10 min, and 2 µL of MS grade trypsin (Promega) was added to each sample. The samples were digested overnight at the ambient temperature on a rocker. An additional 1 µL of trypsin was added to each sample in the morning, and the samples were incubated for an additional 2 hours. The final peptide mixtures were acidified by the addition of 10% TFA to a final concentration of 1% and briefly spun down to precipitate digitonin using a benchtop centrifuge. The supernatants were desalted using 10 mg StrataX SPE cartridges (Phenomenex), and the desalted peptides were lyophilized to dryness in a SpeedVac (Thermo Fisher).

Each sample was resuspended in 25 µL 0.2% formic acid in HPLC-MS grade water (Fisher Scientific). Peptide concentrations of the samples were obtained using NanoDrop at A280. The volumes corresponding to 1 µg of peptides of each sample were injected on a 75 µm ID x 360 µm OD column packed in-house [DOI: 10.1021/acs.analchem.8b02766] with 1.7 µm

BEH C18 particles (Waters) to the final length of 35 cm. The column was kept at 50°C, and the peptides were separated over a 60 min gradient using Dionex nanoMate 3000 at the flow rate of 335 nL/min with mobile phase A consisting of 0.2% formic acid and mobile phase B consisting of 0.2% formic acid in 70% acetonitrile. The peptides were ionized into Orbitrap Eclipse (Thermo Scientific) for analysis. MS1 scans were obtained in the Orbitrap at resolution of 240,000, a maximum injection time (max IT) of 50 ms, and over the range of 300-1,350 m/z. Precursor ions with charge states of +2 to +5 were isolated in the quadrupole with 0.5 Da isolation window and fragmented at normalized collision energy of 25%. Subsequent MS2 analysis was performed in the ion trap using turbo scan with max IT of 17 ms over the range of 150-1,350 m/z with APD enabled. Dynamic exclusion was set to 15 s.

RAW files were searched in MaxQuant (version 1.6.10.43) [DOI: 10.1038/nbt.1511], against the reviewed database of human proteins and their isoforms (Homo sapiens, downloaded from Uniprot). All parameters were set to defaults, except for LFQ quantification was enabled with the minimum ratio count of 1, and match-between-runs was enabled. Protein group list was filtered for reverse identifications, contaminants, and entries "identified by site only." Protein groups containing missing values (zeros) in more than 50% of samples were removed. The remaining missing values were imputed using the web-based tool Argonaut [DOI: 10.1016/j.patter.2020.100122] , which was also used to share and explore the dataset.

7.4.7. RNA-seq immunoprecipitation analysis

All mRNA sequencing was performed at the University of Chicago Genomics Facility. Samples were obtained in biological replicates, starting from WT and 3xFlag-FKBP11 microsomes prepared as described above, but without micrococcal nuclease treatment. Affinity-

purified FKBP11-ribosome complexes were obtained as described above, but using RNAse-free water and including Superasin in the Solubilization and Wash buffers; mRNA was isolated by Trizol extraction and oligo-dT purification. Total membrane-associated mRNAs were isolated similarly. After cDNA library preparation, fragment sizes were determined by Bioanalyzer, and samples were pooled for sequencing on an Illumina HiSeq 4000.

Analysis was done at the University of Chicago CRI Bioinformatics Core Facility. 102 bp pair-end sequence reads were trimmed using Trimmomatic (v0.36) (Bolger et al., 2014) and trimmed reads were aligned to human GRCh38 reference transcriptome using STAR (v2.7.3a) (Dobin et al., 2013). Gene transcript abundance was quantified by featureCounts using the Subread package (v1.6.4) (Liao et al., 2013). Only genes with a mean CPM higher than 0.5 (from two or three biological replicates) were considered confidently identified and used in the analysis. Enrichment scores were calculated as follows: Enrichment = (IP abundance/Total membrane abundance)Flag / (IP abundance/Total membrane abundance)WT.

7.4.8. Analysis of steady-state expression levels

The effect of different siRNAs on the steady-state levels of endogenous EpCAM and cathepsin Z (CTSZ) was monitored by SDS-PAGE and western blot. WT HEK293 cells were cultured in 6-well plates and siRNA depletion was performed over a period of 72 hours using ThermoFisher Lipofectamine RNAiMAX reagent. A first round of siRNA treatment was performed in the presence of DMEM and 10% tetracycline-free FCS using a transfection mixture of 3 µl siRNA at 10 µM, 4 µl transfection reagent, and 300 µL ThermoFisher Gibco Opti-MEM. After incubation for 48 hours, cells were reseeded on a new plate and a second round of identical siRNA treatment was performed. After 24 hours, cells were harvested using trypsinization,

washed in ice-cold PBS, and lysed in RIPA buffer for 30 min on ice. The relative concentration of whole cell lysate was analysed using stain-free gel imaging, and normalized protein loads were run in SDS-PAGE cells. Western blot was used to probe the relative expression levels of endogenous EpCAM and CTSZ, and to verify knockdown of FKBP11 and FKBP2.

7.4.9. Flow cytometry analysis of reporter cell lines

The effect of different siRNAs on a stably expressed EpCAM-GFP-2A-RFP reporter cell line was analysed by flow cytometry as described previously (Chitwood, 2020, Sundaram, Yamsek, Zhong et al., 2022). siRNA depletion was performed as above. 8 hrs prior to analysis, expression of the fluorescent reporter construct was induced with 100 ng/ml doxycycline. Cells were then collected by trypsinization, washed once in ice-cold PBS, resuspended in 1 ml PBS, and passed through a 70 µm filter. Flow cytometry was performed using a Becton Dickinson LSRII 4-15 instrument. Live cells were gated by forward and side scatter. Additional gating for relatively high levels of the soluble fluorescent protein reporter (RFP) was used to focus on the population of cells with productive translation of the reporter construct. Between 15,000 and 20,000 RFP-positive cells were collected. Data were analysed using FlowJo (version 10.8.1).

References

1. Akopian, D., Shen, K., Zhang, X. & Shan, S. O. Signal recognition particle: An essential protein-targeting machine. Annual Review of Biochemistry **82**, 693–721 (2013).

2. Alanay, Y. et al. TMCO1 deficiency causes autosomal recessive cerebrofaciothoracic dysplasia. American Journal of Medical Genetics, Part A **164**, 291–304 (2014).

3. Almedom, R. B. et al. An ER-resident membrane protein complex regulates nicotinic acetylcholine receptor subunit composition at the synapse. EMBO Journal **28**, 2636–2649 (2009).

4. Almén, M. S., Nordström, K. J. V., Fredriksson, R. & Schiöth, H. B. Mapping the human membrane proteome: A majority of the human membrane proteins can be classified according to function and evolutionary origin. BMC Biology **7**, 50 (2009).

5. Anghel, S. A., McGilvray, P. T., Hegde, R. S. & Keenan, R. J. Identification of Oxa1 Homologs Operating in the Eukaryotic Endoplasmic Reticulum. Cell Reports **21**, 3708–3716 (2017).

6. Attwood, M. M., Krishnan, A., Almén, M. S. & Schiöth, H. B. Highly diversified expansions shaped the evolution of membrane bound proteins in metazoans. Scientific Reports **7**, (2017).

7. Bai, L., You, Q., Feng, X., Kovach, A. & Li, H. Structure of the ER membrane complex, a transmembrane-domain insertase. Nature **584**, 475–478 (2020).

8. Barlowe, C. K. & Miller, E. A. Secretory protein biogenesis and traffic in the early secretory pathway. Genetics **193**, 383–410 (2013).

9. Bernstein, H. D. et al. Model for signal sequence recognition from amino acid sequence of 54k subunit of signal recognition particle. Nature **340**, 482–486 (1989).

10. Bischoff, L., Wickles, S., Berninghausen, O., Van Der Sluis, E. O. & Beckmann, R. Visualization of a polytopic membrane protein during SecY-mediated membrane insertion. Nature Communications **5**, (2014).

11. Blobel, G. Intracellular protein topogenesis (protein translocation across membranes/protein integration into membranes/posttranslocational sorting/topogenic sequences/ phylogeny of membranes and compartments). Cell Biology vol. 77 1496–1500 https://www.pnas.org (1980).

12. Blomen, V. A. et al. Gene essentiality and synthetic lethality in haploid human cells. Science **350**, 1092–1096 (2015).

13.
Bonnefoy, N., Fiumera, H. L., Dujardin, G. & Fox, T. D. Roles of Oxa1-related inner-membrane translocases in assembly of respiratory chain complexes. Biochimica et Biophysica Acta - Molecular Cell Research **1793**, 60–70 (2009).

14.
Bonnefoy, N., Chalvet, F., Hamel, P., Slonimski, P. & Dujardin, G. OXA1, a Saccharomyces cerevisiae Nuclear Gene whose Sequence is Conserved from Prokaryotes to Eukaryotes Controls Cytochrome Oxidase Biogenesis. J. Mol. Bio **239**, 201–212 (1994).

15.
Borowska, M. T., Dominik, P. K., Anghel, S. A., Kossiakoff, A. A. & Keenan, R. J. A YidC-like Protein in the Archaeal Plasma Membrane. Structure **23**, 1715–1724 (2015).

16.
Bozkurt, G. et al. Structural insights into tail-anchored protein binding and membrane insertion by Get3. (MAC Pub, 2009).

17.
Bozkurt, G. et al. The structure of Get4 reveals an α-solenoid fold adapted for multiple interactions in tail-anchored protein biogenesis. FEBS Letters **584**, 1509–1514 (2010).

18.
Braunger, K. et al. Structural basis for coupling protein transport and N-glycosylation at the mammalian endoplasmic reticulum. https://www.science.org.

19.
Brodsky, J. L., Goeckeler, J. & Schekmantt, R. BiP and Sec63p are required for both co-and posttranslational protein translocation into the yeast endoplasmic reticulum (DnaJ/heat shock proteins/70-kDa heat shock protein). Cell Biology vol. 92 9643–9646 https://www.pnas.org (1995).

20.
Burdon, K. P. et al. Genome-wide association study identifies susceptibility loci for open angle glaucoma at TMCO1 and CDKN2B-AS1. Nature Genetics **43**, 574–578 (2011).

21.
Caglayan, A. et al. Whole-exome sequencing identified a patient with TMCO1 defect syndrome and expands the phenotic spectrum. Clinical Genetics **84**, 394–395 (2013).

22.
Canul-Tec, J. C. et al. Structure and allosteric inhibition of excitatory amino acid transporter 1. Nature **544**, 446–451 (2017).

23.
Chartron, J. W., M Suloway, C. J., Zaslaver, ayan & Clemons, W. M. Structural characterization of the Get4/Get5 complex and its interaction with Get3. (2010) doi:10.1073/pnas.1006036107/-/DCSupplemental.

24.
Chavan, M., Yan, A. & Lennarz, W. J. Subunits of the translocon interact with components of the oligosaccharyl transferase complex. Journal of Biological Chemistry **280**, 22917–22924 (2005).

25.

Cherepanova, N. A., Shrimal, S. & Gilmore, R. Oxidoreductase activity is necessary for N-glycosylation of cysteine-proximal acceptor sites in glycoproteins. Journal of Cell Biology **206**, 525–539 (2014).

26. Cherepanova, N. A., Venev, S. V., Leszyk, J. D., Shaffer, S. A. & Gilmore, R. Quantitative glycoproteomics reveals new classes of STT3A- And STT3B-dependent N-glycosylation sites. Journal of Cell Biology **218**, 2782–2796 (2019).

27. Chevet, E. et al. Phosphorylation by CK2 and MAPK enhances calnexin association with ribosomes. EMBO Journal **18**, 3655–3666 (1999).

28. Chitwood, P. J. & Hegde, R. S. An intramembrane chaperone complex facilitates membrane protein biogenesis. Nature **584**, 630–634 (2020).

29. Chitwood, P. J., Juszkiewicz, S., Guna, A., Shao, S. & Hegde, R. S. EMC Is Required to Initiate Accurate Membrane Protein Topogenesis. Cell **175**, 1507-1519.e16 (2018).

30. Cioffi, J. A., Allen, K. L., Lively, M. O. & Kemper, B. Parallel effects of signal peptide hydrophobic core modifications on co-translational translocation and post-translational cleavage by purified signal peptidase. Journal of Biological Chemistry **264**, 15052–15058 (1989).

31. Connolly, T. & Gilmore, R. The Signal Recognition Particle Receptor Mediates the GTP-Dependent Displacement of SRP from the Signal Sequence of the Nascent Polypeptide. Cell vol. 57 599–610 (1969).

32. Conti, B. J., Devaraneni, P. K., Yang, Z., David, L. L. & Skach, W. R. Cotranslational Stabilization of Sec62/63 within the ER Sec61 Translocon Is Controlled by Distinct Substrate-Driven Translocation Events. Molecular Cell **58**, 269–283 (2015).

33. Conti, B. J., Elferich, J., Yang, Z., Shinde, U. & Skach, W. R. Cotranslational folding inhibits translocation from within the ribosome-Sec61 translocon complex. Nature Structural and Molecular Biology **21**, 228–235 (2014).

34. Cui, X. A., Zhang, H. & Palazzo, A. F. P180 promotes the ribosome-independent localization of a subset of mRNA to the endoplasmic reticulum. PLoS Biology **10**, (2012).

35. Dalbey, R. E., Kuhn, A., Zhu, L. & Kiefer, D. The membrane insertase YidC. Biochimica et Biophysica Acta - Molecular Cell Research **1843**, 1489–1496 (2014).

36. Denic, V., Dötsch, V. & Sinning, I. Endoplasmic reticulum targeting and insertion of tail-anchored membrane proteins by the GET pathway. Cold Spring Harbor Perspectives in Biology **5**, (2013).

37.

Deshaies, R. J., Sanders, S. L., Feldheim, D. A., & Schekman Randy. Assembly of yeast Sec proteins involved in translocation into the endoplasmic reticulum into a membrane-bound multisubunit complex. Nature **349**, 806–808 (1991).

38. Deshaies, R. & Schekman, R. A Yeast Mutant Defective at an Early Stage in Import of Secretory Protein Precursors into the Endoplasmic Reticulum. 633–645 (1987).

39. Dettmer, U. et al. Transmembrane protein 147 (TMEM147) is a novel component of the Nicalin-NOMO protein complex. Journal of Biological Chemistry **285**, 26174–26181 (2010).

40. Devaraneni, P. K. et al. Stepwise insertion and inversion of a type II signal anchor sequence in the ribosome-Sec61 translocon complex. Cell **146**, 134–147 (2011).

41. Dudek, J. et al. ERj1p has a basic role in protein biogenesis at the endoplasmic reticulum. Nature Structural and Molecular Biology **12**, 1008–1014 (2005).

42. Ernst, S., Schönbauer, A. K., Bär, G., Börsch, M. & Kuhn, A. YidC-driven membrane insertion of single fluorescent Pf3 coat proteins. Journal of Molecular Biology **412**, 165–175 (2011).

43. Evans, E. A., Gilmoret, R., Blobel, G. & Robbins, P. Purification of microsomal signal peptidase as a complex (canine pancreatic microsomes/posttranslational precursor processing/gradient sievorptive chromatography/multisubunit membrane protein/glycoprotein subunits)'-Dimethoxybenzidine dihydrochloride was from East-man Kodak. Streptomyces griseus endo-p3-N-acetylglucosa-minidase H (EC 3.2.1.96) was a gift from. vol. 83 581–585 https://www.pnas.org (1986).

44. Fons, R. D., Bogert, B. A. & Hegde, R. S. Substrate-specific function of the translocon-associated protein complex during translocation across the ER membrane. Journal of Cell Biology **160**, 529–539 (2003).

45. Fredriksson, R. & Schiöth, H. B. The repertoire of G-protein-coupled receptors in fully sequenced genomes. Molecular Pharmacology **67**, 1414–1425 (2005).

46. Ge, Y., Draycheva, A., Bornemann, T., Rodnina, M. V. & Wintermeyer, W. Lateral opening of the bacterial translocon on ribosome binding and signal peptide insertion. Nature Communications **5**, (2014).

47. Gemmer, M. et al. Visualization of translation and protein biogenesis at the ER membrane. Nature **614**, 160–167 (2023).

48. Gogala, M. et al. Structures of the Sec61 complex engaged in nascent peptide translocation or membrane insertion. Nature **506**, 107–110 (2014).

49.

Gorlich, D., Prehn, S., Hartmann, E., Kalies, K.-U. & Rapoport', T. A. A Mammalian Homolog of SEC6lp and SECYp Is Associated with Ribosomes and Nascent Polypeptides during Translocation. Cell vol. 71 499–503 (1992).

50. Gorlich, D. & Rapoport, T. A. Protein Translocation into Proteoliposomes Reconstituted from Purified Components of the Endoplasmic Reticulum Membrane. Cell vol. 75 615–630 (1993).

51. Guna, A., Volkmar, N., Christianson, J. C. & Hegde, R. S. The ER membrane protein complex is a transmembrane domain insertase. https://www.science.org.

52. Haffner, C. et al. Nicalin and its binding partner Nomo are novel Nodal signaling antagonists. EMBO Journal **23**, 3041–3050 (2004).

53. Halic, M. et al. Structure of the signal recognition particle interacting with the elongation-arrested ribosome. http://www.rna.icmb.utexas.edu/ (2004).

54. Halic, M. et al. Signal recognition particle receptor exposes the ribosomal translocon binding site. Science **312**, 745–747 (2006).

55. HARTMANN, E. et al. A tetrameric complex of membrane proteins in the endoplasmic reticulum. European Journal of Biochemistry **214**, 375–381 (1993).

56. He, S. & Fox, T. D. Membrane Translocation of Mitochondrially Coded Cox2p: Distinct Requirements for Export of N and C Termini and Dependence on the Conserved Protein Oxalp. Molecular Biology of the Cell vol. 8 1449–1460 (1997).

57. Hegde, R. S. & Keenan, R. J. The mechanisms of integral membrane protein biogenesis. Nature Reviews Molecular Cell Biology **23**, 107–124 (2022).

58. Heinrich, S. U., Mothes, W., Brunner, J. & Rapoport, T. A. The Sec61p Complex Mediates the Integration of a Membrane Protein by Allowing Lipid Partitioning of the Transmembrane Domain or TM sequence is inserted into the channel (for review, see Matlack et al., 1998). In the case of a signal se-quence, the hydrophobic segment binds in an N cyt C lum (cyt, cytosol; lum, lumenal) orientation to a specific site at the interface between the channel and lipid formed. Cell vol. 102 233–244 (2000).

59. Hell, K., Neupert, W. & Stuart, R. A. Oxa1p acts as a general membrane insertion machinery for proteins encoded by mitochondrial DNA. EMBO Journal **20**, 1281–1288 (2001).

60. Heo, P., Culver, J. A., Miao, J., Pincet, F. & Mariappan, M. The Get1/2 insertase forms a channel to mediate the insertion of tail-anchored proteins into the ER. Cell Reports **42**, (2023).

61. Hessa, T. et al. Recognition of transmembrane helices by the endoplasmic reticulum translocon. www.nature.com/nature (2005).

62.
Hori, O. et al. Deletion of SERP1/RAMP4, a Component of the Endoplasmic Reticulum (ER) Translocation Sites, Leads to ER Stress. Molecular and Cellular Biology **26**, 4257–4267 (2006).
63.
Itskanov, S. & Park, E. Structure of the posttranslational Sec protein-translocation channel complex from yeast. https://www.science.org (2019).
64.
Itskanov, S. et al. A common mechanism of Sec61 translocon inhibition by small molecules 1 2. doi:10.1101/2022.08.11.503542.
65.
Jaskolowski, M. et al. Molecular basis of the TRAP complex function in ER protein biogenesis. Nature Structural and Molecular Biology **30**, 770–777 (2023).
66.
Jonikas, M. C. et al. Comprehensive characterization of genes required for protein folding in the endoplasmic reticulum. Science **323**, 1693–1697 (2009).
67.
Jung, S. jun, Jung, Y. & Kim, H. Proper insertion and topogenesis of membrane proteins in the ER depend on Sec63. Biochimica et Biophysica Acta - General Subjects **1863**, 1371–1380 (2019).
68.
Jung, S. jun, Kim, J. E. H., Reithinger, J. H. & Kim, H. The Sec62-Sec63 translocon facilitates translocation of the C-terminus of membrane proteins. Journal of Cell Science **127**, 4270–4278 (2014).
69.
Junne, T., Schwede, T., Goder, V. & Spiess, M. The Plug Domain of Yeast Sec61p Is Important for Efficient Protein Translocation, but Is Not Essential for Cell Viability. Molecular Biology of the Cell **17**, 4063–4068 (2006).
70.
Kamat, S., Yeola, S., Zhang, W., Bianchi, L. & Driscoll, M. NRA-2, a nicalin homolog, regulates neuronal death by controlling surface localization of toxic caenorhabditis elegans DEG/ENaC channels. Journal of Biological Chemistry **289**, 11916–11926 (2014).
71.
Kedrov, A., Kusters, I., Krasnikov, V. V. & Driessen, A. J. M. A single copy of SecYEG is sufficient for preprotein translocation. EMBO Journal **30**, 4387–4397 (2011).
72.
Kedrov, A. et al. Elucidating the native architecture of the YidC: Ribosome complex. Journal of Molecular Biology **425**, 4112–4124 (2013).
73.
Keenan, R. J., Freymann, D. M., Walter, P. & Stroud, R. M. Crystal Structure of the Signal Sequence Binding Subunit of the Signal Recognition Particle sequence and functional conservation with their eukary-otic counterparts, SRP54, SRP RNA, and the SRP re-ceptor. Ffh is essential for viability of Escherichia coli. Cell vol. 94 181–191 (1998).
74.

Kelleher, D. J., Karaoglu, D., Mandon, E. C. & Gilmore, R. Oligosaccharyltransferase Isoforms that Contain Different Catalytic STT3 Subunits Have Distinct Enzymatic Properties binding site-induced alterations in the binding affinity of the catalytic site for the oligosaccharide donor and the tripeptide acceptor. A combination of protein biochemistry and yeast ge-netics led to the identification of the eight subunits. Molecular Cell vol. 12 101–111 (2003).

75. Kelleher, D. J. & Gilmore, R. An evolving view of the eukaryotic oligosaccharyltransferase. Glycobiology **16**, (2006).

76. Klenner, C., Yuan, J., Dalbey, R. E. & Kuhn, A. The Pf3 coat protein contacts TM1 and TM3 of YidC during membrane biogenesis. FEBS Letters **582**, 3967–3972 (2008).

77. Konno, M. et al. Calumin, a Ca2+-binding protein on the endoplasmic reticulum, alters the ion permeability of Ca2+ release-activated Ca2+ (CRAC) channels. Biochemical and Biophysical Research Communications **417**, 784–789 (2012).

78. Kostova, K. K. et al. CAT-tailing as a fail-safe mechanism for efficient degradation of stalled nascent polypeptides. https://www.science.org.

79. Kubota, K., Yamagata, A., Sato, Y., Goto-Ito, S. & Fukai, S. Get1 stabilizes an open dimer conformation of Get3 ATPase by binding two distinct interfaces. Journal of Molecular Biology **422**, 366–375 (2012).

80. Kumazaki, K. et al. Structural basis of Sec-independent membrane protein insertion by YidC. Nature **509**, 516–519 (2014).

81. Kumazaki, K. et al. Crystal structure of Escherichia coli YidC, a membrane protein chaperone and insertase. Scientific Reports **4**, (2014).

82. Kutay, U., Hartmann, E. & Rapaport, T. A class of membrane proteins with a C-terminal anchor. Trends in Cell Biology **3**, 72–75 (1993).

83. Lang, S. et al. Different effects of Sec61α, Sec62 and Sec63 depletion on transport of polypeptides into the endoplasmic reticulum of mammalian cells. Journal of Cell Science **125**, 1958–1969 (2012).

84. Lewis, A. J. O. & Hegde, R. S. A unified evolutionary origin for the ubiquitous protein transporters SecY and YidC. BMC Biology **19**, (2021).

85. Li, H., Chavan, M., Schindelin, H., Lennarz, W. J. & Li, H. Structure of the Oligosaccharyl Transferase Complex at 12 Å Resolution. Structure **16**, 432–440 (2008).

86. Liaci, A. M. et al. Structure of the human signal peptidase complex reveals the determinants for signal peptide cleavage. Molecular Cell **81**, 3934-3948.e11 (2021).

87.
Lipp, J., Dobberstein, B. & Haeuptle, M.-T. Signal Recognition Particle Arrests Elongation of Nascent Secretory and Membrane Proteins at Multiple Sites in a Transient Manner*. THE JOURNAL OF BIOLOGICAL CHEMISTRY vol. 262 1680–1684 (1987).

88.
Louie, R. J. et al. A yeast phenomic model for the gene interaction network modulating CFTR-ΔF508 protein biogenesis. http://genomemedicine.com/content/4/12/103 (2013).

89.
Mariappan, M. et al. The mechanism of membrane-associated steps in tail-anchored protein insertion. Nature **477**, 61–69 (2011).

90.
Martoglio, B., Hofmann, M. W., Brunner, J. & Dobberstein, B. The Protein-Conducting Channel in the Membrane of the Endoplasmic Reticulum Is Open Laterally toward the Lipid Bilayer. Cell vol. 81 207–214 (1995).

91.
Mary, C. et al. Residues in SRP9/14 essential for elongation arrest activity of the signal recognition particle define a positively charged functional domain on one side of the protein. RNA **16**, 969–979 (2010).

92.
Mason, N., Ciufo, L. & Brown, J. Elongation arrest is a physiologically important function of signal recognition particle. EMBO Journal **19**, 4164–4174 (2000).

93.
Mateja, A. et al. The structural basis of tail-anchored membrane protein recognition by Get3. Nature **461**, 361–366 (2009).

94.
Matlack, K. E. S., Mothes, W. & Rapoport, T. A. Protein Translocation: Review Tunnel Vision channel by an interaction between SRP and its mem-brane receptor. Targeting in posttranslational pathways also requires a signal sequence but does not require. Cell vol. 92 381–390 (1998).

95.
Mccormick, P. J., Miao, Y., Shao, Y., Lin, J. & Johnson, A. E. Cotranslational Protein Integration into the ER Membrane Is Mediated by the Binding of Nascent Chains to Translocon Proteins pore, the translocon must also regulate molecular move-ment in the plane of the membrane because the TM sequences in a nascent membrane protein must be iden-tified and moved laterally from the aqueous pore into the hydrophobic interior of the ER membrane. Such a. Molecular Cell vol. 12 329–341 (2003).

96.
McDowell, M. A. et al. Structural Basis of Tail-Anchored Membrane Protein Biogenesis by the GET Insertase Complex. Molecular cell **80**, 72–86 (2020).

97.
McGilvray, P. T. et al. An ER translocon for multi-pass membrane protein biogenesis. eLife **9**, 1–43 (2020).

98.

McKenna, M., Simmonds, R. E. & High, S. Mechanistic insights into the inhibition of Sec61-dependent co- and post-translational translocation by mycolactone. Journal of Cell Science **129**, 1404–1415 (2016).

99. McKenna, M., Simmonds, R. E. & High, S. Mycolactone reveals the substrate-driven complexity of Sec61-dependent transmembrane protein biogenesis. Journal of Cell Science **130**, 1307–1320 (2017).

100. Meacock, S. L., Lecomte, F. J. L., Crawshaw, S. G. & High, S. Different Transmembrane Domains Associate with Distinct Endoplasmic Reticulum Components during Membrane Integration of a Polytopic Protein. Molecular Biology of the Cell **13**, 4114–4129 (2002).

101. Moore, M., Goforth, R. L., Mori, H. & Henry, R. Functional interaction of chloroplast SRP/FtsY with the ALB3 translocase in thylakoids: Substrate not required. Journal of Cell Biology **162**, 1245–1254 (2003).

102. Moore, M., Harrison, M. S., Peterson, E. C. & Henry, R. Chloroplast Oxa1p homolog albino3 is required for post-translational integration of the light harvesting chlorophyll-binding protein into thylakoid membranes. Journal of Biological Chemistry **275**, 1529–1532 (2000).

103. Mori, H., Summer, E. J., Ma, X. & Cline, K. Component Specificity for the Thylakoidal Sec and Delta pH-dependent Protein Transport Pathways. The Journal of Cell Biology vol. 146 45–55 http://www.jcb.org (1999).

104. Morimoto, M. et al. Bi-allelic CCDC47 Variants Cause a Disorder Characterized by Woolly Hair, Liver Dysfunction, Dysmorphic Features, and Global Developmental Delay. American Journal of Human Genetics **103**, 794–807 (2018).

105. Mothes, W., Jungnickel, B., Brunner, J. & Rapoport, T. A. Signal Sequence Recognition in Cotranslational Translocation by Protein Components of the Endoplasmic Reticulum Membrane. The Journal of Cell Biology vol. 142 355–364 http://www.jcb.org (1998).

106. Mukamel, R. E. et al. Repeat polymorphisms underlie top genetic risk loci for glaucoma and colorectal cancer. Cell **186**, 3659-3673.e23 (2023).

107. Müller, L. et al. Evolutionary Gain of Function for the ER Membrane Protein Sec62 from Yeast to Humans. Molecular Biology of the Cell **21**, 691–703 (2010).

108. Myronidi, I., Ring, A., Wu, F. & Ljungdahl, P. O. ER-localized Shr3 is a selective co-translational folding chaperone necessary for amino acid permease biogenesis. The Journal of cell biology **222**, (2023).

109. Nagamori, S., Smirnova, I. N. & Kaback, H. R. Role of YidC in folding of polytopic membrane proteins. Journal of Cell Biology **165**, 53–62 (2004).

110.
Neugebauer, S. A., Baulig, A., Kuhn, A. & Facey, S. J. Membrane protein insertion of variant MscL proteins occurs at YidC and SecYEG of Escherichia coli. Journal of Molecular Biology **417**, 375–386 (2012).

111.
Ng, B. G. et al. Mutations in the translocon-associated protein complex subunit SSR3 cause a novel congenital disorder of glycosylation. Journal of Inherited Metabolic Disease **42**, 993–997 (2019).

112.
Nguyen, D. et al. Proteomics reveals signal peptide features determining the client specificity in human TRAP-dependent ER protein import. Nature Communications **9**, (2018).

113.
Nilsson, I. & Von Heijne, G. Determination of the distance between the oligosaccharyltransferase active site and the endoplasmic reticulum membrane. Journal of Biological Chemistry **268**, 5798–5801 (1993).

114.
Nilsson, I. M. et al. Photocross-linking of nascent chains to the STT3 subunit of the oligosaccharyltransferase complex. Journal of Cell Biology **161**, 715–725 (2003).

115.
O'donnell, J. P. et al. The architecture of EMC reveals a path for membrane protein insertion. eLife **9**, 1–56 (2020).

116.
O'Keefe, S. et al. An alternative pathway for membrane protein biogenesis at the endoplasmic reticulum. Communications Biology **4**, (2021).

117.
Ogg, S. C. & Walter, P. SRP Samples Nascent Chains for the Presence of Signal Sequences by Interacting with Ribosomes at a Discrete Step during Translation Elongation. Cell vol. 81 1075–1084 (1995).

118.
Osborne, A. R., Rapoport, T. A. & Van Den Berg, B. Protein translocation by the Sec61/SecY channel. Annual Review of Cell and Developmental Biology **21**, 529–550 (2005).

119.
Overington, J. P., Al-Lazikani, B. & Hopkins, A. L. How many drug targets are there? Nature Reviews Drug Discovery **5**, 993–996 (2006).

120.
Panzner, S., Dreier, L., Hartmann, E., Kostka, S. & Rapoport', T. A. Posttranslational Protein Transport in Yeast Reconstituted with a Purified Complex of Set Proteins and Kar2p. Cell vol. 61 561–570 (1995).

121.
Park, E. & Rapoport, T. A. Mechanisms of Sec61SecY-mediated protein translocation across membranes. Annual Review of Biophysics **41**, 21–40 (2012).

122.

Peschke, M. et al. SRP, FtsY, DnaK and YidC Are Required for the Biogenesis of the E. coli Tail-Anchored Membrane Proteins DjlC and Flk. Journal of Molecular Biology **430**, 389–403 (2018).

123. Pfeffer, S. et al. Structure of the mammalian oligosaccharyl-transferase complex in the native ER protein translocon. Nature Communications **5**, (2014).

124. Plath, K. & Rapoport, T. A. Spontaneous Release of Cytosolic Proteins from Posttranslational Substrates before their Transport into the Endoplasmic Reticulum. The Journal of Cell Biology vol. 151 167–178 http://www.jcb.org/cgi/content/full/151/1/167 (2000).

125. Plath, K., Wilkinson, B. M., Stirling, C. J. & Rapoport, T. A. Interactions between Sec Complex and Prepro-Factor during Posttranslational Protein Transport into the Endoplasmic Reticulum. Molecular Biology of the Cell **15**, 1–10 (2004).

126. Pleiner, T. et al. Structural basis for membrane insertion by the human ER membrane protein complex. Science **369**, 433–436 (2020).

127. Pool, M. R. A trans-membrane segment inside the ribosome exit tunnel triggers RAMP4 recruitment to the Sec61p translocase. Journal of Cell Biology **185**, 889–902 (2009).

128. Richard, M., Boulin, T., Robert, V. J. P., Richmond, J. E. & Bessereau, J. L. Biosynthesis of ionotropic acetylcholine receptors requires the evolutionarily conserved ER membrane complex. Proceedings of the National Academy of Sciences of the United States of America **110**, (2013).

129. Ron, D. et al. The ER membrane protein complex interacts cotranslationally to enable biogenesis of multipass membrane proteins. (2018) doi:10.7554/eLife.37018.001.

130. Rosemond, E. et al. Regulation of M3 muscarinic receptor expression and function by transmembrane protein 147. Molecular Pharmacology **79**, 251–261 (2011).

131. Sachelaru, I. et al. YidC occupies the lateral gate of the SecYEG translocon and is sequentially displaced by a nascent membrane protein. Journal of Biological Chemistry **288**, 16295–16307 (2013).

132. Sadlish, H., Pitonzo, D., Johnson, A. E. & Skach, W. R. Sequential triage of transmembrane segments by Sec61α during biogenesis of a native multispanning membrane protein. Nature Structural and Molecular Biology **12**, 870–878 (2005).

133. Satoh, T., Ohba, A., Liu, Z., Inagaki, T. & Satoh, A. K. dPob/EMC is essential for biosynthesis of rhodopsin and other multi-pass membrane proteins in Drosophila photoreceptors. doi:10.7554/eLife.06306.001.

134.

Schaffitzel, C. et al. Structure of the E. coli signal recognition particle bound to a translating ribosome. Nature **444**, 503–506 (2006).

135.

Schröder, K. et al. Control of glycosylation of MHC class II-associated invariant chain by translocon-associated RAMP4. EMBO Journal **18**, 4804–4815 (1999).

136.

Schuenemann, D. et al. A novel signal recognition particle targets light-harvesting proteins to the thylakoid membranes. Plant Biology vol. 95 10312–10316 www.pnas.org. (1998).

137.

Schuldiner, M. et al. The GET Complex Mediates Insertion of Tail-Anchored Proteins into the ER Membrane. Cell **134**, 634–645 (2008).

138.

Seitl, I., Wickles, S., Beckmann, R., Kuhn, A. & Kiefer, D. The C-terminal regions of YidC from Rhodopirellula baltica and Oceanicaulis alexandrii bind to ribosomes and partially substitute for SRP receptor function in Escherichia coli. Molecular Microbiology **91**, 408–421 (2014).

139.

Serdiuk, T. et al. YidC assists the stepwise and stochastic folding of membrane proteins. Nature Chemical Biology **12**, 911–917 (2016).

140.

Shakoori, A. et al. Identification of a five-pass transmembrane protein family localizing in the Golgi apparatus and the ER. Biochemical and Biophysical Research Communications **312**, 850–857 (2003).

141.

Shanmugam, S. K. & Dalbey, R. E. The Conserved Role of YidC in Membrane Protein Biogenesis. Microbiology Spectrum **7**, (2019).

142.

Shao, S. & Hegde, R. S. Membrane protein insertion at the endoplasmic reticulum. Annual Review of Cell and Developmental Biology **27**, 25–56 (2011).

143.

Shao, S. & Hegde, R. S. A calmodulin-dependent translocation pathway for small secretory proteins. Cell **147**, 1576–1588 (2011).

144.

Sharma, S. et al. Association of genetic variants in the TMCO1 gene with clinical parameters related to glaucoma and characterization of the protein in the eye. Investigative Ophthalmology and Visual Science **53**, 4917–4925 (2012).

145.

Shibatani, T., David, L. L., McCormack, A. L., Frueh, K. & Skach, W. R. Proteomic analysis of mammalian oligosaccharyltransferase reveals multiple subcomplexes that contain Sec61, TRAP, and two potential new subunits. Biochemistry **44**, 5982–5992 (2005).

146.

Shrimal, S., Cherepanova, N. A. & Gilmore, R. DC2 and KCP2 mediate the interaction between the oligosaccharyltransferase and the ER translocon. Journal of Cell Biology **216**, 3625–3638 (2017).

147.

Slaymaker, I. M. et al. Rationally engineered Cas9 nucleases with improved specificity. Science **351**, 84–88 (2016).

148. Smalinskaitė, L., Kim, M. K., Lewis, A. J. O., Keenan, R. J. & Hegde, R. S. Mechanism of an intramembrane chaperone for multipass membrane proteins. Nature **611**, 161–166 (2022).

149. Sommer, N., Junne, T., Kalies, K. U., Spiess, M. & Hartmann, E. TRAP assists membrane protein topogenesis at the mammalian ER membrane. Biochimica et Biophysica Acta - Molecular Cell Research **1833**, 3104–3111 (2013).

150. Sun, S., Li, X. & Mariappan, M. Signal sequences encode information for protein folding in the endoplasmic reticulum. Journal of Cell Biology **222**, (2023).

151. Talbot, B. E., Vandorpe, D. H., Stotter, B. R., Alper, S. L. & Schlondorff, J. S. Transmembrane insertases and N-glycosylation critically determine synthesis, trafficking, and activity of the nonselective cation channel TRPC6. Journal of Biological Chemistry **294**, 12655–12669 (2019).

152. Taylor, M. R. et al. The zebrafish pob gene encodes a novel protein required for survival of red cone photoreceptor cells. Genetics **170**, 263–273 (2005).

153. Thapa, K. et al. Dysregulation of the calcium handling protein, CCDC47, is associated with diabetic cardiomyopathy. Cell and Bioscience **8**, (2018).

154. Tian, S. et al. Proteomic Analysis Identifies Membrane Proteins Dependent on the ER Membrane Protein Complex. Cell Reports **28**, 2517-2526.e5 (2019).

155. Tong, M. & Jiang, Y. FK506-Binding Proteins and Their Diverse Functions.

156. Uchihashi, T., Iino, R., Ando, T. & Noji, H. High-speed atomic force microscopy reveals rotary catalysis of rotorless F 1-ATPase. Science **333**, 755–758 (2011).

157. Vabulas, R. M., Raychaudhuri, S., Hayer-Hartl, M. & Hartl, F. U. Protein folding in the cytoplasm and the heat shock response. Cold Spring Harbor perspectives in biology **2**, (2010).

158. Van Bloois, E., Jan Haan, G., De Gier, J. W., Oudega, B. & Luirink, J. F1F0 ATP synthase subunit c is targeted by the SRP to YidC in the E. coli inner membrane. FEBS Letters **576**, 97–100 (2004).

159. Van Den Berg, B. et al. X-ray structure of a protein-conducting channel. www.nature.com/nature (2003).

160. Vembar, S. S. & Brodsky, J. L. One step at a time: Endoplasmic reticulum-associated degradation. Nature Reviews Molecular Cell Biology **9**, 944–957 (2008).

161.

Voigt, S., Jungnickel, B., Hartmann, E. & Rapoport, T. A. Signal Sequence-dependent Function of the TRAM Protein during Early Phases of Protein Transport across the Endoplasmic Reticulum Membrane.

162. Volkmar, N. et al. The ER membrane protein complex promotes biogenesis of sterol-related enzymes maintaining cholesterol homeostasis. Journal of Cell Science **132**, (2019).

163. Von Heijne, G. Signal Sequences The Limits of Variation. J. Mol. Biol vol. 184 99–105 (1985).

164. Walter, P. & Blobel, G. Translocation of Proteins Across the Endoplasmic Reticulum III. Signal Recognition Protein (SRP) Causes Signal Sequence-dependent and Site-specific Arrest of Chain Elongation that is Released by Microsomal Membranes. THE JOURNAL OF CELL BIOLOGY vol. 91 557–561 (1981).

165. Wang, F., Brown, E. C., Mak, G., Zhuang, J. & Denic, V. A chaperone cascade sorts proteins for posttranslational membrane insertion into the endoplasmic reticulum. Molecular Cell **40**, 159–171 (2010).

166. Wang, F., Chan, C., Weir, N. R. & Denic, V. The Get1/2 transmembrane complex is an endoplasmic-reticulum membrane protein insertase. Nature **512**, 441–444 (2014).

167. Wang, Q. C. et al. TMCO1 is an ER Ca2+ load-activated Ca2+ channel. Cell **165**, 1454–1466 (2016).

168. Watson, H. Biological membranes. Essays in Biochemistry **59**, 43–70 (2015).

169. Wu, H. & Hegde, R. S. Mechanism of signal-anchor triage during early steps of membrane protein insertion. Molecular Cell **83**, 961-973.e7 (2023).

170. Xin, B. et al. Homozygous frameshift mutation in TMCO1 causes a syndrome with craniofacial dysmorphism, skeletal anomalies, and mental retardation. Proceedings of the National Academy of Sciences of the United States of America **107**, 258–263 (2010).

171. Xiong, L. et al. ER complex proteins are required for rhodopsin biosynthesis and photoreceptor survival in Drosophila and mice. Cell Death and Differentiation **27**, 646–661 (2020).

172. Yamaguchi, A. et al. Stress-associated Endoplasmic Reticulum Protein 1 (SERP1)/Ribosome-associated Membrane Protein 4 (RAMP4) Stabilizes Membrane Proteins during Stress and Facilitates Subsequent Glycosylation. The Journal of Cell Biology vol. 147 1195–1204 http://www.jcb.org (1999).

173. Yamamoto, S. et al. Contribution of calumin to embryogenesis through participation in the endoplasmic reticulum-associated degradation activity. Developmental Biology **393**, 33–43 (2014).

174. Yip, M. C. J., Sedor, S. F. & Shao, S. Mechanism of client selection by the protein quality-control factor UBE2O. Nature Structural and Molecular Biology **29**, 774–780 (2022).

175. Young, B. P., Craven, R. A., Reid, P. J., Willer, M. & Stirling, C. J. Sec63p and Kar2p are recquired for the translocation of SRP-dependent precursors into the yeast endoplasmic reticulum in vivo. EMBO Journal **20**, 262–271 (2001).

176. Zafar, S., Nasir, A. & Bokhari, H. Computational analysis reveals abundance of potential glycoproteins in Archaea, Bacteria and Eukarya. (2011).

177. Zalisko, B. E., Chan, C., Denic, V., Rock, R. S. & Keenan, R. J. Tail-Anchored Protein Insertion by a Single Get1/2 Heterodimer. Cell Reports **20**, 2287–2293 (2017).

178. Zhang, M. et al. Calumin, a novel Ca2+-binding transmembrane protein on the endoplasmic reticulum. Cell Calcium **42**, 83–90 (2007).

179. Zhu, L., Kaback, H. R. & Dalbey, R. E. YidC protein, a molecular chaperone for LacY protein folding via the SecYEG protein machinery. Journal of Biological Chemistry **288**, 28180–28194 (2013).

180. Zong, G. et al. Ipomoeassin F Binds Sec61α to Inhibit Protein Translocation. Journal of the American Chemical Society **141**, 8450–8461 (2019).